JUSTUS-LIEBIG-
UNIVERSITÄT
GIESSEN

The Prp19 and Msl5-Mud2 complexes coordinate transcription with nuclear mRNP assembly

Dissertation

zur Erlangung des Doktorgrades der Naturwissenschaften

(Dr. rer. nat.)

am Fachbereich 08 für Biologie und Chemie

der Justus-Liebig-Universität Gießen

Vorgelegt von

Laura Henke-Schulz

Gießen, 2023

Die vorliegende Arbeit wurde am Institut für Biochemie (Fachbereich 08) der Justus-Liebig-Universität Gießen, unter Leitung von Prof. Dr. Katja Sträßer, erstellt.

Dissertation eingereicht: Juni 2023

Erstgutachter: Prof. Dr. Katja Sträßer

Fachbereich 08: Biologie und Chemie
Institut für Biochemie
Justus-Liebig-Universität Gießen

Zweitgutachter: Apl. Prof. Dr. Elena Evguenieva-Hackenberg

Department of Biology and Chemistry
Institute of Microbiology and Molecular biology
Justus-Liebig-University

1 List of content

2 Zusammenfassung

Der Prozess der Genexpression ist komplex und umfasst mehrere Schritte. Im ersten Schritt synthetisiert die RNA-Polymerase II (RNAPII) mRNA, die dann eine ko-transkriptionelle Prozessierung wie das Anfügen einer 5'-Kappen-Struktur, das Herausspleißen der Introns und Polyadenylierung durchläuft. Die prozessierte mRNA wird dann in ein Boten-Ribonukleoprotein-Partikel (mRNP) verpackt, in das Zytoplasma transportiert und schließlich in ein Protein übersetzt. TREX ist ein Schlüsselspieler der mRNP-Biogenese, da er die Transkription mit dem mRNA-Export koppelt. Zusätzlich wurde entdeckt, dass der Prp19-Komplex (Prp19C), der für seine Rolle im Spleißen bekannt ist, eine wesentliche Rolle bei der Genexpression spielt, indem er die Transkriptionselongation unterstützt und TREX an den transkribierten Genen stabilisiert – oder rekrutiert. Der Prp19C besteht aus acht Kernproteinen. Die essentiellen Untereinheiten sind Prp19, Cef1, Clf1, Syf1, Cwc2 und Prp46 und die nicht-essentiellen Untereinheiten sind Isy1, Ntc20, Syf2 und Snt309. Es ist jedoch unbekannt, ob diese essentiellen als auch die nicht-essentiellen Untereinheiten des Prp19Cs eine Rolle bei der Stabilisierung von TREX an transkribierten Genen und bei der Transkription spielen.

In dieser Arbeit wurde festgestellt, dass Ntc20 während der Transkriptionselongation keine Rolle spielt. Die Deletion von *ISY1* führt zu einer veränderten Rekrutierung von RNAPII und Prp19C/TREX an den transkribierten Genen. Es ist bereits bekannt, dass Snt309 den Prp19C stabilisiert, dies wurde in dieser Arbeit bestätigt. Cwc15 und Syf2 stabilisieren die Interaktion zwischen TREX, Prp19C und mit der Transkriptionsmaschinerie. Darüber hinaus ist Cwc15 für eine effiziente Transkriptionselongation unerlässlich.

Msl5 ist ein Verzweigungspunkt-bindendes Protein, das eine wichtige Rolle während des Spleißens spielt und mit Mud2 interagiert. Mud2 ist auch an der Transkriptionselongation beteiligt. PAR-CLIP-Analysen von Baejen et al. (2014), welche von Minocha at al. (2018) erneut analysiert und publiziert wurden ergaben, dass Msl5 mit intronlosen mRNAs interagiert, seine Funktion in der Biogenese von intronlosen mRNAs ist jedoch unbekannt. Daher sollte untersucht werden, ob Msl5 eine Rolle bei der Transkription spielt. In dieser Arbeit wurde festgestellt, dass Msl5 für stabile Niveaus von Prp19C und TREX an transkribierten Genen benötigt wird. Wenn Msl5 fehlt, ist zudem der effiziente Export von mRNA bei 37°C beeinträchtigt.

Zusammenfassend wurde in dieser Studie gezeigt, dass die nicht-essentiellen Untereinheiten von Prp19C eine spezifische Funktion besitzen und eine neue Funktion von Msl5 während der Transkription und des mRNA-Exports aufzeigt.

3 Summary

The process of gene expression is complex and involves multiple steps. In the first step, RNA polymerase II (RNAPII) synthesizes mRNA, which then undergoes co-transcriptional processing such as 5′-end capping, splicing, and polyadenylation. The processed mRNA is then packaged into a messenger ribonucleoprotein particle (mRNP), transported to the cytoplasm, and eventually translated into a protein. TREX is a key player of mRNP biogenesis by coupling transcription to nuclear mRNA export. Additionally, the Prp19 complex (Prp19C), well-known for its role in splicing, has been discovered to play an important role in gene expression by supporting transcription elongation by stabilizing TREX at transcribed genes.

Prp19C contains eight core proteins; the essential subunits are Prp19, Cef1, Clf1, Syf1, Cwc2, and Prp46 and the non-essential subunits are Isy1, Ntc20, Syf2, and Snt309. However, it is unknown if the individual non-essential subunits of Prp19C play a role in maintaining TREX at transcribed genes and in transcription. In this study, I found out that Ntc20 does not have a role during transcription elongation. However, deletion of *ISY1* leads to a loss of Prp19C and TREX occupancy's at transcribed genes. Deletion of *SNT309* elicits many effects, which in the end can be explained by a destabilization of the Prp19C. Cwc15 and Syf2 facilitate the interaction between TREX and Prp19C, as well as with the transcription machinery. Moreover, Cwc15 is essential for efficient transcription elongation.

Msl5 is the branch point binding protein that plays a crucial role in splicing and interacts with Mud2. Recent research has shown that Mud2 is also involved in transcription elongation. Published PAR-CLIP data showed that Msl5 crosslinks to intronless mRNAs. However, its function in the biogenesis of intronless mRNAs remains unknown. Therefore, I wanted to investigate whether Msl5 has a role in transcription. In this work, I found out that Msl5 is needed for full occupancy of Prp19C and therefore TREX at transcribed genes. Further, if Msl5 is missing efficient export of mRNA is impaired at 37°C.

In sum, this study is the first to determine specific functions for the non-essential subunits of Prp19C and further a novel function of Msl5 during transcription and nuclear mRNA export.

4 Introduction

4.1 Gene expression

The central dogma of molecular biology is that genetic information is stored in DNA and transcribed into RNA. The RNA is later translated into proteins. These proteins are responsible for most functional activities in all organisms (Crick 1970). This fundamental process occurs in all living cells and is also called gene expression. Gene expression is a complex process that is closely linked and highly regulated at every step, from transcription, over mRNA processing and nuclear mRNA export, translation to mRNA degradation.

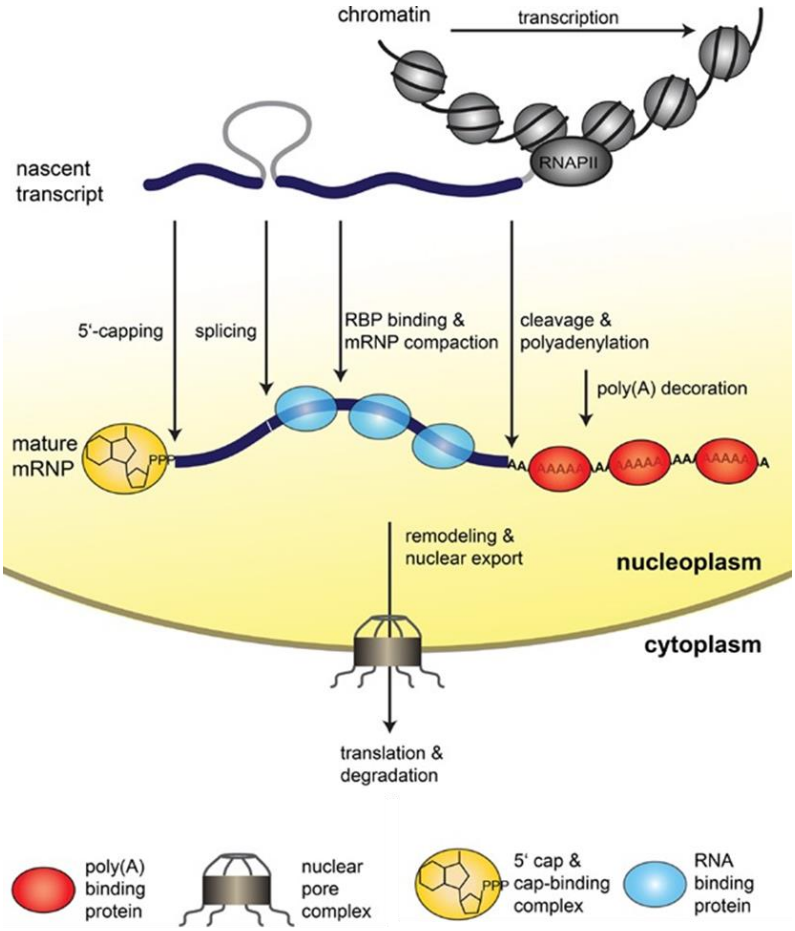

Figure 1: Gene expression. The nascent mRNA is transcribed by RNA polymerase II (RNAPII) and undergoes various processing events until the mRNA is matured and ready to be exported. Already during transcription, several proteins bind to the nascent mRNA and the nascent mRNA is covered by different RNA binding proteins (RBPs) and proteins complexes. The different RBPs regulate the processing of the mRNA like 5' capping, splicing and 3' end formation. During these processes the mRNA is remodeled until it is ready to be exported from the nucleus through the nuclear pore complexes to the cytoplasm, where it is translated and later degraded. Blue and red circles indicate different RBPs that bind to the mRNA (Meinel and Sträßer 2015).

Eukaryotic cells are divided into a nuclear and a cytoplasmic compartment. The DNA is stored inside the nucleus, where the nascent pre-mRNAs is synthesized by the DNA-dependent RNA-polymerase II (RNAPII). Already during the synthesis of nascent pre-mRNAs several RNA-binding proteins (RBPs) bind to the nascent pre-mRNA and the mRNA is processed by capping, splicing, 3'-end processing and polyadenylation. The mRNA is then compacted and packed into a messenger ribonucleoprotein particle (mRNP). If the mRNA is correctly processed and packaged it gets exported through one of the nuclear pore complexes into the cytoplasm where the mRNA is translated into proteins (Figure 1).

4.2 mRNA synthesis

The first step of gene expression is the synthesis of mRNA. In *Saccharomyces cerevisiae* (*S. cerevisiae*) the mRNA is synthesized by the RNAPII, which consists of 12 subunits. Transcription of a gene takes place in three stages: initiation, elongation, and termination. Every step is highly regulated and therefore a multitude of other proteins and transcription factors are involved in this process (Schier and Taatjes 2020; Thomas and Chiang 2006).

4.2.1 Transcription initiation

The C-terminal domain (CTD) of Rpb1, which is the largest subunit of RNAPII, is essential for the coordination of the different steps of transcription. The CTD only exists in eukaryotes and has a highly conserved consensus sequence. The consensus sequence consists of a heptapeptide ($Y_1S_2P_3T_4S_5P_6S_7$), which is repeated 26 times in *S. cerevisiae* and 52 in humans. Different kinases and phosphatases phosphorylate or dephosphorylate the serine, tyrosine and threonine residues of the heptapeptide during transcription process (Hsin and Manley 2012; Dahmus 1995).

It has long been known that the RNAPII assembles with transcription factors and forms a large preinitiation complex (PIC), which is even bigger than a ribosome (Liu, Bushnell, and Kornberg 2013). The core proteins of the PIC which consists of eight core complexes: TFIIA,TFIIB, TFIID, TFIIE, TFIIF, TFIIH, unphosphorylated RNAPII, and the mediator complex (Hahn 2004). The mediator complex binds to the unphosphorylated CTD of RNAPII. The TATA-box binding protein (TBP), a subunit of TFIID, binds to the

TATA box, which is located 30-100 bp upstream of the transcription start site (TSS). This interaction leads to a sharp bend of the promoter DNA. TBP recruits TFIIA, then TFIIB binds to the promotor. During this process TFIIB recruits the non-phosphorylated RNAPII and TFIIF to the promotor and together they stabilize the PIC. Subsequently, TFIIF joins the growing complex and recruits TFIIH. TFIIH possesses subunits that contain protein kinase and DNA helicase activity. This kinase phosphorylates the S_5 and S_7 residues of the RNAPII CTD, and the helicase unwinds the DNA at the promoter region. These ATP-dependent events lead to the transition from a closed to an open PIC, causing the transcription bubble to form. RNAPII engages with the template strand of the transcription bubble and RNA synthesis begins. After the synthesis of approximately 10 nucleotides of nascent mRNA, RNAPII leaves the promoter region, which is called promotor clearance (Mermelstein, Flores, and Reinberg 1989; Holstege and Timmers 1997; Schier and Taatjes 2020).

4.2.2 Transcription elongation

The transition from transcription initiation to elongation is marked by a change in the phosphorylation pattern of the CTD. The cyclin-dependent protein kinases Bur1 and Ctk1 phosphorylate S_2. Simultaneously, Rtr1 and Ssu72 dephosphorylate S_5 (Keogh, Podolny, and Buratowski 2003; Lee and Greenleaf 1989; Mosley et al. 2009; Rosado-Lugo and Hampsey 2014). At the same time, the elongation factors Paf1, Spt4, Spt5, Spt6 are recruited to RNAPII and start the elongation. Paf1 interacts with RNAPII and it further is involved in histone modification and in mRNA 3' end processing (Wade et al. 1996; Jaehning 2010). Spt6 can bind to histones and provides that RNAPII can passage through the chromatinized DNA (Narain et al. 2021). Spt5 is conserved form yeast to human and binds directly to RNAPII, depletion of Spt5 even causes the degradation of RNAPII (Hu et al. 2021; Aoi et al. 2021). Furthermore, Spt5 binds to Spt4 which leads to the formation of a heterodimer together they stimulate transcription elongation (Ehara and Sekine 2018; Hirtreiter et al. 2010). The transition from transcription elongation to transcription termination is signaled by decreasing levels of Y_1 and S_2 phosphorylation. Y_1 is dephosphorylated at the poly(A) site and S_2 at the termination site (Mayer et al. 2012).

4.2.3 Transcription termination

The last step of transcription is transcription termination. At this step RNAPII releases the transcript and dissociates from the DNA. When RNAPII reaches the poly(A) signal (AAUAA) two protein complexes, CPSF (cleavage and polyadenylation specify factor) and CSTF (cleavage stimulation factor) recognize the poly(A) signal on the synthesized RNA (Richard and Manley 2009). In eukaryotes, two models of transcription termination are favored, the “torpedo model” and the “allosteric model”. The torpedo model requires the endonucleolytic cleavage of the nascent RNA and a 5’-3’ exonuclease (Rat1) activity, which can trigger the release of RNAPII. When Rat1 catches up with the transcribing RNAPII, it triggers transcript release by disrupting RNAPII-mRNA contacts, which in turn allows the release of the RNAPII from the DNA (Kim et al. 2004). The allosteric model proposes that termination occurs due to a structural change and the loss of some associated proteins from RNAPII which in turn leads to a release of the DNA strand after passing the poly(A) signal (Rosonina, Kaneko, and Manley 2006). When transcription is completed RNAPII has to be recycled in order to start a new round of transcription. RNAPII needs to be released from all transcription elongation termination factors. Furthermore, the CTD of RNAPII needs to be reverted to its unphosphorylated state (Rosonina, Kaneko, and Manley 2006).

4.3 mRNA processing, mRNP formation and nuclear export

During transcription, the nascent mRNA is processed co-transcriptionally and packaged into an mRNP by a variety of RBPs. To obtain mature mRNA the nascent mRNA has to be capped, spliced and polyadenylated at its 3’ end. These steps are closely linked to the different steps of transcription.

4.3.1 Capping

Shortly after transcription initiation, mRNAs are capped co-transcriptionally at their 5’ end. The cap is essential for RNA stability, splicing, polyadenylation, mRNA export and for the efficient translation of the mRNA (Shatkin and Manley 2000). The cap of all mRNAs consists of a guanine nucleotide that is methylated at the N7 position and is linked to the first nucleotide of the mRNA through an unusual 5’-5’ phosphate linkage

(Zhai and Xiang 2014). The recruitment of the capping enzyme complex (RNA triphosphatase, guanylyltransferase, and the 7-methyltransferase) is dependent on the phosphorylation of S_5 of the CTD (Komarnitsky, Cho, and Buratowski 2000). The capping reaction consists of three steps. First, Cet1, removes the γ-phosphate from the 5' triphosphate. Next, Ceg1, a guanyltransferase, adds a guanine monophosphate to the 5'-end diphosphate. The last step is the addition of a methyl group to the N7 atom of the terminal guanine group, which is performed by the methyltransferase Abd1 (Martinez-Rucobo et al. 2015; Ramanathan, Robb, and Chan 2016; Rodriguez et al. 1999). Next, the cap binding complex (CBC) binds the cap, CBC consists of small subunit and large subunit (in *S. cerevisiae* the small subunit is called Cbp20 and the large subunit is called Cbp80) and is important for several downstream processes like splicing, polyadenylation and mRNA export (Flaherty et al. 1997). After nuclear mRNA export to the cytoplasm, the cap is important for the initiation of protein synthesis and is bound by the general translation initiation factor eIF4E (Nojima et al. 2007; Topisirovic et al. 2011).

4.3.2 Splicing

The DNA of eukaryotic cells consists of intronic and exonic regions. Introns derive from the term intragenic region, and exons derive from the term expressed regions. During splicing, introns are removed and the exons are religated (Gilbert 1978). In *S. cerevisiae*, only ~5% of genes contain introns, which is only a small amount but these genes are essential to live. This is due to the fact that 30% of all mRNAs in the cell contain introns. The reason behind this is the high expression of mRNA for genes coding for ribosomal proteins (since most of these mRNAs do contain an intron), or other highly transcribed genes that contain introns. However, in *S. cerevisiae*, most mRNAs only contain a single intron per gene (Ares, Grate, and Pauling 1999; Hossain and Johnson 2014; Parenteau et al. 2011). Splicing occurs largely co-transcriptionally and is a two-step transesterification reaction which is carried out by the spliceosome. The spliceosome is a large ribonucleoprotein complex and consist of five small nuclear RNAs (snRNAs) U1, U2, U4, U5 and U6 and numerous associated proteins (Reed 2003; Herzel et al. 2017; Wahl, Will, and Lührmann 2009). Three conserved sequences define introns: the 5' splice site (5'SS), the internal branch point (BP) with the polypyrimidine track and the 3' splice site (3'SS). The splicing reaction occurs in a step-wise manner. At first the U1 snRNP recognizes the 5' splice site while Mud2 do recognizes the 3' splice site. Msl5 binds the BP sequence in the intron, and Mud2 binds the polypyrimidine tract. Subsequently, Mud2 interacts with Msl5 in a BP-dependent manner. U2 is recruited to

the BP, displacing Msl5 and Mud2 and leading to the formation of complex A at the splice site (Figure 2). The tri-snRNP consisting of U4/U6-U5 is recruited to the 5' splice site region and form the complex B. Complex B undergoes some rearrangements that allow the release of U1 and U4. Prp19C binds to (for more details see 4.4) the complex B which leads to further rearrangements and to the activated complex B*. Now the complex performs the first catalytic step of splicing, which leads to pre-mRNA cleavage at the 5' splice site and ligation of the 5' end of the intron to the adenosine of the BP leading to a so-called lariat structure. The newly created complex is now called complex C. During the second catalytic step, the cleavage at the 3' splice site of the pre-mRNA occurs. This leads to ligation of the 5' and 3' ends of the two exons. The now called post-splicing complex undergoes further remodeling and releases all the snRNPs and all involved factors. These can now be recycled and used in the next round of splicing (Ohi et al. 2005; Will and Lührmann 2011).

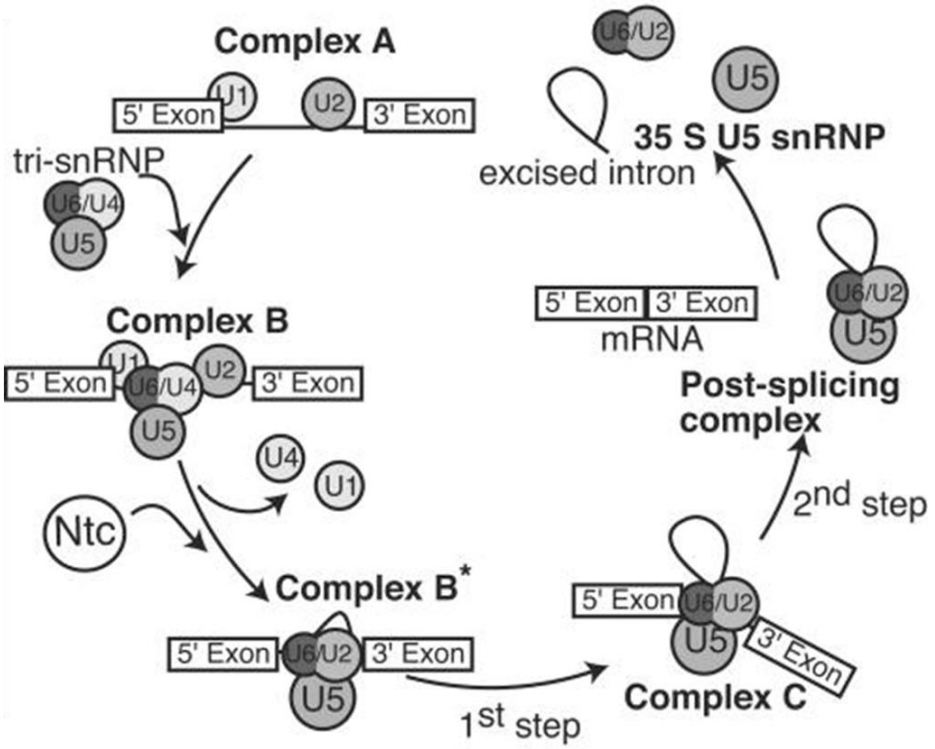

Figure 2: Schematic model of pre-mRNA splicing. Splicing starts with recognition of 5' splice site and the branch point by U1 and U2 snRNAs, respectively, leading to formation of Complex A. Association of U5/U4-U6 tri-snRNP to complex A resulting in Complex B. After several rearrangements and the addition of the NTC (Prp19C), complex B* is formed. Two catalytic steps are performed to remove the intron and ligate the exons. The spliced mRNA is released and factors involved in the process are released and recycled. (Ohi et al. 2005)

4.3.3 3’ end processing

The last step to obtain a mature mRNA is cleavage and polyadenylation. For polyadenylation to occur, the mRNA needs to be released from RNAPII by mRNA cleavage. The cleavage and polyadenylation specificity factor (CPSF) consists of more than 20 proteins and mediates the cleavage at the 3’ untranslated region (3’ UTR) is followed by the addition of the poly(A) tail. CPSF components such as Rna14, Rna15 and Pcf11 are recruited via the S_2 phosphorylation of the CTD and motifs inside the 3’ UTR of the pre-mRNA (Minvielle-Sebastia et al. 1991; Amrani et al. 1997; Moore and Proudfoot 2009). The nuclease Cft2 cleaves the nascent mRNA, and the poly(A) polymerase Pap1 adds the poly(A) tail (Zhao, Kessler, and Moore 1997; Casañal et al. 2017). Poly(A) binding proteins, like Nab2, bind the poly(A) tail as it is synthesized to stabilize the mRNA. The length of the poly(A) tail is important for the stability of poly(A) tail (Soucek, Corbett, and Fasken 2012). The final length of the poly(A) tail is controlled by Pab1 and Nab2 (Kelly et al. 2010; Brambilla et al. 2019).

4.3.4 TREX complex

A key player of mRNP assembly is the TREX complex. It couples transcription to nuclear mRNA export (Figure 3). TREX is evolutionarily conserved from yeast to human (Strässer et al. 2002; Xie and Ren 2019). In *S. cerevisiae*, TREX is a multiprotein complex consisting of the THO complex, the SR-like proteins Gbp2 and Hrb1, the DEAD-box RNA-helicase Sub2 and the export adaptor Yra1 (Strässer et al. 2002; Xie et al. 2021; Wegener and Müller-McNicoll 2019). THO complex is a pentameric subcomplex (Tho2, Hpr1, Thp2, Tex1 and Mft1). THO and therefore TREX are recruited to RNAPII-transcribed genes by several mechanisms. THO interacts with the Prp19C and Mud2, both of which also function in splicing. Prp19C is recruited through the direct or indirect interaction with the Rpb1 and Mud2 is recruited by the S_2 phosphorylated CTD to the transcribed genes (Chanarat, Seizl, and Strässer 2011; Minocha et al. 2018). THO also interacts directly with the S_2 phosphorylated CTD to be recruited to transcribed genes and also with the nascent mRNA (Meinel and Sträßer 2015). Mutants of the THO complex have a defect in transcription elongation and an increased number of R-loops, hence TREX is also important to prevent hyper-recombination events (Jimeno et al. 2002; Chávez and Aguilera 1997). The SR-like proteins Hrb1 and Gbp2 are involved in spicing (Hackmann et al. 2014). The DEAD-box helicase Sub2 binds to the THO complex and recruits Yra1 (Strässer and Hurt 2000). Yra1 binds to Mex67-Mtr2 and then

facilitates the export of the mature mRNA from the nucleus to the cytoplasm, where ribosomes are responsible for the synthesis of the encoded proteins (Jimeno et al. 2002; Strässer et al. 2002). It has been shown that the ubiquitylated Hpr1 can directly interact with ubiquitylated Mex67. Knowing this, it could be concluded, that Yra1 is not the only TREX component which can recruit Mex67-Mtr2 to the mRNP (Gwizdek et al. 2005; Hobeika et al. 2007; Hobeika et al. 2009). Besides, the TREX complex the Thp1-Sac3-Sus1-Cdc31 (THSC) complex, which is located the nuclear pore can also export mRNAs.

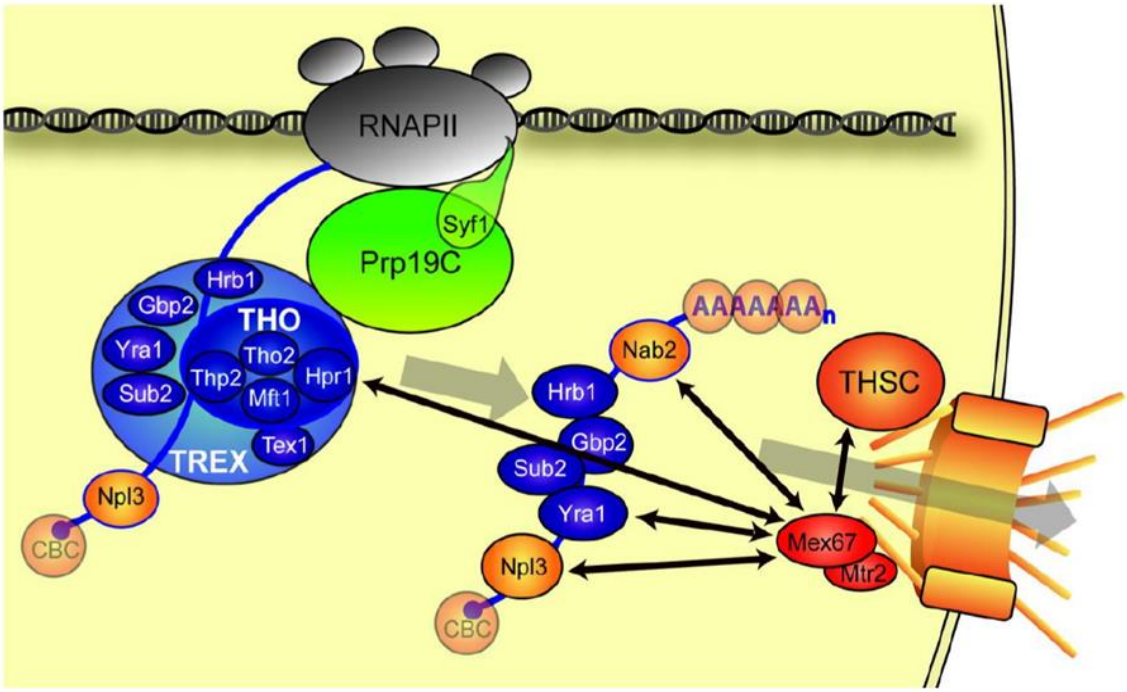

Figure 3: Schematic overview of mRNP formation and export to the cytoplasm. During transcription, the TREX complex is recruited to the transcription machinery and couples transcription to mRNA export. The Prp19C component Syf1 binds RNAPII *via* its C-terminus and stabilizes the occupancy of TREX to transcribed genes. Simultaneously, several mRNA-binding proteins are recruited to the mRNA, which itself undergoes several remodeling steps to form an mRNP. The Mex67-Mtr2 export receptor is recruited to the mature mRNP by direct interaction with TREX components Yra1 and/or Hpr1, Nab2, Npl3 and the THSC complex. Mex67-Mtr2 then exports the mRNP through the nuclear pore complex into the cytoplasm. (Chanarat et al. 2012)

4.3.5 nuclear mRNA export

In eukaryotes, translation takes place in the cytoplasm. Hence, to be able to be translated, the mature mRNA needs to be exported from the nucleus into the cytoplasm. This process is highly regulated and conserved from yeast to human (Katahira 2012). The export of the mature mRNA is mediated by the nuclear pore complex (NPC). The NPC is a large multiprotein complex with a size of 52 MDa or even ~82 MDa, including

the membrane, cargo and nuclear transport factors (NTRs) (Kim et al. 2018). The NPC consists of approximately 30 different nucleoporins (Nups), which are mostly conserved across eukaryotes (Rout et al. 2000). The NPC can be divided into three different sections: the nuclear basket, the central channel (inner ring) and the cytoplasmic complex (Beck and Hurt 2017).

Once the nascent mRNA has been successfully processed and packaged into an mRNP, it can be transported through the NPC into the cytoplasm. This process is mediated by the essential and highly conserved export receptor Mex67-Mtr2 (Santos-Rosa et al. 1998). Mex67-Mtr2 binds RNA directly, but only with very low affinity (Katahira et al. 1999). Mex67-Mtr2 is recruited to mRNAs by the direct interaction with mRNA-binding proteins. One of these proteins is Yra1, mentioned above (4.3.4 TREX complex). Yra1 is part of the TREX complex, and thus Yra1 is an export adaptor to increase the efficiency of mRNA export. Yra1 binds to the DEAD-box helicase Sub2. Mex67-Mtr2 then interacts with Yra1 (Strässer and Hurt 2001). Besides Yra1, the THO component Hpr1 interacts directly with Mex67 when both proteins are ubiquitinylated (Hobeika et al. 2009). If Npl3 is dephosphorylated, it also interacts with Mex67-Mtr2 (Gilbert and Guthrie 2004). Nab2 is also essential for the export of the mRNP, it interacts with Mex67-Mtr2 and Yra1 and built a ternary complex (Hector et al. 2002; Iglesias et al. 2010). Next to the interaction to Yra1 and Mex67-Mtr2, Nab2 can also interact with the Mlp1, which is located at the NPC. The interaction of Nab2 and Mlp1 is one final quality control step for the mRNA before it is exported (Fasken, Stewart, and Corbett 2008; Galy et al. 2004). Mex67 interacts with nucleoporins that contain phenylalanine and glycine repeats (FG repeats). These repeats are mostly unfolded and stretch into the inner channel of the NPC (Katahira et al. 1999, Strasser et al. 2000, Hobeika et al. 2009).

When the mRNP reaches the cytoplasmic side, the mRNP undergoes a remodeling step, causing the release of Mex67 and Nab2 from the mRNP (Lund and Guthrie 2005; Adams and Wente 2020). This remodeling step is carried out by the ATP-dependent DEAD-box helicase Dbp5. Dbp5 binds to the mRNP already in the nucleus and shuttles together with it to the cytoplasm. At the cytosolic side, Dbp5 is activated by Gle1 and inositol hexaphophate (IP6) in an ATP-dependent manner. This step is crucial to ensure the directionality of nuclear mRNA export (Linder and Jankowsky 2011; Ashkenazy-Titelman et al. 2022). During the mRNP remodeling the export factors are released and get reimported into the nucleus (Tran et al. 2007). The mRNA is now ready for translation inside the cytoplasm.

4.4 The Prp19 complex (Prp19C)

Prp19C is named after its component Prp19 and was first identified in 1993 as splicing factor in *S. cerevisiae* (Cheng et al. 1993). Prp19C is conserved from yeast to human and mostly known for its function in splicing. However, it is involved in many more processes than splicing (Chanarat et al. 2012) such as genome stability (Idrissou and Maréchal 2022), lipid droplet formation (Cho et al. 2007), and transcription elongation (Chanarat et al. 2012). In humans, there are three different Prp19-like complexes known, compared to only one in yeast (Chanarat and Sträßer 2013). In *S. cerevisiae*, Prp19C contains eight core subunits. The four essential ones are Prp19, Cef1, Syf1, and Clf1 and the four non-essential ones are Snt309, Syf2, Isy1, and Ntc20 (Grote et al. 2010; Chanarat et al. 2012; Fabrizio et al. 2009). Prp19C has 26 further associated proteins (Ohi et al. 2002; Chanarat and Sträßer 2013). In addition to the eight core proteins of *S. cerevisiae*, human Prp19C has additional core proteins, namely PRL1/PRLG1, AD002/HSPC148, CTNNBL1/NAP, and HSP73. The yeast orthologs of PRL1/PRLG1 and AD002/HSPC148 are Prp46 and Cwc15, the other two proteins do not have orthologues in *S. cerevisiae* (Grote et al. 2010).

During splicing, Prp19C and its associated proteins interact with the spliceosome during or after the dissociation of the U4 snRNP. Prp19C stabilizes the association of the U5 and U6 snRNPs by promoting RNA-RNA interaction between U5 and U6 in the activated spliceosomal B*complex, which catalyzes the first transesterification reaction and remains bound throughout the second step of splicing (Chan and Cheng 2005; Chan et al. 2003; Tarn et al. 1994; Fabrizio et al. 2009). It has been shown that if components of the Prp19C are deleted or depleted free U4 snRNPs accumulate. This indicates that Prp19C has a role in spliceosome biogenesis and recycling (Hogg, McGrail, and O'Keefe 2010).

In addition to splicing, Prp19C has a role in transcription elongation in *S. cerevisiae* (Chanarat et al. 2012). Syf1, an essential protein of Prp19C, interacts with RNAPII. A mutant of Syf1, *syf1-37*, it is not viable at 37°C and is not able to interact with RNAPII anymore, due to the lack of its C-terminus. In *syf1-37* mutant cells, part of TREX falls off while transcribing genes leading to a lower transcription efficiency. Therefore, Syf1 and the whole Prp19C are needed for the occupancy of TREX at transcribed genes. Until now it is not known if the non-essential subunits of the Prp19C play a role in this process and how the two complexes interact with each other. Since the *syf1-37* mutant impairs

transcription but not splicing, it also leaves the question if *S. cerevisiae* contains more than one Prp19C subcomplex, like in human cells, that have not been found yet.

In this study, I focus on the non-essential proteins of Prp19C, namely Isy1, Ntc20, Syf2, Snt309 and the Prp19C related protein Cwc15. All of these Prp19C components are recruited to the spliceosome in the same manner as Prp19. None of the single deletion mutants of these non-essential subunits show a strong phenotype (Chen et al. 2001; Chen et al. 2002; Chen et al. 1998; Ohi et al. 2002). Cwc15 is involved in pre-mRNA splicing and interacts directly with the essential subunit Cef1 (Ohi et al. 2002). Three of the other five non-essential proteins, namely Isy1, Ntc20 and Syf2 have overlapping functions in modulating Syf1. Together with Syf1 they form a subcomplex (Figure 4) (Chen et al. 2002). Double deletion of *ISY1* and *NTC20* causes a severe growth defect and a strong accumulation of non-spliced mRNAs (Chen et al. 2001). The combined deletion of *ISY1*, *NTC20* and *SYF2* is lethal, however, none of the double deletion is (Chen et al. 2001; Chen et al. 2002). Deletion of *SNT309* leads to the accumulation of non-spliced mRNAs at elevated temperatures (Chen et al. 1998). Snt309 interacts exclusively with Prp19 (Figure 4), and the absence of Snt309 results in destabilization of the whole Prp19C (Chen et al. 1999). Taken together, the non-essential proteins show no severe effects if deleted separately, but combined deletions show more severe phenotypes. Therefore, some proteins may compensate the deletion of another non-essential Prp19C component.

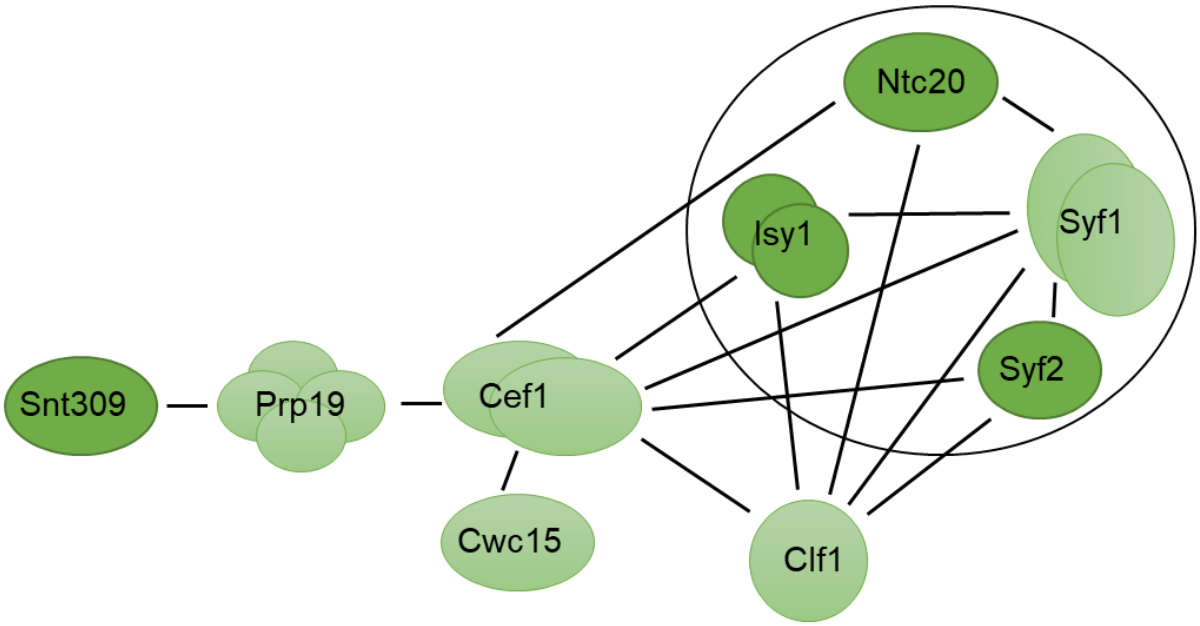

Figure 4: Schematic model showing interactions between the components of the Prp19C components. Proteins encoded by essential genes are shown in light green and non-essential genes in dark green. Lines represent the interaction between the respective other proteins. The circle indicates stable association of Syf1, Syf2, Isy1 and Ntc20 in a subcomplex (Adapted from Chen et al. 2002).

4.5 The branchpoint binding protein Msl5

In a study PAR-CLIP analysis of mRNP biogenesis factors showed that Mud2 as well as Msl5 is not only bound to intron-containing genes but also to intronless genes (Baejen et al. 2014). Since the role of Mud2 in transcription has already been demonstrated (Minocha et al. 2018), it was intriguing to investigate whether Msl5 plays a part in transcription as well.

Mud2 consists of 527 amino acids and is not essential. In *S. cerevisiae*, Mud2 has an RRM (RRM3) domain and 2 RRM-like domains which seem to be important for transcription elongation (Minocha et al. 2018), whereas the mammalian orthologue U2AF65 contains three RRM domains (RRM1, RRM2 and RRM3). The RRM domains are required for the interaction of Mud2 with the RNA (Abovich and Rosbash 1997). Msl5 directly interacts with Mud2. Together they build a stable heterodimer (Wang et al. 2008).

Msl5 (Mud2 synthetic lethal 5) is also called branchpoint binding protein (BBP) which describes its role during splicing. The mammalian orthologue is *SF1* (splicing factor 1) (Abovich and Rosbash 1997; Arning et al. 1996). Msl5 is a highly conserved protein which consists of 476 amino acids (as). Msl5 has a K-homology (KH) domain and a

QUA2 domain. Deletion of the KH domain is lethal. These domains are essential for the interaction of Msl5 with RNA (Figure 5). Furthermore, Msl5 contains Zn knuckle modules and a proline-rich region in its C-terminus (Chang, Schwer, and Shuman 2012).

Figure 5: Schematic illustration of the domain organization of Msl5. The 476 as long polypeptide Msl5. Pink shows the interaction site with Mud2, light blue the interaction site with Prp40. The KH-QUA2 domain is marked in blue, orange highlights the Zn knuckle domains and the proline-rich domain is marked in yellow (Chang, Schwer, and Shuman 2012).

In early spliceosome assembly, the U1 snRNP binds to the 5' splice site of the nascent pre-mRNA. Here, the U1 snRNP interacts with the branchpoint region through the binding of the U1 snRNP protein Prp40. Prp40 therefore interacts directly with Msl5. Msl5 binds Mud2 and Mud2 is bound to the 3' splice site (Figure 6) (Wang et al. 2008).

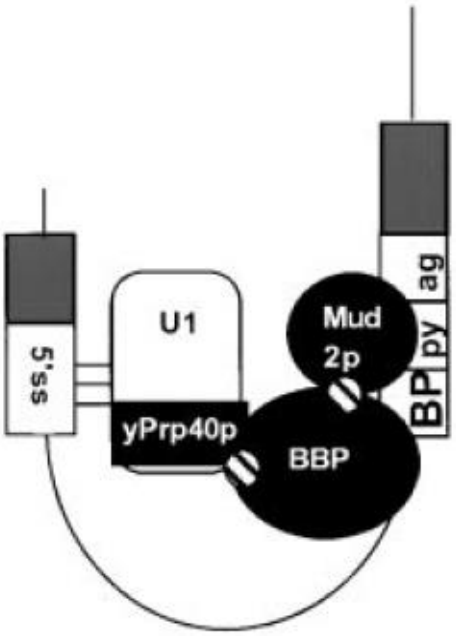

Figure 6: Schematic model of the Cross-Intron Interaction. Proteins are indicated by closed ovals and are defined in the text. The interaction between the branchpoint region (BP), the polypyrimidine region (py), and the 3' ss (splice site) region (ag) is displayed (Abovich and Rosbash 1997).

Deletion in Msl5 of amino acids 2-56 (Wang et al. 2008) or 34-56 (Chang, Schwer, and Shuman 2012) of Msl5 leads to loss of Mud2 interaction.

The commitment complex commits the pre-mRNA to the splicing pathway in an ATP-independent manner (Legrain, Seraphin, and Rosbash 1988). In *S. cerevisiae*, there are two commitment complexes; the Commitment complex 1 (CC1) only needs the 5' splice site for its assembly, whereas the formation of commitment complex 2 (CC2) depends on the presence of a branch point sequence (Séraphin and Rosbash 1991). The heterodimer Msl5-Mud2 is present in CC2, however, it is absent in the pre-spliceosomal complex and in the mature spliceosome. Therefore, the heterodimer is released form the spliceosomal machinery during the transition phase from CC2 to pre-spliceosomal complex formation. Furthermore, no splicing defects occur if the CC1 performs splicing or if Msl5 is depleted or/and *MUD2* is deleted (Rutz and Séraphin 1999; Wang et al. 2008). Msl5 and Mud2 also interact with each other in an RNA-independent manner *in vitro*. As mentioned above, this interaction is only essential during the formation of CC2 (Berglund, Abovich, and Rosbash 1998; Rutz and Séraphin 2000).

Furthermore, it has been shown that Msl5 interacts with the nuclear envelope associating protein Mlp1 (Galy et al. 2004; Bonnet and Palancade 2015) and that it plays a role in the nuclear retention of the pre-mRNA (Rutz and Séraphin 2000).

4.6 Aim of this study

Gene expression is a fundamental process and encompasses several steps. The mRNA is synthesized by RNA polymerase II (RNAPII), largely co-transcriptionally processed by 5′-end capping, splicing and polyadenylation, packaged into a messenger ribonucleoprotein particle (mRNP), exported to the cytoplasm and finally translated into a protein. A key player in mRNP biogenesis is TREX, a conserved complex coupling transcription to nuclear mRNA export. The Prp19 complex (Prp19C) is mainly known for its function in splicing. Previously, the Straesser lab uncovered a second function of Prp19C in gene expression: It functions in transcription elongation by ensuring occupancy of TREX at transcribed genes (Chanarat, Seizl, and Strässer 2011). Further Mud2 is needed for the full recruitment of Prp19C and TREX to the transcribed genes. Mud2 is recruited to the transcription machinery by the phosphorylated CTD of RNAPII (Minocha et al. 2018).

The aim of this study is to elucidate the role of the five non-essential subunits of Prp19C: Cwc15, Isy1, Ntc20, Syf2 and Snt309. First, I want to perform ChIP experiments to assess, whether the non-essential subunits are important for the occupancy of Prp19C and TREX, I want to investigate how deletion of each of these non-essential subunits influences the interaction of Prp19C with TREX, Mud2 and the RNAPII. Next, I want to know if the non-essential Prp19C subunits function in stability of the Prp19C-TREX, Prp19C-Mud2 and Prp19C-RNAPII interaction to do so I want to purify the native protein complexes. Furthermore, I wanted to investigate if any of the non-essential proteins have a role in transcription to do so I want to perform growth assays and *in vivo* transcription assays.

In addition to the investigation of Prp19C, I also want to discover a potential novel function of the essential protein Msl5. Msl5 is the branch point binding protein involved in splicing and interacts with Mud2. Mud2 is also known to be involved in splicing, but new findings revealed that Mud2 is also involved in transcription elongation (Minocha et al. 2018). In addition, PAR-CLIP analysis showed that Msl5 also crosslinks to intronless mRNAs (Baejen et al. 2014). Therefore, I want to discover the function of Msl5 in the biogenesis of intronless mRNAs. To do this, I want to perform ChIP experiments, to investigate, whether the occupancy of Prp19C, TREX, Mud2 and RNAPII changes when Msl5 is depleted. Further, I want to investigate, weather the mRNP composition changes or if nuclear mRNA export is impaired when Msl5 is depleted. To do so I want to purify

the native mRNP. In the end, I want to elucidate, what role Msl5 plays at intronless genes and how Msl5 functions in this process.

5 Materials

5.1 Chemicals and consumables

Chemicals and consumables provided by the respective supplier in this work are listed in (Table 1)*Table 1*.

Table 1: List of the used chemicals with their respective supplier.

Name of the equipment	**Supplier**
2-Propanol	Carl Roth
5-Fluoroorotic acid (5-FOA)	Apollo Scientific Ltd
6-Azuracil (6-AU)	Sigma-Aldrich
Acetic acid	VWR Chemicals
Acrylamide (29:1) 40 %	AppliChem
Adenine hemisulfate salt	Sigma-Aldrich
Agar Bacteriology grade	AppliChem
Agarose	Applichem
Ammonium persulfate (APS)	VWR Chemicals
Ampicillin	Applichem
ANTI-FLAG M2 Affinity Gel	Sigma-Aldrich
BactoTM Peptone	BD Biosciences
BactoTM Yeast extract	BD Biosciences
Bovine serum albumin (BSA)	Carl Roth
Bromophenol blue	Applichem
Calcium chloride ($CaCl_2$)	Fluka
Calmodulin Affinity resin	Agilent Technologies
Chloroform	Merck
Coomassie Brilliant Blue G-250	Applichem
Coomassie Brilliant Blue R-250	Applichem
D-Galactose	Applichem
D-Glucose Monohydrate	Sigma-Aldrich
D-Raffinose	Roth
D-Sorbitol Carl Roth	D-Sorbitol Carl Roth
Dimethyl sulfoxide (DMSO)	Grüssing
Disodium hydrogen phosphate (Na_2HPO_4)	Sigma-Aldrich
Dithiothreitol (DTT)	Sigma-Aldrich
dNTPs (dATP, dTTP, dCTP, dGTP)	Thermo Fisher Scientific
Dynabeads^{TM} M-280 Tosylactivated	Invitrogen

Dynabeads™ Protein G	Invitrogen
ECL Solution	Applichem
Ethanol	Fisher Chemical
Ethylenediaminetetraacetic acid (EDTA)	Sigma-Aldrich
Ethylene glycol-bis(aminoethyl ether) tetra acetic acid (EGTA)	Merck
FLAG Peptide	Sigma-Aldrich
Formaldehyde	ORG Laborchemie
Formamide	Merck
Gel loading dye, purple (6x)	NEB
Gel loading dye, purple (6x) w/o SDS	NEB
Geneticin (G418)	ThermoFisher (Gibco)
Glycerol	Carl Roth
Glycine	Labochem international
HDGreen™ DNA stain	Intas
HEPES	Carl Roth
Hydrochloric acid (HCl)	Carl Roth
IgG Sepharose 6 Fast Flow	GE Healthcare
Indol-3-acetid acid (IAA)	Sigma-aldrich
L-Arginine-HCl	Biomol GmbH
L-Aspartic acid	Sigma-Aldrich
Leupeptin (Hemisulfate)	Carl Roth
L-Histidine	Sigma-Aldrich
L-Isoleucine	Sigma-Aldrich
Lithium acetate ($C_2H_3LiO_2$)	Carl Roth
L-Arginine-HCl	Biomol GmbH
L-Aspartic acid	Sigma-Aldrich
Lithium chloride (LiCl)	Merck
L-Leucine	Sigma-Aldrich
L-Lysine Monohydrochloride	Sigma-Aldrich
L-Methionine	Sigma-Aldrich
L-Phenylalanine	Sigma-Aldrich
L-Threonine	Sigma-Aldrich
L-Tryptophan	Sigma-Aldrich
L-Tyrosine	Sigma-Aldrich
L-Valine	Biomol GmbH
Lithium acetate (LiOAc)	Carl Roth

Lithium chloride (LiCl)	Merck
Magnesium chloride ($MgCl_2$)	Merck
Magnesium sulfate (MgSO4)	Carl Roth
Methanol	Merck-Millipore
Octylphenoxypolyethoxyethanol (IGEPAL CA-630; NP-40)	Sigma-Aldrich
Pepstatin A	Applichem GmbH
phenyl methane sulfonyl fluoride (PMSF)	Carl Roth
Phosphoric acid	Carl Roth
Polyethylene glycol (PEG) 3800/4000	Carl Roth
Polyethylene glycol (PEG) 8000	Fluka
Polylysine	Sigma-Aldrich
Polysorbate 20 (Tween 20)	Merck
Ponceau S	Serva
Potassium acetat (CH_3CO_2K)	Applichem
Potassium chloride (KCl)	ORG Laborchemie
Potassium hydroxide (KOH)	Merck
Powdered milk, fat free, blotting grade	Carl Roth
Rothi-Mount FluorCare DAPI	Carl Roth
Salmon sperm DNA (SSD)	Applichem
Sodium acetate ($C_2H_3NaO_2$)	Merck
Sodium carbonate (Na_2CO_3)	Merck
Sodium chloride (NaCl)	Merck
Sodium citrate	Carl Roth
Powdered milk, fat free, blotting grade	Carl Roth
Rothi-Mount FluorCare DAPI	Carl Roth
Salmon sperm DNA (SSD)	Applichem
Sodium acetate ($C_2H_3NaO_2$)	Merck
Sodium carbonate (Na_2CO_3)	Merck
Sodium carbonate (Na_2CO_3)	Merck
Sodium chloride (NaCl)	Merck
Sodium citrate	Carl Roth
Sodium deoxycholate	Sigma-Aldrich
Sodium dihydrogen phosphate (NaH_2PO_4)	Sigma-Aldrich
Sodium dodecyl sulfate (SDS)	Serva
Sodium hydroxide (NaOH)	Merck
Sulfosalicylic acid	Merck
Tetramethylethylendiamin (TEMED)	Carl Roth

Trichloroacetic acid (TCA)	Merck
Tris(hydroxymethyl)aminomethane (Tris)	Applichem
Triton X-100	Applichem
Tryptone BioChemica	Applichem
Uracil	Sigma-Aldrich
Urea	Applichem
Yeast nitrogen base, w/o amino acids	Formedium
Sodium deoxycholate	Sigma-Aldrich
Sodium dihydrogen phosphate (NaH_2PO_4)	Sigma-Aldrich
Sodium dodecyl sulfate (SDS)	Serva
Sodium hydroxide (NaOH)	Merck
Sulfosalicylic acid	Merck
Tetramethylethylendiamin (TEMED)	Carl Roth
Trichloroacetic acid (TCA)	Merck
Tris(hydroxymethyl)aminomethane (Tris)	Applichem
Triton X-100	Applichem
Tryptone BioChemica	Applichem
Uracil	Sigma-Aldrich
Urea	Applichem
Yeast nitrogen base, w/o amino acids	Formedium

5.2 Equipment and devices

Equipment and devices provided by the respective supplier in this work are listed in Table 2.

Table 2: Equipment and devices.

Name of the equipment	**Supplier**
70 Ti	Beckman Coulter
Agarose gel electrophoresis system	Southern biological
AM100, micro scale	Mettler-Toledo
Apollo, liquid nitrogen container	Cryotherm
Avanti JXN-26 with JLA-8.1, JA-10	Beckman Coulter
Bioruptor UCL 200	Diagenode
ChemoCam Imager ECL HR 16-3200	Intas
CME microscope	Leica

CO8000 Cell Density Meter	WPA
Delta Vision Ultra fluorescence microscope	Cytiva
Dissection microscope MSM 400	Singer Instruments
Electrophoresis Power Supply Consort E835	Neolab
Electrophoresis Power Supply EPS 3500	Pharmacia Biotech
Eppendorf centrifuge 5424	Eppendorf
Eppendorf centrifuge 5430R	Eppendorf
Eppendorf centrifuge 5415D	Eppendorf
FastPrep-24TM 5G	MP Biomedicals
Freezer/Mill 6870D	Spex SamplePrep
Frezzer Forma 900 Series	Thermo Scientific
Gel iX20 Transilluminator/gel docu	Intas
Hera safe, laminar flow cabinet	Thermo Fisher Scientific
HeraFreeze HFU T Series	Thermo Fisher Scientific
Heidolph shaker duomax 1030	Neolab
IKA KS 4000 ic control, shaking incubator	IKA Labortechnik
IKAMAG RCT, magnetic stirrer	IKA Labortechnik
Incubators	Memmert
Innova 44 shaking incubator	New Brunswick
JLA-8.1, JA-25.50, JA-10	JLA-8.1, JA-25.50, JA-10
LED bluelight transilluminator	Nippon genetics
Megafuge 40R, 75003180R	Thermo Scientific
Milli-Q integral water purification system	Merck
Mini-Protean Tetra Electrophoresis Cell	Bio-Rad Laboratories
Multitron Pro / Labotron shaker	Infors HT
Nano Drop ND - 1000 Spectrometer	Thermo Scientific
Optima XPN-80 Ultracentrifuge	Beckman Coulter
PeqStar XS Thermocycler	Peqlab
Personal Thermocycler	Biometra
Pipetboy acu	IBS Integra Biosciences
Pipettes 20, 100, 200, 1000	Brand
Pipettes 2, 5000	Gilson
PM2000, scale	Mettler-Toledo
pH 211 Microprocessor pH meter	HANNA instruments
Pulverisette	Fritsch
Research Pipettes 2, 10, 20, 100, 200, 1000	Gilson
Rotator	neoLab

StepOnePlus Real Time PCR System	Applied Biosystems
SW22, shaking waterbath	Julabo
T3 Thermocycler	Biometra
Thermomixer compact	Eppendorf
Thermomixer 5436	Eppendorf
Trans-Blot Turbo Transfer System	Bio-Rad Laboratories
Typhoon FLA 9500	GE Healthcare
Vakulan CVC 3000	Vacuubrand
VF2, vortex mixer	IKA Labortechnik
VX-150, autoclave	Systec
WT 12, tumbling shaker	Biometra

5.3 Buffers

Buffers were prepared with water filtered by the Milli-Q-synthesis System (Millipore/Merck) and autoclaved at 120°C for 20 min. Heat-sensitive solutions and buffers were sterile-filtered (0.22 µm) (Table 3).

Table 3: List of the used buffers and their composition.

Buffer	**Composition**
AE buffer	10 mM TRIS-HCl pH 7.4, 50 mM NaOAc, 10 mM EDTA
Coomassie stain solution	0.25% (w/v) Coomassie Brilliant Blue R-250, 30% (v/v), ethanol, 10% (v/v) acetic acid
1x PBS	137 mM NaCl, 2.7 mM KCl, 20 mM NaH_2PO_4, 10 mM Na_2HPO_4 (pH 7.5)
Protease inhibitor (100x)	8 ng/ml Leupeptin, 137 ng/ml Pepstatin A, 17 ng/ml PMSF, 0.33 mg/ml Benzamidine,solved in 100% EtOH (p.a.)
20x SSC	3 M NaCl, 0.3 M sodium citrate
4x SDS sample buffer	0.2 M TRIS-HCl (pH 6.8), 40% (v/v) glycerol, 8% (w/v), SDS, some mg of bromophenol blue, 0.1 M DTT
SDS-PAGE running buffer	25 mM TRIS, 0.1% (w/v) SDS, 0.19 mM glycine
4x separating SDS gel buffer	3 M TRIS, 0.4% (w/v) SDS, pH 8.8 (HCl)
Semi-Dry-Blotting-buffer	25 mM TRIS, 192 mM glycine, 20% (w/v) methanol

4x stacking SDS-gel buffer	0.5 M TRIS, 0.4% (w/v) SDS, pH 6.8 (HCl)
1x TAE	40 mM TRIS, 2 mM EDTA, pH 8.0; 20 mM acetic acid
1x TBST	137 mM NaCl, 2.7 mM KCl, 12.5 mM TRIS-HCl 0.1% (v/v) Tween-20
1 x TBE	100 mM TRIS; 100 mM H_3BO_3; 2,5 mM EDTA
1 x TE	1 mM EDTA, 10 mM TRIS-HCl, pH 8.0
prehybridization buffer	50 % formamide, 10 % dextran sulphate, 125 µg/ml *E. coli* tRNA, 500 µg ml herring sperm DNA, 4 x SSC, 0.02
pre-treatment solution	7.5 % β-mercaptoethanol, 1.85 M NaOH
TAP buffer	100 mM NaCl, 50 mM HEPES-KOH pH 7.5, 1.5 mM MgCl2, 0.15 % NP-40
wash buffer (FISH)	1.2 M sorbitol, 0.1 M potassium phosphate dibasic pH 6.4

5.4 Media

Media was prepared with water filtered by the Milli-Q-synthesis System (Millipore/Merck) and autoclaved at 120°C for 20 min. Media recipes are listed in Table 4.

Table 4: Media and agar plates used for cultivation of all organisms.

Media	**composition**
LB medium	1 % (w/v) tryptone; 0.5 % (w/v) yeast extract;0.5 % (w/v), NaCl; (2 % (w/v) agar for plates)
Synthetic dropout complete (SDC)	0.67% (w/v) yeast nitrogen base; 0.06% (w/v) complete, synthetic mix of aa; drop out as required; 2% (w/v) glucose; (2% (w/v) agar for plates)
Synthetic complete dropout medium (SRC) with raffinose	0.67 % (w/v) yeast nitrogen base; 0.06 % (w/v) completesynthetic mix of aa; drop out as required; 2 % (w/v) raffinose; (2 % (w/v) agar for plates)
SDC-FAA	0.67 % (w/v) yeast nitrogen base; 0.06 % (w/v) complete, synthetic mix of aa; drop out as required; 2 % (w/v) glucose; 2 % (w/v) agar for plates, g 5-FAA
SDC-FOA	0.67 % (w/v) yeast nitrogen base; 0.06 % (w/v) complete, synthetic mix of aa; drop out as required; 2 % (w/v) glucose; 2 % (w/v) agar for plates, 1 g 5-FOA
SOC	2 g tryptone, 0.5 g yeast extract, 10 mM NaCl, 0.5 mM KCl, 10 mM MgCl2, 10 mM MgSO4 dissolve in up to 100 ml water and adjust pH to 7.0
Yeast full medium (YPD)	2 % (w/v) peptone; 2 % (w/v) glucose; 1 % (w/v) yeast extract; (2% (w/v) agar for plates)
Yeast full medium (YPG) (with galactose)	2 % (w/v) peptone; 2 % (w/v) galactose; 1 % (w/v) yeast, extract; (2 % (w/v) agar for plates)

5.5 Organisms

5.5.1 *S. cerevisiae* strains

S. cerevisiae strains used are listed in Table 4.

Table 4: Yeast strains

Strain	Strain Background	Genotype	Reference
wild-type	BY4741	*MATa; his3Δ1; leu2Δ0; met15Δ0; ura3Δ0*	(Strässer and Hurt 2000)
wild-type	W303	*MATa; ade2-1; his3-11, 15; ura3-1; leu2-3, 112; trp1-1; can1-100; rad5-535*	(Thomas and Rothstein 1989)
MUD2-HA	BY4741	*MATa; ura3Δ0; leu2Δ0; his3Δ1; met15Δ0; MUD2-HA::HIS3*	Rashmi Minocha
SYF1-TAP MUD2-HA	BY4741	*MATa; ura3Δ0; leu2Δ0; his3Δ1; met15Δ0; SYF1-TAP::URA, MUD2-HA::HIS*	Rashmi Minocha
SYF1-TAP MUD2-HA Δcwc15	BY4741	*MATa; ura3Δ0; leu2Δ0; his3Δ1; met15Δ0; SYF1-TAP::URA3; MUD2-HA::HIS3; Δcwc15::kanMX4*	Rashmi Minocha
SYF1-TAP MUD2-HA Δisy1	BY4741	*MATa; ura3Δ0; leu2Δ0; his3Δ1; met15Δ0; SYF1-TAP::URA3; MUD2-HA::HIS3; Δisy1::kanMX4*	Rashmi Minocha
SYF1-TAP MUD2-HA Δntc20	BY4741	*MATa; ura3Δ0; leu2Δ0; his3Δ1; met15Δ0; MUD2-HA::HIS3; SYF1-TAP::URA3; Δntc20::kanMX4*	Rashmi Minocha
SYF1-TAP MUD2-HA Δsyf2	BY4741	*MATa; ura3Δ0; leu2Δ0; his3Δ1; met15Δ0; MUD2-HA::HIS3; SYF1-TAP::URA3; Δsyf2::kanMX4*	Rashmi Minocha
SYF1-TAP MUD2-HA Δsnt309	BY4741	*MATa; ura3Δ0; leu2Δ0; his3Δ1; met15Δ0; MUD2-HA::HIS3; SYF1-TAP::URA3; Δsnt309::kanMX4;*	this study
SYF1-HA	BY4741	*MATa; ura3Δ0; leu2Δ0; his3Δ1; met15Δ0; SYF1-HA::HIS3*	Rashmi Minocha
HPR1-TAP SYF1-HA	BY4741	*MATa; ura3Δ0; leu2Δ0; his3Δ1; met15Δ0; SYF1-HA::HIS3; HPR1-TAP::URA3*	Rashmi Minocha
HPR1-TAP SYF1-HA Δcwc15	BY4741	*MATa; ura3Δ0; leu2Δ0; his3Δ1; met15Δ0; HPR1-TAP::URA3; SYF1-HA::HIS3; Δcwc15::kanMX4;*	Rashmi Minocha

HPR1-TAP SYF1-HA Δisy1	BY4741	*MATa; ura3Δ0; leu2Δ0; his3Δ1; met15Δ0; HPR1-TAP::URA3; SYF1-HA::HIS3; Δisy1::kanMX4*	Rashmi Minocha
HPR1-TAP SYF1-HA Δntc20	BY4741	*MATa; ura3Δ0; leu2Δ0; his3Δ1; met15Δ0; HPR1-TAP::HIS3; SYF1-HA::URA3; Δntc20::kanMX4;*	Rashmi Minocha
HPR1-TAP SYF1-HA Δsyf2	BY4741	*MATa; ura3Δ0; leu2Δ0; his3Δ1; met15Δ0; HPR1-TAP::URA3; SYF1-HA::HIS3; Δsyf2::kanMX4*	Rashmi Minocha
HPR1-TAP SYF1-HA Δsnt309	BY4741	*MATa; ura3Δ0; leu2Δ0; his3Δ1; met15Δ0; HPR1-TAP::URA3; SYF1-HA::HIS3; Δsnt309::kanMX4*	this study
HPR1-TAP SYF1-HA Δcwc15 Δsyf2	BY4741	*MATa; ura3Δ0; leu2Δ0; his3Δ1; met15Δ0; HPR1-TAP::URA3; SYF1-HA::HIS3; Δsyf2::kanMX4; Δcwc15::LEU2;*	this study
SYF1-TAP	BY4741	*MATa; ura3Δ0; leu2Δ0; his3Δ1; met15Δ0; SYF1-TAP::URA3;*	Chanarat, Sittinan
SYF1-TAP Δcwc15	BY4741	*MATa; ura3Δ0; leu2Δ0; his3Δ1; met15Δ0; SYF1-TAP::URA3; Δcwc15::kanMX4*	Rashmi Minocha
SYF1-TAP Δisy1	BY4741	*MATa; leu2Δ0; met15Δ0; his3Δ1; ura3Δ0, SYF1-TAP::URA3; Δisy1::kanMX4*	Rashmi Minocha
SYF1-TAP Δntc20	BY4741	*MATa; ura3Δ0; leu2Δ0; his3Δ1; met15Δ0; SYF1-TAP::URA3; Δntc20::kanMX4*	Rashmi Minocha
SYF1-TAP Δsyf2	BY4741	*MATa; ura3Δ0; leu2Δ0; his3Δ1; met15Δ0; SYF1-TAP::URA3; Δsyf2::kanMX4*	Rashmi Minocha
SYF1-TAP Δsnt309	BY4741	*MATa; leu2Δ0; met15Δ0; ura3Δ0 SYF1-TAP::URA3; Δsnt309*::kanMX4	this study
HPR1-TAP	BY4741	*MATa, his3Δ1; leu2Δ0; lys2Δ0; ura3Δ0; HPR1-TAP::URA3*	Röther, Susanne
HPR1-TAP Δcwc15	BY4741	*MATa; ura3Δ0; leu2Δ0; his3Δ1; met15Δ0; HPR1-TAP::URA3; Δcwc15::kanMX4*	Rashmi Minocha
HPR1-TAP Δisy1	BY4741	*MATa; ura3Δ0; leu2Δ0; his3Δ1; met15Δ0; HPR1-TAP::URA3; Δisy1::kanMX4*	Rashmi Minocha
HPR1-TAP Δntc20	BY4741	*MATa; ura3Δ0; leu2Δ0; his3Δ1; met15Δ0; HPR1-TAP::URA3; Δntc20::kanMX4*	Rashmi Minocha
HPR1-TAP Δsyf2	BY4741	*MATa; ura3Δ0; leu2Δ0; his3Δ1; met15Δ0; Δsyf2::kanMX4; HPR1-TAP::URA3*	Rashmi Minocha
HPR1-TAP Δsnt309	BY4741	*MATa; ura3Δ0; leu2Δ0; his3Δ1; met15Δ0; HPR1-TAP::URA3; Δsnt309::kanMX4*	Rashmi Minocha

Δdst1	W303	*MATa; ura3-1; trp1-1; his3-11,15; leu2-3,112; ade2-1; can1-100; GAL+; Δdst1::HIS3*	Karakasili, Eleni
Δcwc15	W303	*MATa; ura3-1; trp1-1; his3-11,15; leu2-3,112; ade2-1; can1-100; GAL+; Δcwc15::kanMX4*	this study
Δisy1	W303	*MATa; ura3-1; trp1-1; his3-11,15; leu2-3,112; ade2-1; can1-100; GAL+; Δisy1::kanMX4*	this study
Δntc20	W303	*MATa; ura3-1; trp1-1; his3-11,15; leu2-3,112; ade2-1; can1-100; GAL+; Δntc20::kanMX4*	this study
Δsyf2	W303	*MATa; ura3-1; trp1-1; his3-11,15; leu2-3,112; ade2-1; can1-100; GAL+; Δsyf2::kanMX4*	this study
Δsnt309	W303	*MATa; ura3-1; trp1-1; his3-11,15; leu2-3,112; ade2-1; can1-100; GAL+; Δsnt309*::kanMX4	this study
Δcwc15 Δdst1	W303	*MATa; ura3-1; trp1-1; his3-11,15; leu2-3,112; ade2-1; can1-100; GAL+; Δdst1::HIS3; Δcwc15::kanMX4*	this study
Δisy1 Δdst1	W303	*MATa; ura3-1; trp1-1; his3-11,15; leu2-3,112; ade2-1; can1-100; GAL+; Δdst1::HIS3; Δisy1::kanMX4*	this study
Δntc20 Δdst1	W303	*MATa; ura3-1; trp1-1; his3-11,15; leu2-3,112; ade2-1; can1-100; GAL+; Δdst1::HIS, Δntc20::kanMX4*	this study
Δsyf2 Δdst1	W303	*MATa; ura3-1; trp1-1; his3-11,15; leu2-3,112; ade2-1; can1-100; GAL+; Δdst1::HIS3; Δsyf2::kanMX4*	this study
Δsnt309 Δdst1	W303	*MATa; ura3-1; trp1-1; his3-11,15; leu2-3,112; ade2-1; can1-100; GAL+; Δdst1::HIS3; Δsnt309::kanMX4*	this study
Δcwc15	BY4741	*MATa; his3Δ1; leu2Δ0; met15Δ0; ura3Δ0 Δcwc15::kanMX4*	Euroscarf
Δisy1	BY4741	*MATa; his3Δ1; leu2Δ0; met15Δ0; ura3Δ0 Δisy1::kanMX4*	Euroscarf
Δntc20	BY4741	*MATa; his3Δ1; leu2Δ0; met15Δ0; ura3Δ0 Δntc20::kanMX4*	Euroscarf
Δsyf2	BY4741	*MATa; his3Δ1; leu2Δ0; met15Δ0; ura3Δ0 Δsyf2::kanMX4*	Euroscarf
Δsnt309	BY4741	*MATa; his3Δ1; leu2Δ0; met15Δ0; ura3Δ0 Δsnt309::kanMX4*	Euroscarf
TAP-HPR1 SYF1-HA	BY4741	*MATa; his3Δ1; leu2Δ0; met15Δ0; ura3Δ0; TAP-HPR1; SYF1-HA::HIS3*	this study

TAP-HPR1 SYF1-HA Δcwc15	BY4741	*MATa; ura3Δ0; leu2Δ0; his3Δ1; met15Δ0; NTAP-HPR1; SYF1-HA::HIS3; Δcwc15::kanMX4*	this study
TAP-HPR1 SYF1-HA Δsyf2	BY4741	*MATa; ura3Δ0; leu2Δ0; his3Δ1; met15Δ0; NTAP-HPR1; SYF1-HA::HIS3; Δsyf2::kanMX4*	this study
TAP-HPR1 SYF1-HA Δcwc15 Δsyf2	BY4741	*MATa; ura3Δ0; leu2Δ0; his3Δ1; met15Δ0; NTAP-HPR1; SYF1-HA::HIS3; Δsyf2::kanMX4; Δcwc15::LEU24*	this study
HPR1-TAP	W303	*MATa; ura3-1; trp1-1; his3-11,15; leu2-3,112; ade2-1; can1-100; GAL+; HPR1-TAP::TRP1*	this study
HPR1-TAP Δcwc15 Δsyf2	W303	*MATa; ura3-1; trp1-1; his3-11,15; leu2-3,112; ade2-1; can1-100; GAL+; HPR1-TAP::TRP1; Δsyf2::kanMX4; Δcwc15::LEU2*	this study
MSL5-TAP	W303	*MATa; ura3-1; trp1-1; his3-11,15; leu2-3,112; ade2-1; can1-100; GAL+; MSL5TAP::TRP1*	this study
OsTIR1	W303	*MATa; ura3-1; trp1-1; his3-11,15; leu2-3,112; ade2-1; can1-100; GAL+; osTIR1::URA*	Kristin Hühn
MSL5-AID	W303	*MATa; ura3-1; trp1-1; his3-11,15; leu2-3,112; ade2-1; can1-100; GAL+; osTIR1::URA; MSL5-AID::HYG*	this study
MSL5-AID Δmud2	W303	*MATa; ura3-1; trp1-1; his3-11,15; leu2-3,112; ade2-1; can1-100; GAL+; osTIR1::URA; MSL5-AID::HYG; Δmud2::KanMX*	this study
Δmud2	W303	*MATa; ura3-1; trp1-1; his3-11,15; leu2-3,112; ade2-1; can1-100; GAL+; Δmud2::KanMX*	this study
Δmud2	W303	*MATa; ura3-1; trp1-1; his3-11,15; leu2-3,112; ade2-1; can1-100; GAL+; Δmud2::TRP*	this study
MSL5-TAP Δmud2	W303	*MATa; ura3-1; trp1-1; his3-11,15; leu2-3,112; ade2-1; can1-100; GAL+; MSL5-TAP::TRP; Δmud2::KanMX*	this study
MUD2-TAP MSL5-AID	W303	*MATa; ura3-1; trp1-1; his3-11,15; leu2-3,112; ade2-1; can1-100; GAL+; osTIR1::URA; MSL5-AID::HYG; MUD2-TAP::TRP*	this study
RPB1 shuffle MSL5-TAP	W303	*MATa; ura3-1; trp1-1; his3-11,15; leu2-3,112; ade2-1; can1-100; GAL+; Δrpb1::HIS; MSL5-TAP::TRP*	this study
RBP3-TAP Ribozyme active	BY4741	*MATa; his3Δ1; leu2Δ0; met15Δ0; ura3Δ0; RPB3-TAP::HIS3; Ribo-YCT1::KanMX*	(Meinel et al. 2013)

RBP3-TAP Ribozyme silent	BY4741	*MATa; his3Δ1; leu2Δ0; met15Δ0; ura3Δ0; RPB3-TAP::HIS3;RiboMut-YCT1::KanMX*	(Meinel et al. 2013)
HPR1-TAP Ribozyme active	BY4741	*MATa; his3Δ1; leu2Δ0; met15Δ0; ura3Δ0; HPR1-TAP::HIS3; Ribo-YCT1::KanMX*	(Meinel et al. 2013)
HPR1-TAP Ribozyme silent	BY4741	*MATa; his3Δ1; leu2Δ0; met15Δ0; ura3Δ0; HPR1-TAP::HIS3;RiboMut-YCT1::KanMX*	(Meinel et al. 2013)
MSL5-TAP Ribozyme active	BY4741	*MATa; his3Δ1; leu2Δ0; met15Δ0; ura3Δ0; MSL5-TAP::HIS3; Ribo-YCT1::KanMX*	this study
MSL5-TAP Ribozyme silent	BY4741	*MATa; his3Δ1; leu2Δ0; met15Δ0; ura3Δ0; MSL5-TAP::HIS3;RiboMut-YCT1::KanMX*	this study
MUD2-TAP Ribozyme active	BY4741	*MATa; his3Δ1; leu2Δ0; met15Δ0; ura3Δ0; MUD2-TAP::HIS3; Ribo-YCT1::KanMX*	this study
MUD2-TAP Ribozyme silent	BY4741	*MATa; his3Δ1; leu2Δ0; met15Δ0; ura3Δ0; MUD2-TAP::HIS3;RiboMut-YCT1::KanMX*	this study
SYF1-TAP Ribozyme active	BY4741	*MATa; his3Δ1; leu2Δ0; met15Δ0; ura3Δ0; SYF1-TAP::HIS3; Ribo-YCT1::KanMX*	this study
SYF1-TAP Ribozyme silent	BY4741	*MATa; his3Δ1; leu2Δ0; met15Δ0; ura3Δ0; SYF1-TAP::HIS3;RiboMut-YCT1::KanMX*	this study
MSL5-TAP SYF1 shuffle	W303	*MATa; ura3-1; trp1-1; his3-11,15; leu2-3,112; ade2-1; can1-100; GAL+; MSL5-TAP::TRP; Δsyf1:KanMX*	this study
MSL5 Δhpr1	W303	*MATa; ura3-1; trp1-1; his3-11,15; leu2-3,112; ade2-1; can1-100; GAL+; MSL5-TAP::TRP; Δhpr1:KanMX*	this study
MSL5-AID SYF1-TAP	W303	*MATa; ura3-1; trp1-1; his3-11,15; leu2-3,112; ade2-1; can1-100; GAL+; osTIR1::URA; MSL5-AID::HYG; SYF1-TAP::TRP*	this study
MSL5-AID HPR1-TAP	W303	*MATa; ura3-1; trp1-1; his3-11,15; leu2-3,112; ade2-1; can1-100; GAL+; osTIR1::URA; MSL5-AID::HYG; HPR1-TAP::TRP*	this study
MSL5-HA	W303	*MATa; ura3-1; trp1-1; his3-11,15; leu2-3,112; ade2-1; can1-100; GAL+; MSL5-HA::HIS*	this study
MSL5 shuffle	W303	*MATa; ura3-1; trp1-1; his3-11,15; leu2-3,112; ade2-1; can1-100; GAL+; Δmsl5::KanMX*	this study
MSL5 shuffle MUD2-FTPA	W303	*MATa; ura3-1; trp1-1; his3-11,15; leu2-3,112; ade2-1; can1-100; GAL+; Δmsl5::KanMX; MUD2-FTPA::TRP*	this study

CBC20-FTPA HPR1-HA SYF1-MYC	W303	*MATa; ura3-1; trp1-1; his3-11,15; leu2-3,112; ade2-1; can1-100; GAL+; CBC20-FTPA::HIS; HPR1-HA::LEU; SYF1-MYC::TRP*	this study
CBC20-FTPA HPR1-HA SYF1-MYC MSL5-AID	W303	*MATa; ura3-1; trp1-1; his3-11,15; leu2-3,112; ade2-1; can1-100; GAL+; CBC20-FTPA::HIS; HPR1-HA::LEU; SYF1-MYC::TRP; osTIR1::URA; MSL5-AID::HYG*	this study
CBC20-FTPA MEX67-HA YRA1-MYC	W303	*MATa; ura3-1; trp1-1; his3-11,15; leu2-3,112; ade2-1; can1-100; GAL+; CBC20-FTPA::HIS; MEX67-HA::LEU; YRA1-MYC::TRP*	this study
CBC20-FTPA MEX67-HA YRA1-MYC MSL5-AID	W303	*MATa; ura3-1; trp1-1; his3-11,15; leu2-3,112; ade2-1; can1-100; GAL+; CBC20-FTPA::HIS; MEX67-HA::LEU; YRA1-MYC::TRP; osTIR1::URA; MSL5-AID::HYG*	this study
MSL5-AID Δmex67 MEX67mCHERRY	W303	*MATa; ura3-1; trp1-1; his3-11,15; leu2-3,112; ade2-1; can1-100; GAL+; osTIR1::URA; MSL5-AID::HYG; Δmex67::TRP*	this study
Δmex67 MEX67mCHERRY	W303	*MATa; ura3-1; trp1-1; his3-11,15; leu2-3,112; ade2-1; can1-100; GAL+;; Δmex67::TRP*	this study

5.5.2 *E. coli* strains

Escherichia coli (*E. coli*) strains used for in this work is listed in Table 5.

Table 5: E. coli strain list.

Strain	Genotype	Reference
DH5α	F− endA1 glnV44 thi-1 recA1 relA1 gyrA96 deoR nupG θ80dlacZΔM15Δ(lacZY AargG)U169 hsdR17K(r-Km+B) λ−	(Doherty et al. 1993)

5.6 Plasmids

Plasmids used in this work is listed in Table 6.

Table 6: List of used plasmids.

Plasmid	Description	Reference
pBS1479	for C - terminal TAP - tagging with TRP1 marker	(Puig et al. 2001)
pBS1539	for C-terminal TAP-tagging of a protein by genomic integration with the URA3 marker	(Puig et al. 2001)
pBS1776	for N-terminal TAP-tagging of a protein by genomic integration with the LEU2 marker	(Puig et al. 2001)
pFA6a-FTpA-HIS3	for C - terminal FtpA - tagging with HIS3 marker	(Kressler et al. 2012)
pHyg-AID-GFP (2354)	pHyg-AID*-GFP	(Nishimura et al. 2009)
pRS315	pBlueScript based yeast centromere vector with LEU2 marker	(Sikorski and Hieter 1989)
pRS315 MEX67-mCherry	ORF + 500 bp of 5' of *MEX67-mCherry* are cloned into pRS315	This study
pRS315 *MSL5*-HA	ORF + 500 bp of 5' and 500 bp of 3' UTR of *MSL5-HA* was cloned into pRS315	This study
pRS315 *MSL5*-HA *Δ2-56*	ORF + 500 bp of 5' and 500 bp of 3' UTR of *MSL5-HA Δ2-56* was cloned into pRS315	This study
pRS315 *MSL5*-HA *Δ34-56*	ORF + 500 bp of 5' and 500 bp of 3' UTR of *MSL5-HA Δ34-56* was cloned into pRS315	This study
pRS315-TAP	pBlueScript based yeast centromere vector with LEU marker and TAP-tag	(Röther and Strässer 2007)
pRS315-SYF1	a HincII-SpeI fragment containing *SYF1* ORF was cloned into pRS315	(Chanarat, Seizl et al. 2011)
pRS315-syf1-37	Same as pRS315-*SYF1* but with C-terminal deletion mutant *syf1-37*	(Chanarat, Seizl et al. 2011)
pRS316	pBlueScript based yeast centromere vector with URA1 marker	(Sikorski and Hieter 1989)
pRS425	high copy number plasmid, 2μ, with LEU2 maker	(Sikorski and Hieter 1989)
pRS425 *MUD2*	ORF + 500 bp of 5' and 500 bp of 3' UTR of *MUD2* was cloned into pRS425	This study
pRS425 *MUD2*-TAP	ORF + 500 bp of 5' of *MUD2-TAP* was cloned into pRS425	This study

pYM15	for C-terminal HA-tagging with the HIS3MX6 marker	Euroscarf
pYM15_LEU marker	for C-terminal HA-tagging with the LEU2 marker	This study
pY1WT(14)	plasmid coding for Rpb1 with a CTD containing 14 wild-type repeats	(West and Corden 1995)
pY1WT(9)A2(6)	plasmid coding for Rpb1 with a CTD containing 9 wild-type and 6 S2A repeats	(West and Corden 1995)
pY1WT(7)A5(7)	plasmid coding for Rpb1 with a CTD containing 7 wild-type and 7 S5A repeats	(West and Corden 1995)
pRS316-*GAL10::ACT1*	GAL10 promoter sequence in front of ACT1 ORF in pRS316	(Chanarat et al. 2012)

5.7 Oligonucleotides

In the tables 8-11 are the oligonucleotides listed which were used in this work.

Table 7: Oligonucleotides used for genomic tagging.

Name	**Number**	**Sequence (5'-3')**
Hpr1-TAP fwd	BB11	ATGCAGCTACTTCGAACATTTCTAATGGTTCATCTACCCAAGATATGAAAtccatggaaaagagaag
Hpr1-TAP rev	BB12	TAAAATCTATCTGAATTGTTTGGGACACTATGCATGAATTTCTTATCAGTtacgactcactataggg
Mud2-HA fwd	RM113	CTTATATAGATGAGGACGACTTTGACATGATGGAAGCAACCCAACTTTCCcgtacgctgcaggtcgac
Mud2-HA rev	RM114	ATGAATACTCAATTCTTTACTTAATTTCGCTCTACAAAATAGACCATTTAatcgatgaattcgagctcg
Mud2-TAP fwd	RM9	CTTATATAGATGAGGACGACTTTGACATGATGGAAGCAACCCAACTTTCCtccatggaaaagagaag
Mud2-TAP rev	RM10	ATAATGAATACTCAATTCTTTACTTAATTTCGCTCTACAAAATAGACCATtacgactcactataggg
Syf1-HA fwd	RM36	CAAAAAAGAACTTATGGTTTCGAAAATGATGCATGATTTTACATAGCTTATATCAatcgatgaattcgagctcg
Syf1-HA rev	RM37	ACCCAATCAACCTCTTCATATTCGATTAATCCAGATGAAATAGAACTAGATATTcgtacgctgcaggtcgac
Syf11-TAP fwd	RM119	CAATCAACCTCTTCATATTCGATTAATCCAGATGAAATAGAACTAGATATTtccatggaaaagagaag
Syf1-TAP rev	RM120	CAAAAAAGAACTTATGGTTTCGAAAATGATGCATGATTTTACATAGCTTATAtacgactcactataggg
Msl5-TAP fwd	LH18	CATTAACAAACCTACACCTCCGGGACTGCAAGGGCCTCCCGGATTATCCATGGAAAAGAGAAG
Msl5-TAP rev	LH19	CCTTCAACACAAATAAAAAAAAAATGCAGATATTGTATAATGGGAGTGTATTATACGACTCACTATAGGG
Msl5-AID fwd	LH24	CCTTCAACACAAATAAAAAAAAAATGCAGATATTGTATAATGGGAGTGTA TTA CTGATATCATCGATGAATTC

Msl5-AID rev	LH25	CCTTCAACACAAATAAAAAAAAATGCAGATATTGTATA ATGGGAGTGTA TTA CTGATATCATCGATGAATTC
Cbp20-FTPA fwd	PK159	AGACCAGGTTTCGATGAAGAAAGAGAAGATGATAACT ACGTACCTCAG GATCACGACGGTGACTAC
Cbp20-FTPA rev	PK160	ATATATCTGTGTGTAGAATCTTTCTCAGATATAAATTGA TTGATTCTA ATCGATGAATTCGAGCTCG
Mex67 S2	PK369	TAAACTGTATATTTTTTGTGATACTGTGCGGCTGAAAC AGGGAACAATATCATTAATCGATGAATTCGAGCTCG
Mex67 S3	PK370	AAAGGGTTTTCAGAGTAGCATGAATGGCATCCCTAGA GAAGCATTTGTGCAGTTCCGTACGCTGCAGGTCGAC
Yra1 S2	PK386	AAAATTAAATTTAATAAAACCAAATTAAATCAAACAAAA AATTGACAATTAATTAATCGATGAATTCGAGCTCG
Yra1 S3	PK387	TAAGAAAAGTCTTGAAGATCTGGACAAGGAAATGGCG GACTATTTCGAAAAGAAACGTACGCTGCAGGTCGAC
Hpr1 S2	KG1	GCTACTTCGAACATTTCTAATGGTTCATCTACCCAAGA TATGAAACGTACGCTGCAGGTCGAC
Hpr1 S3	KG2	ATGAATTTCTTATCAGTTTAAAATTTCTATTAAGAGGAT AATTTAATCGATGAATTCGAGCTCG

Table 8: Oligonucleotides for qPCR.

Name	**Sequence (5′–3′)**
YER_fwd	TGCGTACAAAAAGTGTCAAGAGATT
YER_rev	ATGCGCAAGAAGGTGCCTAT
PMA1-5'- fwd	GTTTTTCGTCGGTCCAATTCA
PMA1-5'-rev	AACCGGCAGCCAAAATAGC
PMA1-M-fwd	AAATCTTGGGTGTTATGCCATGT
PMA1-M-rev	CCAAGTGTCTAGCTTCGCTAACAG
PMA1-3'-fwd	CAGAGCTGCTGGTCCATTCTG
PMA1-3'-rev	GAAGACGGCACCAGCCAAT
DBP2-5'-fwd	CCAAAGCCAATCACCACTTTC
DBP2-5'-rev	CAGCCTTCACTTCATTCAAAACG
DBP2-M-fwd	CGTGACTGGGTTCTACAAGAGTTTAG
DBP2-M-rev	GGCCACATCAGTAGCAACCAT
DBP2-3'-fwd	CTTCACCGAACAAAACAAAGGTT
DBP2-3'-rev	TCGGGAGGAATATTTTGATTAGCT
DBP2-intron-fwd	ACGCATACATACGCTTCGTTG
DBP2-intron-rev	AATCTACCCTTGTACAAATGCCA
ACT1-5'-fwd	TGGTATGTTCTAGCGCTTGCAC
ACT1-5'-rev	ATCTCTCGAGCAATTGGGACC
ACT1-M-fwd	GTATTGTCACCAACTGGGACG

ACT1-M-rev	TCTGGGGCAACTCTCAATTCG
ACT1-3'-fwd	TCAGAGCCCCAGAAGCTTTG
ACT1-3'-rev	TTGGTCAATACCGGCAGATTC
ILV5-5'-fwd	AAGAGAACCTTTGCTTTGGC
ILV5-5'-rev	TTGGCTTAACGAAACGGGCA
ILV5-M-fwd	TGCCGCTCAATCAGAAACCT
ILV5-M-rev	GGGAGAAACCGTGGGAGAAG
ILV5-3'-fwd	TGGTACCCAATCTTCAAGAATGC
ILV5-3'-rev	ACCGTTCTTGGTAGATTCGTACA
CCW12-5'-fwd	ACTGTCGCTTCTATCGCCGC
CCW12-5'-rev	TTGGCTGACAGTAGCAGTGG
CCW12-M-fwd	CTGTCTCCCCAGCTTTGGTT
CCW12-M-rev	GGCACCAGGTGGTGTATTGA
CCW12-3'-fwd	TGAAGCTCCAAAGAACACCACC
CCW12-3'-rev	AGCAGCAGCACCAGTGTAAG
RPL9B-5'-fwd	TCCCAGAAGGTGTTACTGTCAG
RPL9B-5'-rev	TCAAAGTACCTCTTGGACCGAC
RPL9B-M-fwd	ACATTGTTGAAAAGGATGGTGC
RPL9B-M-rev	CGTTTCTGATCTTCTTGTCACC
RPL9B-3'-fwd	AGGACGAAATCGTCTTATCTGGT
RPL9B-3'-rev	CAGATTTGTTGCAAGTCAGCGG
RPL28-5'-fwd	ACTAGAAAGCACAGAGGTCACG
RPL28-5'-rev	ACCGTCTTGGTTCTTTCATTCC
RPL28-M-fwd	TGGTTGTAGAGAGCGCAATTATG
RPL28-M-rev	GGTTTTCAACTGGACATTTTATCG
RPL28-3'-fwd	TGGAAGCCAGTCTTGAACTTGG
RPL28-3'-rev	TTGGTCTCTCTTGTCTTCTGGGA
RPS14B-5'-fwd	ACGTGAAAGGGGTGATATCCTG
RPS14B-5'-rev	ACCCGATCACAGTCTCCATC
RPS14B-M-fwd	GCAGAAGTTCTGTTTACTAACAAC
RPS14B-M-rev	TGAGAGTTATCGCGAGCTTG
RPS14B-3'-fwd	AAGACCCCAGGACCAGGTG
RPS14B-3'-rev	GATACGGCCAATCCTCAAACCAG
GAL1-5'-fwd	GTGACTTCTCGGTTTTACCTTTAGCT
GAL1-5'-rev	AATGGATGGATTTTTCTCGTTCA

GAL1-M-fwd	ATCATGCTCTATACGTTGAGTTC
GAL1-M-rev	TGCGGAAATTTAAACGGAGTAGC
GAL1-3'-fwd	GGTGGTTGTACTGTTCACTTGGTT
GAL1-3'-rev	TCATTGGCAAGGGCTTCTTT
MSL5-3' fwd	TCCGGGAGGCCCTTGCAGT
MSL5-3' rev	CCCGGTATGACTACGGTACAATC
MUD2-3' fwd	CCTTGGAGGCAGCAAAACA
MUD2-3' rev	GGAAAGTTGGGTTGCTTCCATC
MEX67-3' fwd	GCGGCTAAATCCCGTACAACT
MEX67-3' rev	CTGCACAAATGCTTCTCTAGGG
YRA1-3' fwd	GCCGACAGGATCAAGGCTA
YRA1-3' rev	GTCCGCCATTTCCTTGTCCA
MTR2-3' fwd	ATTTTGGCATTTCCCTGCA
MTR2-3' rev	AGCAGAGAATCCTCGGG
SYF1-3' fwd	GGTGTTGGAATCCAACATGC
SYF1-3' rev	CGAATATGAAGAGGTTGATTGGG

Table 9: Oligonucleotide sequences used for cloning and colony PCR.

Name	Number	Sequence (5'-3')
Del. Isy1 fwd	LH001	GGAGGCATACTGAAAGTGTG
Del Isy1 rev	LH002	CCACCACTGGTTGTTTCATTG
Col. Isy1 fwd	LH003	CGCCAGCGGCAAATTTTTT
Del. Cwc15 fwd	LH004	CCTCCTCATTGTCTCCATCA
Del Cwc15 rev	LH005	GCAGCTTGGACCACGAAAA
Col. Cwc15 fwd	LH006	CCAACCTTGCCCATGCTTGTA
Del. Ntc20 fwd	LH007	GGCTGTTGTCGTGCTACTCAA
Del Ntc20 rev	LH008	GCACAGGATTCGCGAATTAG
Col. Ntc20 fwd	LH009	CCCGGAACAAAAGTCTGCAA
Del. Syf2 fwd	LH010	GACCTTTCTCAGCATTGCATG
Del Syf2 rev	LH011	GAGGCCTTGAAGCAAGAAA
Col. Syf2 fwd	LH012	GAGGTATCAGTGGTATCTTCC
Del.Snt309 fwd	LH013	GATAAATGGGGCCAGGAGT
Del Snt309 rev	LH014	CTTCTCTGCTACCGGTAACT
Col. Snt309 fwd	LH015	GCACGAAATTCCATAGGTCGT
KanMX rev	PK115	gcagcgaggagccgtaatttt
Del. Cwc15 fwd Leu	LH137	GGCTCCATAAAGAACTTGCTCAGAGGCTGGCATTTGAAAGGGCTACAAGACCttaagcaaggattttcttaacttc
Del. Cwc15 rev Leu	LH138	GCTCTTGTCAAAAAAAAAAGATATAAACGTACTATTTATGTATCGTTCCTATGTAAACTGTGGGAATACTCAG
Vector fwd pRS315 Msl5	LH64	GTGTAATGGTTTCAActagagcggccgcca
Vector rev pRS315 Msl5	LH65	CTTCAAAAACTTTTCtggatcccccgggct
Insert fwd pRS315 Msl5	LH66	agcccgggggatccaGAAAAGTTTTTGAAGAGGCGATAGT
Insert rev pRS315 Msl5	LH67	tggcggccgctctagTTGAAACCATTACACGGTTCATCTAGGAGC
Del. Msl5 fwd	LH68	CCCTAATTTGCTACAAGTGCTATTCTATCCCACAATAAAAGGAAATTGTTGGACATGGAGGCCCAGAATA

Del Msl5 rev	LH69	ATACCTTCAACACAAATAAAAAAAAATGCAGATATTGT ATAATGGGAGTGTACAGTATAGCGACCAGCATTC
Col. Msl5 fwd	LH71	GCCTTCTTGTATACAGCACAAA
Del. Syf11	LH72	TCCATATTGGACTCAACTATCCTTCAGTACCGCAAAAC TTATTGTGTCCATATATCCTctagtacactctatatttttttatgcc
Del. Syf11	LH73	TCAGTAATTGCAGAAGGCCGCACCAAAAAAGAACTTA TGGTTTCGAAAATGATGCATGATTTTACATAGCTTATA gcgcctcgttcagaatg
His rev	LH74	gtaattctgctagcctctgc
Vektor fwd pYM15_Leu	LH124	ctgagtattcccacagttgctggccgggtg
Vektor fwd pYM15_Leu	LH125	agaaaatccttgcttaactgtcgattcgatactaacgc
Insert fwd pYM15_Leu	LH126	cgggtcacccggccagcaactgtgggaatactcaggtat
Insert fwd pYM15_Leu	LH127	ttagtatcgaatcgacagttaagcaaggattttcttaacttcttcgg

Table 10: Oligonucleotides used for *in vivo* transcription assay.

Name	**Sequence (5′–3′)**
ACT1-cy5	Cy5- TGGATTGAGCTTCATCACCAACG
GAL10-cy5_96	Cy5- ATTAGCTCTACCACAGTGTGTG
SCR1-cy5	Cy5-TTTACGACGGAGGAAAGACG

5.8 Enzymes

Table 11: Enzymes.

Enzyme	Supplier
RNase A	Thermo Fisher Scientific
Phusion® High-Fidelity DNA Polymerase	NEB
DNase I	Thermo Fisher Scientific
Proteinase K	Sigma Aldrich
Tobacco etch virus (TEV)-protease	self-made
Zymolyase 100T	Carl Roth
Zymolyase 20T	Carl Roth
Taq DNA Polymerase	self-made
T5 Exconuclease	NEB
Taq DNA Ligase	NEB
Restriction Enzymes	NEB

5.9 Antibodies

Primary and secondary antibodies used for immunoblotting are shown in Table 12 and Table 13.

Table 12: List of primary antibodies.

Name	Source	Dilution	Supplier
anti-Cbp80	rabbit, polyclonal	WB: 1:20 000	Görlich lab, Göttingen, Germany
anti-HA	rat, monoclonal	WB: 1:1000	Roche, Basel, Switzerland
anti-HA	rabbit, monoclonal	WB: 1:1000	R&D Systems, Minneapolis, USA
anti-Npl3	rabbit, polyclonal	WB: 1:5000	Guthrie lab, California, San Francisco
anti-myc	rabbit, polyclonal	WB: 1:1000	upstate cell signaling solution, New York, USA
Peroxidase-anti-peroxidase(PAP)	rabbit, polyclonal	WB: 1:5000	Sigma, Taufkirchen, Germany
anti-Pgk1	mouse, monoclonal	1:10 000	Abcam
anti-Sub2	rabbit, polyclonal	WB: 1:10 000	Straesser lab
anti-GFP	Mouse. monoclonal	WB: 1:1000	Merck
8WG16	rabbit, monoclonal	IP: 1:50	BioLegend, San Diego, Kalifornia

Table 13: List of secondary antibodies.

Name	Source	Dilution	Supplier
anti-rabbit-HRPO	goat, monoclonal	1:3.000	Bio-Rad, Hercules, Kalifornia
anti-mouse-HRPO	goat, monoclonal	1:3.000	Bio-Rad, Hercules, Kalifornia

6 Methods

6.1 Standard Methods

If not mentioned otherwise standard molecular cloning techniques like restriction digestion, dephosphorylation of DNA, DNA separation using agarose gel electrophoresis, DNA ligation and transformation in *E. coli* were performed according to (Sambrook and Russell 2001). For small-scale plasmid preparation from *E. coli*, the NucleoSpin® Plasmid (NoLid)-kit or for mid-scale the NucleoSnap Plasmid Midi-kit (Macherey-Nagel) was used. Purifying and gel extraction of DNA samples were carried out by NucleoSpin® Gel and PCR Clean-up-kit (Macherey-Nagel). All plasmids cloned for this study have been confirmed by sequencing (Microsynth). For visualizing DNA or RNA on agarose gels, Intas HDGreenTM was used.

6.2 Molecular cloning methods

6.2.1 Polymerase chain reaction (PCR)

Depending on the required amplicon, Phusion High-Fidelity DNA polymerase (NEB) or Q5® High-Fidelity DNA Polymerase (NEB) (cloning and genomic integration) or self-made Taq DNA polymerase (colony PCR) were used to perform the PCR reaction. A typical PCR reaction for Q5® High-Fidelity DNA Polymerase is shown in the table below. For integration in yeast cells, a PCR reaction with a volume of 300 µl was performed.

Table 14: Standard PCR reaction

COMPONENT	25 µl REACTION	50 µl REACTION	FINAL CONCENTRATION
5X Q5 Reaction Buffer	5 µl	10 µl	1X
10 mM dNTPs	0.5 µl	1 µl	200 µM
10 µM Forward Primer	1.25 µl	2.5 µl	0.5 µM
10 µM Reverse Primer	1.25 µl	2.5 µl	0.5 µM
Template DNA	variable	variable	< 1,000 ng
Q5 High-Fidelity DNA Polymerase	0.25 µl	0.5 µl	0.02 U/µl
Nuclease-Free Water	to 25 µl	to 50 µl	

STEP	TEMP	TIME
Initial Denaturation	98°C	30 seconds
35 Cycles	98°C	5–10 seconds
	50–72°C	10–30 seconds
	72°C	20–30 seconds/kb
Final Extension	72°C	5 minutes
Hold	4–10°C	

6.2.2 Agarose Gel Electrophoresis

To analyze DNA fragments agarose gel electrophoresis was used. 1 % agarose was solved in 1x TAE to prepare an agarose gel. HD Green Plus DNA Stain (Intas) was added to the agarose prior to pouring the agarose gel. The gel was covered with 1XTAE-buffer. PCR samples and the 1 kb DNA ladder (NEB) or 1 kb plus DNA ladder (NEB) were mixed with 6x DNA Loading Dye Purple (NEB) and loaded onto the gel. A voltage of 130 V was applied for approximately 30 min to separate the DNA fragments according to their size. DNA bands were visualized by UV illumination.

6.2.3 Ethanol (EtOH) precipitation

To precipitate DNA, 2.5 volumes of 100 % EtOH and 1/10 volume 3 M NaOAc (pH 5.5) were added to the sample and mixed. After incubation for 20 min at -20°C, the sample was centrifuged at 4°C at 20.000 g for 20 min. Afterwards the sample was washed with 80 % EtOH, the pellet was dried and dissolved in 10 µl autoclaved water.

6.2.4 Plasmid Minipreparation from *E. coli*

To isolate plasmids from *E. coli*, a single colony was picked and transferred to 3 ml LB media containing the respective antibiotics. The culture was incubated on the shaker at 37°C overnight. The cells were harvested by centrifugation. The plasmids were isolated using NucleoSpin Plasmid (NoLid)-kit (Macherey- Nagel) according to the manufacturer's instructions.

6.2.5 Digestion and ligation

For a digestion the appropriate restriction enzymes (NEB) and the corresponding restriction buffer were used. 0.5 µl of each restriction enzyme and 2 µl of corresponding restriction buffer to a digestion volume of 20 µl. The digestion was incubated at the appropriate temperature for 1 h. The digestion was stopped by incubation for 10 min at 80°C. An agarose gel electrophorese was performed to verify the success of the restriction digestion. If the digestion was successful, another agarose gel electrophorese of the whole digestion was made. The resulting bands of the PCR products were excised under UV light. The DNA was purified using the PCR NucleoSpin Gel and PCR Clean-up-kit (Macherey-Nagel) according to the manufacturer's instruction. Restricted plasmids and inserts were ligated in a volume ratio of 1:3 using T4 DNA ligase (NEB) at RT for 1 h or at 16°C overnight. 1-3 µl of the reaction was used for a *E. coli* transformation.

6.2.6 Gibson Assembly

Gibson assembly was used for cloning without restriction sites adapted from Gibson (Gibson et al. 2009). The linear vector backbone and the inserts were generated by PCR. The oligonucleotides were designed to yield PCR fragments with an overlapping region of about 20-25 bp to each other. PCR reaction were DpnI digested after PCR reaction, to remove the vector plasmids, before Gibson assembly. For a typical assembly reaction, 50 ng of vector and a 1:3 ratio of insert to vector was mixed with 15 µl of Gibson assembly master mix and filled up to 20 µl. The mixture was incubated for 60 min at 50°C. For transformation in *E. coli*, 2-5 µl of the mixture was used.

6.3 Transformation of *E. coli*

Competent cells were made as described in the Mix & Go *E. coli* Transformation Kit (Zymo Research Corp.) protocol and stored at -80°C until needed. For each transformation 50 µl competent cells were thawed on ice. 2-5 µl of a Gibson assembly mix (6.2.6) or 1 µl of a plasmid-miniprep (6.2.4) were added to the cells and mixed. The reaction mix were incubated for 30 min on ice. Afterwards the cells were heat shocked at 42°C for 1 min. Immediately after the heat shock, the cells were placed on ice for 1 min. For recovery 400 µl SOC medium was added and incubated for 60 min at 37°C on a shaker at 200 rpm. Afterwards the cells were pelleted at 10.000 g for 20 sec and

pellet was resuspended in 150 µl water. The cell suspension was spread on a selective LB plate and incubated overnight at 37°C.

6.3.1 Colony PCR of *E. coli*

To screen for successful plasmid cloning, single freshly grown colonies were picked and streaked on an LB plate, the rest of the cells were suspended in 20 µl PCR reaction mix. Afterwards the obtained PCR fragments were analyzed on a 1 % agarose gel in TAE. For three positive clones a 3 ml LB culture with appropriate antibiotic was inoculated with freshly grown cells, which were restreaked prior to resuspension in the PCR mix.

6.4 Culture of *S. cerevisiae*

Yeast strains were cultivated in either full media (YPD) or synthetic complete (SC) medium, lacking one specific amino acid or nucleotide on a solid agar plate or in a liquid culture. Unless otherwise specified in a protocol, yeast cultures were cultivated at 30°C and liquid cultures were shaken at 250 rpm. Cell density of the yeast culture was determined with a spectrophotometer at a wavelength of 600 nm. One OD at 600 nm corresponds to app. 2.5X107 cells.

6.4.1 Transformation of *S. cerevisiae*

For transformation of linearized DNA or plasmid in *S. cerevisiae,* an overnight pre-culture was diluted in 50 ml appropriate medium to OD_{600} 0.2. When reaching mid-log phase (OD_{600} 0.6-0.8) after shaking at 200 rpm at 30°C, the culture was harvested at 2.800 g for 3 min and washed once with 10 ml sterile water. The cells were washed once in 500 ml solutionI, transferred to a 2 ml tube and resuspended in 250 µl of solutionI. For each transformation 50 µl of cell suspension were mixed with 5 µl single-stranded carrier DNA (2 mg/ml), 300µl solutionII and 500 ng plasmid DNA or with an EtOH-precipitated 300 µl PCR reaction. As a negative control a mixture without DNA was performed. The mixture was incubated for 30 min on a rotating wheel at RT, the transformation mixture was heat shocked for 10 min at 42°C. To remove the PEG solution, the cells were washed with 1 ml of sterile water. For genomic integration the cells were recovered in

1 ml of YPD for 2-4 h, while shaking at 30°C. After the recovery the cells were pelleted and resuspended in 150 µl water to spread out on selective media. When transforming plasmids, the cells were directly spread out on selective media plates, without recovery. Plates were incubated for 2-4 days at 30°C.

6.4.2 Colony PCR of *S. cerevisiae*

To screen for positive genomic integration of protein tags or genomic deletions, a small amount, of freshly grown yeast colony was picked and suspended in 15 µl zymolyase 20T solution (2.5 mg/mL) to digest the cell wall. The mixture was incubated for 20 min at RT, shifted to 37°C for 5 min and afterwards boiled for 5 min at 95°C. The cell suspension was diluted by adding 50 µl water. Afterwards a PCR reaction with 2 µl of cell suspension were used as template. The performed PCR were visualized and analyzed on a 1 % agarose gel in TAE.

6.4.3 Genomic DNA isolation of *S. cerevisiae*

To isolate genomic DNA of *S. cerevisiae* 10 ml of an OD_{600} (3 min, 3600 rpm). The pellet was washed with 10 ml water. After this wash step, the cells were resuspended in 500 µl of water, 200 µl of TSNTE-buffer (2 % TritonX-100,2 % SDS, 100 mM NaCl, 10 mM TRIS-HCl, pH 8.0, 1 mM EDTA, pH 8.0), 300 µl glass beads and 300 µl phenol:chloroform:isoamylalcohol (25:24:1) were added. The mixture was vortexed for 5 min and a centrifugation for 5 min at 13.000 rpm. After centrifugation the upper phase was transferred to a new reaction tube. An equal volume of chloroform was added, vortexed and centrifuged for 5 min at 13.000 rpm. The upper phase was transferred to a new reaction tube. Genomic DNA was precipitated and resuspended in 100 µl water (6.2.3).

6.4.4 Dot spots of *S. cerevisiae*

Freshly grown yeast cells were picked with a 1 µl loop and suspended in 2 ml of water. To ensure that all spotted strains have the same number of cells the OD_{600} was measured and diluted to 0.10. A 10-fold serial dilution was made four times for each strain. 5 µl of each strain and dilution were spotted on respective media plate, air dried

and incubated at 16°C, 25°C, 30°C and 37°C for up to 2-7 days regarding the desired growth temperature.

6.4.5 6-Azauracil (6-AU) sensitivity assay

In order to test for sensitivity to the drug 6-azauracil (6-AU), the cells of *S. cerevisiae* were transformed with the plasmid pRS316 (containing a *URA3* marker), otherwise uracil in the medium would interfere with the uptake of the drug. SDC-ura agar plates were either supplemented with DMSO (as a control) or 50 µg/ml-150 µg/ml of 6-AU (dissolved in DMSO) were prepared. To test for drug sensitivity, dot spot assays (6.4.4) were performed on the plates. The cells were incubated at 30°C for 2-3 days.

6.4.6 Glycerol stocks

For long term storage of yeast cells, glycerol stocks were prepared. The yeast cells were freshly grown on agar plates for 2 days, scrapped off from plate and resuspended in 1 ml of 50 % sterile glycerol. The cell suspension was flash frozen in liquid nitrogen and stored at -80°C.

6.5 SDS Polyacrylamide Gel Electroporation (SDS-PAGE)

Sodium dodecyl sulfate polyacrylamide gel electrophoresis (SDS-PAGE) was done according to (Laemmli 1970). The gels were cast according to (Sambrook and Russell 2001), using a Mini-Protean II system (Biorad). After electrophoretic separation the proteins were stained with a modified Fairbanks-Coomassie staining method (Fairbanks, Steck, and Wallach 1971; Wong et al. 2000). For staining, the gel was fully covered with Coomassie solution, heated up in a microwave and incubated for 20 min on a shaker. To clear the background, the Coomassie solution was discarded, destain solution was added, heated up and incubated on a shaker. This was repeated until the background was completely destained.

6.6 Western Blotting

To investigate a specific protein, Western Blot is used as detection method. After SDS-PAGE was performed (6.5) the proteins were transferred onto nitrocellulose membrane (Porablot, Macherey & Nagel) using a semi-dry blotting system (Biorad) for 45 min at 25 V based on (Towbin, Staehelin, and Gordon 1979; Sambrook and Russell 2001). The transfer of proteins was verified by Ponceau S staining. After the transfer, the membrane was blocked for 1 h with blocking solution (5 % milk-powder solved in 1x TBST). The primary antibody dissolved in blocking solution was added and incubated overnight at 4°C. Excess of the first antibody was removed by washing the membrane 3 times for 10 min with TBST at room temperature on a shaker. The secondary antibody coupled to the horseradish peroxidase was applied and incubated for 1.5 h. To remove the secondary antibody washing with 1x TBST for 3 times each 10 min, was performed. The visualization of the immunodetected proteins was performed using the CheLuminate-HRP PicoDetect ECL kit (Applichem). Pictures of the blot were taken with the ChemoCam Imager (Intas).

6.7 Quantitative Western Blots

To quantify total protein levels cells were grown to mid-log phase, and 5 OD_{600} units were harvested. The cell pellet was resuspended in 500 µl of water, 150 µl of pre-treatment solution (7.5 % (v/v) β-Mercaptoethanol, 1.85 M NaOH) was added, and the mixture was incubated for 20 min on ice. TCA was added to a final concentration of 10 %, incubated for 20 min on ice and centrifuged for 20 min at 15.000 rpm at 4°C. The supernatant was discarded and the pellet resuspended in 90 µl of 1x SDS-loading buffer, and 10 µl 1 M Tis-base were added. 6 µl of whole cell extract were separated by SDS-PAGE. The signal was imaged using a ChemoCam Imager (Intas) and quantified using ImageJ. Each quantification is based on at least three biologically independent replicates

6.8 RNA isolation

For RNA isolation it is important to prevent contamination with RNAse, therefore all buffers were prepared with DEPC-treated water and all surfaces were cleaned with ethanol. For total RNA isolation cells were grown to an OD_{600} of 0.6-0.8 in the desired media depending on the experiment. The pellet was resuspended in 500 µl AE buffer

(50 mM NaAc; 10 mM EDTA; 10 mM Tris-HCl, pH 7,4). 55 µl 10 % SDS and 500 µl phenol/chloroform/isoamyl ethanol (25:24:1) (PCI). The suspension was incubated for 20 min at 65°CC, 1000 rpm. To sperate the phases the suspension was centrifugated at 14000 rpm for 15 min. The upper phase was taken, mixed with an equal volume of PCI and vortexed. After centrifugation (14000 rpm; 5 min), the upper phase was taken. To eliminate the phenol the suspension was mixed with 400 µl chloroform, vortexed and centrifugated at 14000 rpm for 5 min. The upper phase was taken and an Ethanol precipitation was performed (6.2.3).

To eliminate the DNA a DNA digest was conducted. The pellet after the ethanol precipitation were solved in 39 µl DEPC water, 5 µl 10x DNAse buffer (Thermo Fisher), 5 U DNAseI (Thermo Fisher) and 1 µl RNase Inhibitor (Thermo Fisher) and incubated 1h at 37°C. To stop the DNAse digestion the suspension was deactivated for 10 min at 65°C.The concentration of the RNA was measured with the Nanodrop and was stored at -80°C until further use.

6.9 Reverse transcription

Depending on the experiment different amounts of RNA as a template were used. For *in vivo* experiments 1-10 µg of RNA per reaction were used, for experiments subsequent Q-PCR 100 ng per reaction were used. The reverse transcription M-MulV (NEB) was used, according to the manufacturer's instruction. The cDNA was precipitated and solved in water the amount of water varied between the experiments (*in vivo*: 10 µl; qPCR: 50 µl). The cDNA was stored at -20°C until further use.

6.10 *In vivo* transcription assay

The *in vivo* transcription assays were performed as described in (Minocha et al. 2018). Cells were transformed with a plasmid p*GAL10-ACT1* which has a *URA3* marker containing the *ACT1* gene under a *GAL10* promotor. Cells were grown in SDC-Ura media containing raffinose as a carbon source (2 % w/v). The *GAL10* promotor was induced at OD_{600} 0.8 by addition of 2 % (w/v) galactose for 0, 5, 10, 20 and 30 minutes. At every timepoint 25 ml of culture were harvested. RNA was isolated as described in 6.8. The amount of *GAL10* and *ACT1* mRNA and *SCR1* was measured by primer extension using 5'-Cy5-labeld oligonucleotides specific for *GAL10, ACT1* and *SCR1*, respectively. 5µg, 10 µg and 5 µg of total RNA were used for *ACT1*, *GAL10* and SCR1 reverse transcription

reactions. The cDNA was separated on a 7 M urea 7 % polyacrylamide gel, visualized by using a Typhoon9400 scanner and quantified using ImageJ.

6.11 Tandem Affinity Purification (TAP)

The purification of TAP-tagged proteins was performed as described previously in (Puig et al. 2001). Briefly, 2 l of cell culture were harvested at an OD_{600} of 3.5. The pellets were resuspended in 3 ml of TAP buffer (50 mM Tris-Hcl at pH 7.5, 100 mM NaCl, 1.5 mM MgCl2, 0.15 % NP40, 1 mM DTT, 1.3 µg/mL pepstatin A, 0.28 µg/mL leupeptin, 170 µg/mL PMSF, 330 µg/mL benzamidine) and lysed with a cryomill (Freeer/Mill 6870, Spex Sample Prep). For thawing the lysate 10 ml of TAP buffer was added to the cell powder, centrifuged for 12 min at 4.000 rpm. The supernatant was transferred to a new tube and centrifuged for 1 h at 164.700 g, 4°C. The supernatant was incubated for 1.5 h with IgG-coupled sepharose beads. After the incubation the tube was centrifuged for 3 min, 1.800 rpm at 4°C. The supernatant was discarded and the beads were washed with 10-20 ml lysis buffer. After washing the proteins were eluted for 1 h at 16°C at with TEV protease. The TEV eluates were incubated for 1 h with calmodulin beads and washed with 10 ml of lysis buffer containing 2 mM $CaCl_2$. After elution the copurifying proteins were analyzed by SDS-PAGE and Coomassie staining or Western blotting using antibodies against HA (Roche) and the CTD of Rpb1 (8WG16, Biolegend).

6.12 Fluorescence in situ hybridization (FISH) with oligo d(T)

To visualize poly(A)$^+$ RNA the *in-situ* hybridization assay was performed. The cells were grown in YPD till an OD_{600} of 0.6-0.8. For heat shock FISH the cells were shifted to 37°C with prewarmed median and transferred to a water bath for 1 h. After reaching the desired OD_{600} 10 ml were harvested and crosslinked with 1.25 ml of formaldehyde to a final concentration of 4 % for 1.5 h at RT on a turning wheel. Heat shocked samples were fixed at 37°C for 15 min before transferring to RT. The cells were washed in 100 mM KPO4 (pH 6.4) after fixation, and spheroplasted with 100T zymolyase dissolved in 100 mM KPO4 (pH 6.4) and 1.2 M Sorbitol for 30 min. Spheroplasted cells were washed in sorbitol wash buffer, resuspended in sorbitol wash buffer, and 200 µl were pipetted onto a poly-lysine-coated slide. After 5 min the cell suspension were removed from the cover

slip and then the cover slip was paced in a 6-well chamber. To remove not adhered cell the cover slip was washed once with sorbitol wash buffer. After this the cells were prehybridized at 37°C in prehybridization buffer (50 % formamide, 10 % dextran sulphate, 125 µg/mL of *E. coli* tRNA, 500 µg/mL H.S. DNA, 4x SSC, 0.02 % polyvinyl pyrrolidone, 0.02 % BSA, 0.02 % Ficoll-40) for 1 hour in the 6-well plate. To hybridize with oligo d(T)50-Cy3 0.75 µl of 1 pmol/µl probe was added and incubated at 37°C O/N in the 6-well plate. The slides were washed in 0.05 % SSC at RT for 30 min, allowed to dry for 2-3 h. To mount the cells on the slide 2 µl of ROTI®Mount FluorCare DAPI were placed in the middle of the cover slip and two cover slips were placed on one slide. To visualize the DNA and poly(A)$^+$ RNA the DeltaVision Ultra microscope were used and images were analyzed with ImageJ.

6.13 Live cell imaging

For live imaging of living cells, the pre- and main culture were inoculated in SDC + all media with an 2x excess adenine. The cells were grown to an OD_{600} of 0.5-0.8. After the cells reached their desired OD_{600} 2 ml of the culture were harvested by centrifuging the suspension for 3 min at 3600 rpm. The supernatant was discarded and fresh SDC + all media with an 2x excess adenine were added. 2-5 µl was placed on a coverslip and was directly microscoped after.

6.14 Chromatin Immunoprecipitation (ChIP)

ChIP experiments were performed as described in (Reuter, Meinel, and Sträßer 2015) with some modifications. An overnight culture was used to inoculate the 100 ml yeast main culture, this culture grown to an OD_{600} of 0.8 and crosslinked with 1 % formaldehyde. To stop the crosslinking reaction 12,5 ml of glycine (3 M) were added and incubated for 10 min. The cells were harvested at 3.600 rpm for 3 min and washed twice with 1x PBS. The washed pellets were flash frozen in liquid nitrogen and stored at -80°C till use. Cells were resuspended in 800 µl of low salt buffer and lysed with an equal volume of glass beads. To lyse the cells the FastPrp24G device was used twice for 45 sec (6.5 m/s setting). The lysed cells were sonicated 3 times for 15 min in a Bioruptor (alternating 30 seconds at high energy setting on and 30 seconds off). To clear the lysate the samples were centrifuged once for 5 min and once for 10 min at 13.000 rpm. The

DNA concentration of the samples was measured at the NanoDrop and each sample was adjusted to the lowest measured sample. After adjusting the samples, 10 µl of each lysate were kept at 4°C as an input control sample. TAP-tagged proteins were immunoprecipitated with IgG-coupled Dynabeads (tosylactivated M280, Thermo Scientific) for 2.5 h at RT. For ChIPs of RNAPII 4 µl of the monoclonal antibody 8WG16 (Biolegend) was added for 1.5 h at RT followed by 1 h incubation with Protein G Dynabeads. To wash the magnetic beads 800 µl of wash buffer was used (2x low-salt buffer, 2x high-salt buffer, 2x TLEND, 1x TE). In between the washing steps the sample were on a turning wheel for 2 min. To elute the samples of the beads 130 µl of elution buffer was added and placed on a thermoshaker for 25 min (65°C, 1.000 rpm) The eluates and input samples were treated with proteinase K overnight for 2 h at 37°C and 14 h at 65°C. PCR NucleoSpin® Gel and PCR Clean-up-kit (Macherey-Nagel) was used according to manufacturers' manual and the DNA eluted in 140 µl elution buffer. For quantitative PCR a non-transcribed region (NTR1, 174131-174200 on chr. V) served as negative control. The occupancy of each protein was calculated as its enrichment at the respective gene relative to NTR1 ($[E\text{^}(C_T IP\text{-}C_T Input)]_{NTR}/[E\text{^}(C_T IP\text{-}C_T Input)]_{gene}$).

6.15 Determination of protein stability

The determination of protein stability were performed as described in (Buchanan et al. 2016). The cells were diluted with an overnight culture to an OD_{600} of 0.2 in YPD media. The cultures were cultivated till an OD_{600} of 0.6-0.8. 2.5 OD_{600} units were harvested (3600 rpm, 3 min) and resuspended in 1 ml per timepoint of fresh prewarmed (30°C) YPD media. To equilibrate the cells, they were incubated in the water bath for 5 min. Before adding to a final concentration of 125 µg/ml cycloheximide timepoint 0 were taken. For every timepoint (0, 10, 30, 60, 90 min) 950 µl of cells were taken and 50 µl of 20x stop-mix (20 mM sodium azide, 5 mg/ml bovine serum albumin) were added. The samples were centrifuged for 30 s for 6500 g. Afterwards the pellets were washed with 100 µl of ice-cold H_2O and resuspended in 100 µl of 0.2 M NaOH. The suspension was incubated for 5 min at RT. Following this the samples were centrifuged for 30 s at 18000 g and solved in 100 µl of SDS sample buffer. For fully denatured proteins the sampled were incubated for 5 min at 95°C. To determine the respective protein levels a SDS -PAGE and a subsequent Western Blot were applied as described in 6.5 and 6.6. The signal of the Western Blots was quantified using ImageJ.

6.16 Statistical analysis

If not noted otherwise all data are presented as average ± standard deviation (error bars) of at least three biologically independent experiments. Asterisks indicate the statistical significance (Student's t-test; * = p-value ≤ 0.05; ** = p-value ≤ 0.01; *** = p-value ≤ 0.001).

7 Results

7.1 The role of the non-essential proteins of the Prp19C in the interaction of Prp19C-TREX, Prp19C-Mud2 and Prp19C-RNAPII

Prp19C is conserved from yeast to human and is mostly known for its function in splicing. However, Prp19C is involved in many additional processes including genome stability (Idrissou and Maréchal 2022), lipid droplet formation (Cho et al. 2007) and transcription elongation (Chanarat et al. 2012). The purpose of this study was to identify the role of the non-essential Prp19C components in transcription elongation, since Syf1 is already known to be involved in transcription elongation.

7.1.1 Deletion of the non-essential proteins of the Prp19C does not influence the protein levels of Syf1, Mud2 or Rbp1

Mud2 and Rpb1 are known interaction partners of Prp19C. Therefore, it was interesting to investigate, whether the deletion of any of the non-essential Prp19C components changes the protein levels of Syf1, Mud2 or Rbp1, which are part of the complex or known interaction partners of Prp19C.

To do so, Syf1 and Mud2 were TAP-tagged while for RNAPII an antibody directed against Rpb1 (8WG16) was used. Whole cell extracts were analyzed by Western blot. Syf1 levels do not change if any of the non-essential proteins of its own complex are deleted (Figure 7A). The protein levels of Mud2 are also not influenced by the deletion of any of the non-essential proteins (Figure 7B). When *NTC20* is deleted the levels of Rpb1 are significantly reduced to 80 %, whereas deletion of *CWC15*, *ISY1*, *SYF2* or *SNT309* has no influence on Rpb1 levels (Figure 7).

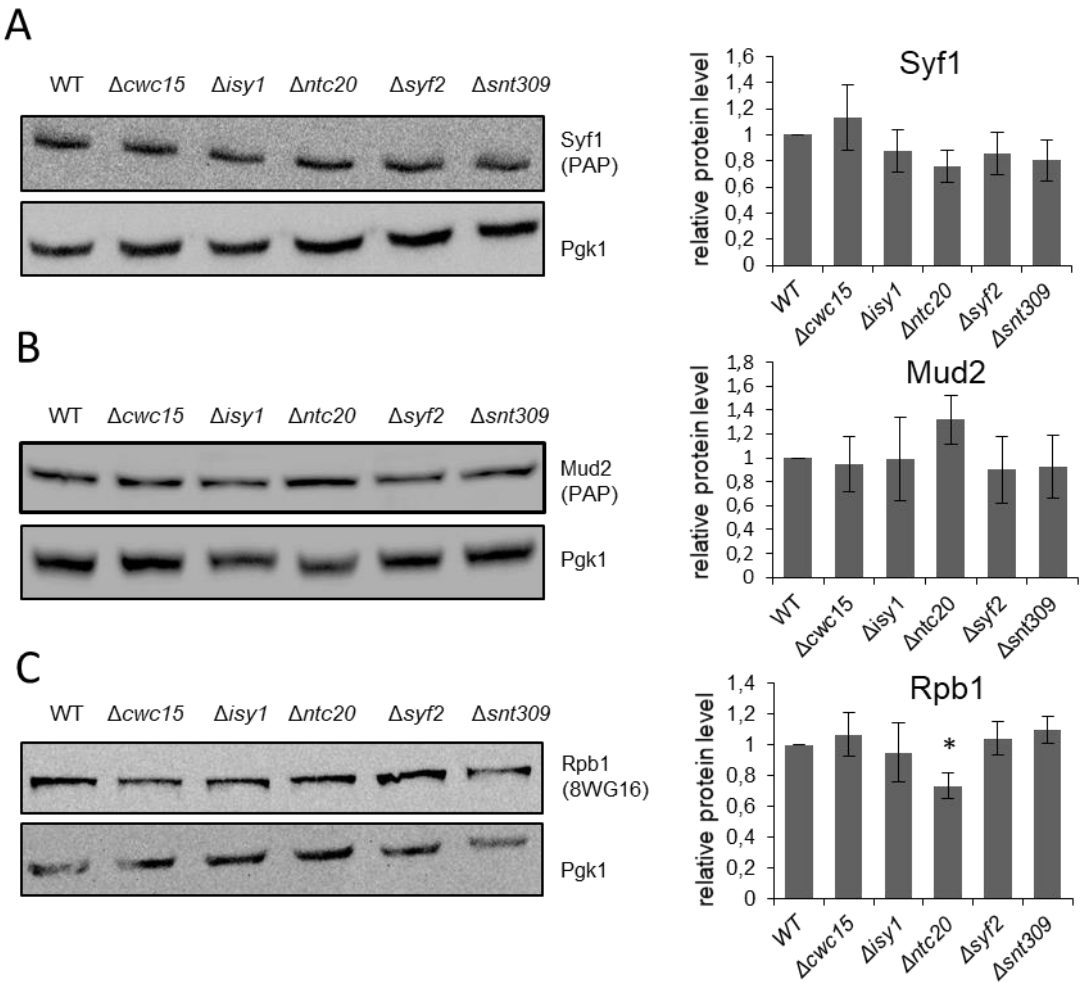

Figure 7: Total levels of Syf1, Mud2 and Rpb1 do not change in deletion mutants of genes encoding the non-essential Prp19C components Cwc15, Isy1, Ntc20, Syf2 and Snt309. (**A**) Western blot analyses (left panel) and quantification of three independent experiments (right panel) of total Syf1 levels in whole cell lysates of deletion mutants of non-essential Prp19C components. The amount of Syf1-TAP was quantified with an antibody directed against protein A (PAP) and normalized to the amount of Pgk1. Values for wild-type cells were set to 1. (**B**) Western blot analyses (left panel) and quantification (right panel) as in (A) except that total levels of Mud2-TAP were determined. (**C**) Western blot analyses (left panel) and quantification (right panel) as in (A) except that total levels of Rpb1 were determined (antibody 8WG16). Total Rpb1 levels slightly decrease in the *Δntc20* mutant.

7.1.2 The non-essential Prp19C subunit Snt309 is crucial for the interaction of Prp19C with Mud2

During transcription elongation Prp19C is recruited to nascent mRNA by Rpb1, the largest subunit of RNAPII, and Mud2. The C-terminus of Syf1 is required for the interaction of the Prp19C with RNAPII, and Mud2 interacts directly with Clf1 (Chanarat,

Seizl, and Strässer 2011; Vincent et al. 2003). The goal was to determine if deleting any of the non-essential proteins leads to a change of interaction between Prp19C-Mud2 and Prp19C-RNAPII. To do so, Prp19C was purified from strains expressing Syf1-TAP in a deletion background of each of the non-essential Prp19C subunits and assessed the co-purification of HA-tagged Mud2 by Western blotting (Figure 8). A strain expressing only Mud2-HA served as a negative control.

The upper panel in Figure 8A shows the purified Syf1-CBP in wild-type and in the five deletion mutants. Western blot analysis showed that deletion of *ISY1* leads to an increased interaction between Prp19C and Mud2 (Figure 8B). In contrast, deletion of *SNT309* causes a significantly reduced interaction between Prp19C and Mud2 (Figure 8B). Therefore, Snt309 appears to be important for the interaction between Prp19C and Mud2.

The interaction between Prp19C and RNAPII is reduced in cells in which *CWC15* and *SNT309* were deleted, suggesting that Cwc15 and Snt309 are important for the interaction between the Prp19C and RNPII in a direct or indirect manner.

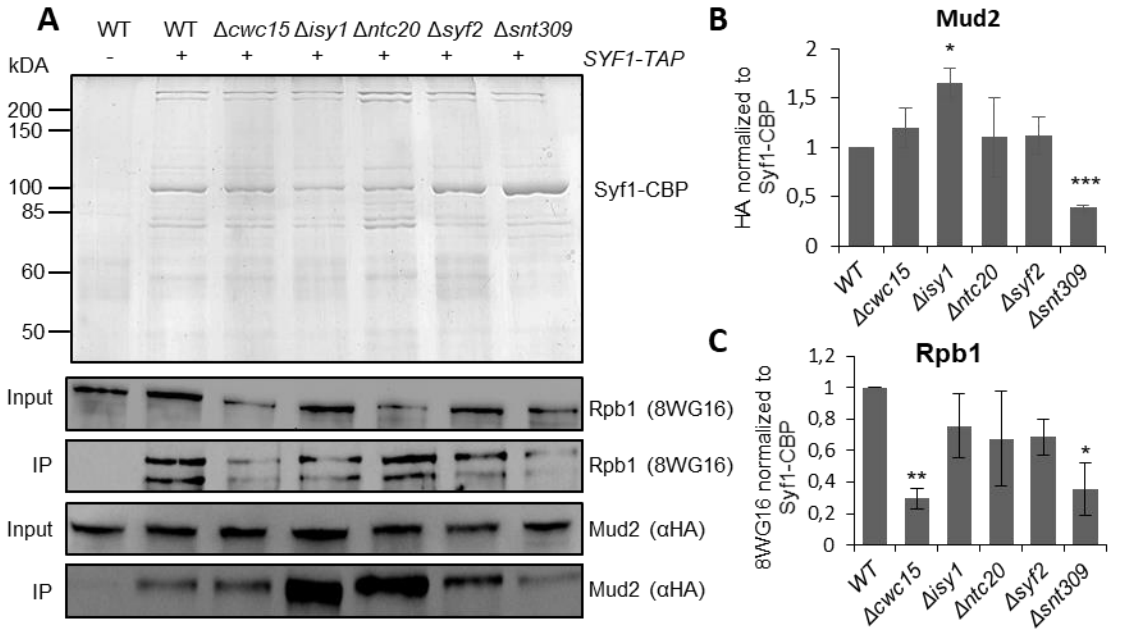

Figure 8: Snt309 is necessary for the interaction between Prp19C-Mud2, Snt309 and Cwc15 are important for the interaction of Prp19C with RNAPII. (**A**) Coomassie-stained SDS-PAGE gel containing the Prp19C eluates via TAP-tagged Syf1 for wild-type (WT) and the five deletion strains (upper panel). The levels of co-purifying HA-tagged Mud2 or RNAPII was assessed by Western blotting with αHA antibodies (αHA) or the antibody 8WG16, respectively. A strain expressing Mud2-HA served as negative control. (**B and C**) Quantification of Western blots of three independent experiments using αHA (B) and 8WG16 (C) as described in (A).

7.1.3 Cwc15, Syf2 and Snt309 play an important role for the interaction of Prp19C with TREX

In a previous publication it has been shown that Prp19C interacts with the TREX complex *in vivo* (Chanarat, Seizl, and Strässer 2011). So far it is not known how these two complexes interact with each other and which proteins are involved in this interaction. To gain insight into the potential involvement of the non-essential proteins in the interaction between Prp19C and the TREX complex, each protein was individually deleted. The TREX complex was subsequently purified, and any alterations in the co-purification of Prp19C were observed (Figure 9A and B).

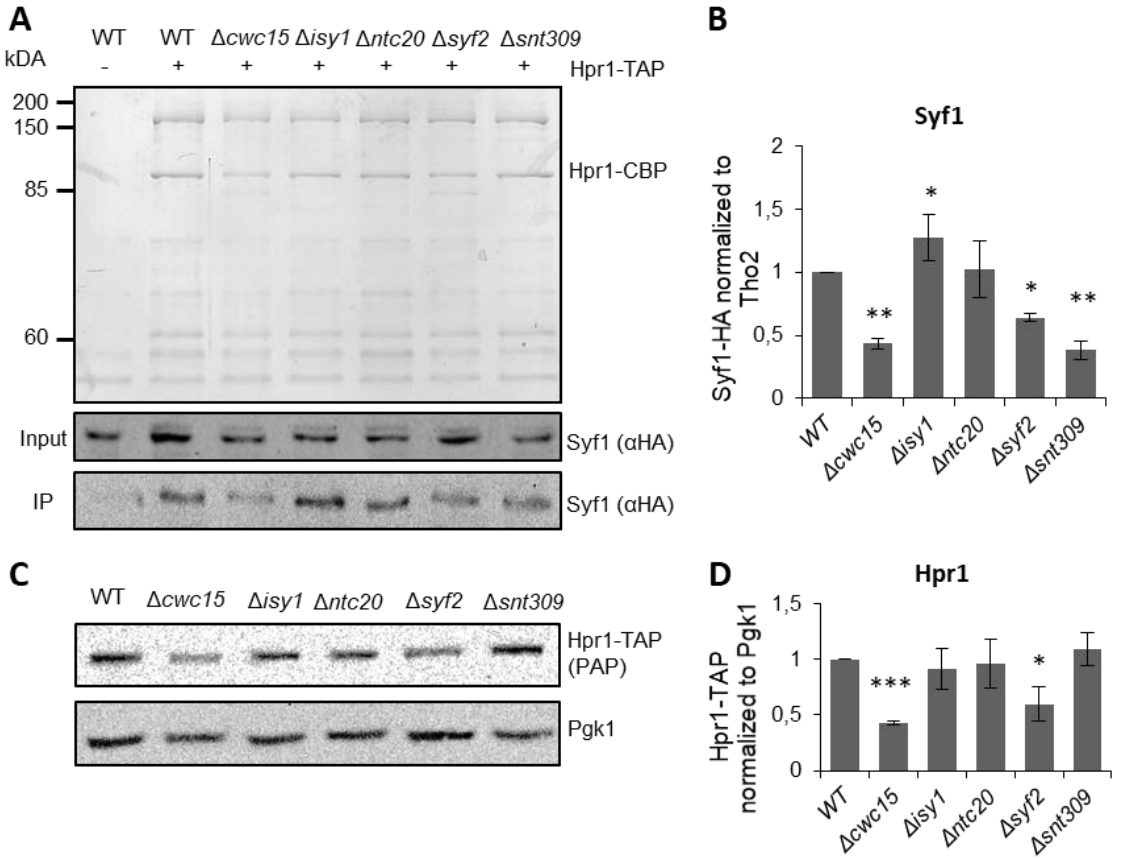

Figure 9: Cwc15, Syf2 and Snt309 are important for the interaction between TREX and Prp19C. (**A**) Coomassie-stained SDS-PAGE gel of TAP eluates from cells expressing Hpr1-TAP and HA-tagged Syf1 in wild-type (WT), Δ*cwc15*, Δ*isy1*, Δ*ntc20,* Δ*syf2* and Δ*snt309* (upper panel). Western blots of input and eluate (IP) using an antibody detecting Syf1-HA (lower panel). A strain expressing only Syf1-HA served as a negative control. (**B**) Quantification of Western blot analysis of three independent purifications as shown in (A). (**C and D**) Deletion of *CWC15* or *SYF2* causes a decrease in total Hpr1 levels. (**C**) Determination of the total level of Hpr1 in the five non-essential deletion mutants of Prp19C components compared to wild-type cells by Western blot analysis. (**D**) Quantification of three independent experiments using an antibody against the TAP-tag (PAP).

In cells where *CWC15* or *SYF2* is deleted a faster migrating band appears below Hpr1-CBP (Figure 9A). In a previous study, it has been confirmed by mass spectrometry that the faster migrating band derived from Hpr1 (Minocha, 2018). In cells where *CWC15*, *SYF2* and *SNT309* are deleted reduced levels of Syf1 co-purify with TREX are detected (Figure 9B), demonstrating that the interaction of Prp19C and TREX is reduced in these mutants. In cells where *ISY1* or *NTC20* is deleted there is no reduced interaction between TREX and Prp19C. Next, the total Hpr1-TAP levels in whole cell lysates was determined. In these, lower total levels of Hpr1 in the absence of either Cwc15 or Syf2 was detected (Figure 9C and D). The deletion of the other non-essential proteins of Prp19C show no differences compared to wild-type. This shows that Cwc15 and Syf2 appear to be important for the interaction of Prp19C and TREX, but in addition, deletion of either protein also leads to the appearance of a protein isoform of Hpr1 with faster migration behavior in SDS-PAGE. Taken together, it could be shown that both proteins, Cwc15 and Syf2, are important for the interaction of Prp19C and TREX.

7.1.4 The double deletion of *CWC15* and *SYF2* leads to an additional faster migrating band

A specific faster migrating band for Hpr1-CBP was observed after purification from cells where either *CWC15* or *SYF2* are deleted (Figure 9A). At the same time, levels of Hpr1-TAP were reduced in whole cell lysates. To investigate this result in more detail, a double deletion strain where both *CWC15* and *SYF2* are deleted was generated.

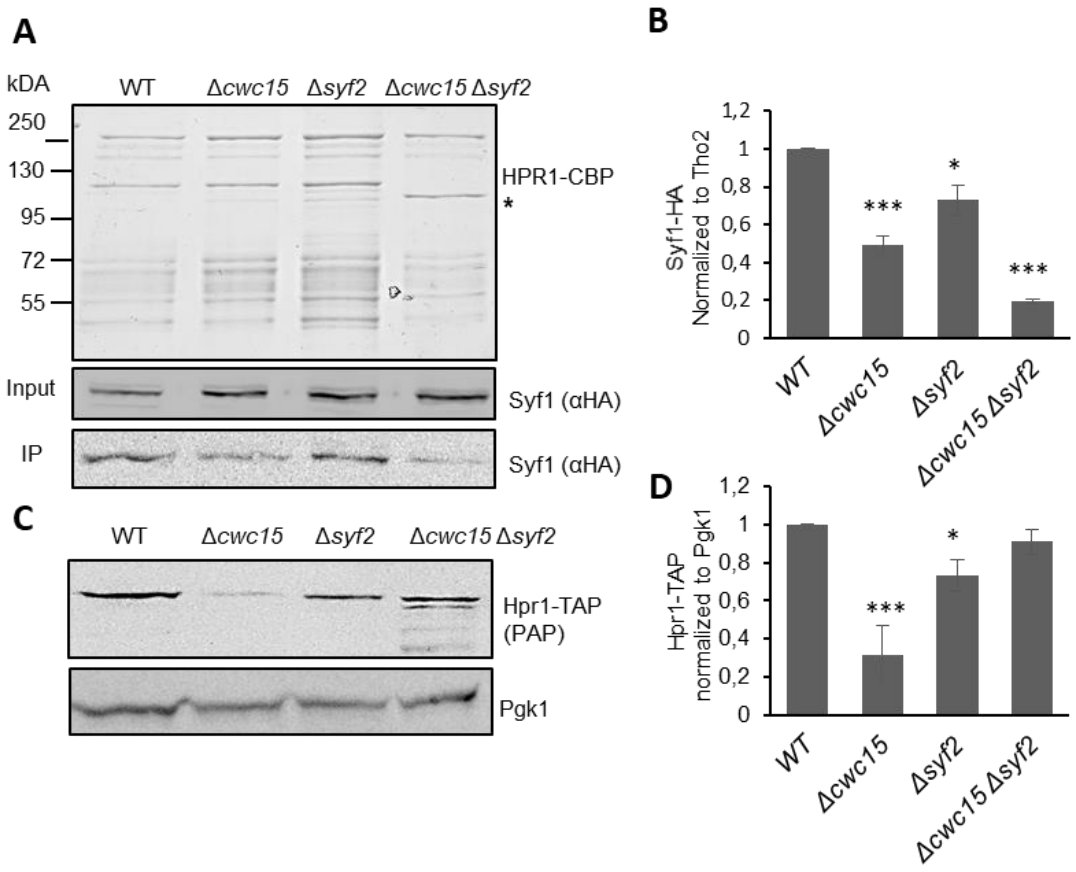

Figure 10: Double deletion of *CWC15* and *SYF2* causes a faster migrating band. (**A**) Upper panel: Purified TREX complex using Hpr1-TAP-tagged and HA-tagged Syf1 in wild-type, Δ*cwc15,* Δ*syf2* and Δ*cwc15* Δ*syf2* mutants. The faster migrating Hpr1-CBP is labelled with an asterisk (*). (**B**) Quantification of three independent purifications as described in (A). (**C**) Western blots to determine the total levels of the TREX subunit Hpr1 in Δ*cwc15,* Δ*syf2* and Δ*cwc15* Δ*syf2* cells compared to wild-type (WT) cells. Deletion of *CWC15* and *SYF2* causes a decrease in total Hpr1 levels, whereas the double deletion does not lead to a reduction. (**D**) Quantification of three independent experiments using an antibody directed against the TAP-tag (PAP).

Hpr1 was tagged at its C-terminus in Δ*cwc15,* Δ*syf2* and Δ*cwc15* Δ*syf2* cells and a TAP purification was performed to see whether the faster migrating band is still visible (Figure 10A). In cells with the double deletion of Δ*cwc15* Δ*syf2* the full-length Hpr1-CBP band was not detectable; in these only the faster migrating product could be visualized. Next, the interaction between TREX and Prp19C in the double deletion mutant was examined. For the double deletion mutant, even an additive effect was observed, the interaction between TREX and Prp19C decreased to only 30 % when compared to the wild-type (Figure 10B). In contrast, the whole cell lysates show an unexpected result for cells where both *CWC15* and *SYF2* are deleted. Here levels of Hpr1-TAP are not reduced but

compared to the wild-type degradation pattern for Hpr1-TAP was observed (Figure 10C and D).

Next, the origin of the faster migrating band was examined. In order to do so, Hpr1 was TAP-tagged at its N-terminus and a purification with cells of the wild-type, Δ*cwc15,* Δ*syf2* and Δ*cwc15* Δ*syf2* cells was performed. From the purification it was analyzed whether the disturbed interaction of TREX and Prp19C and/or the faster migrating version of Hpr1 is still visible.

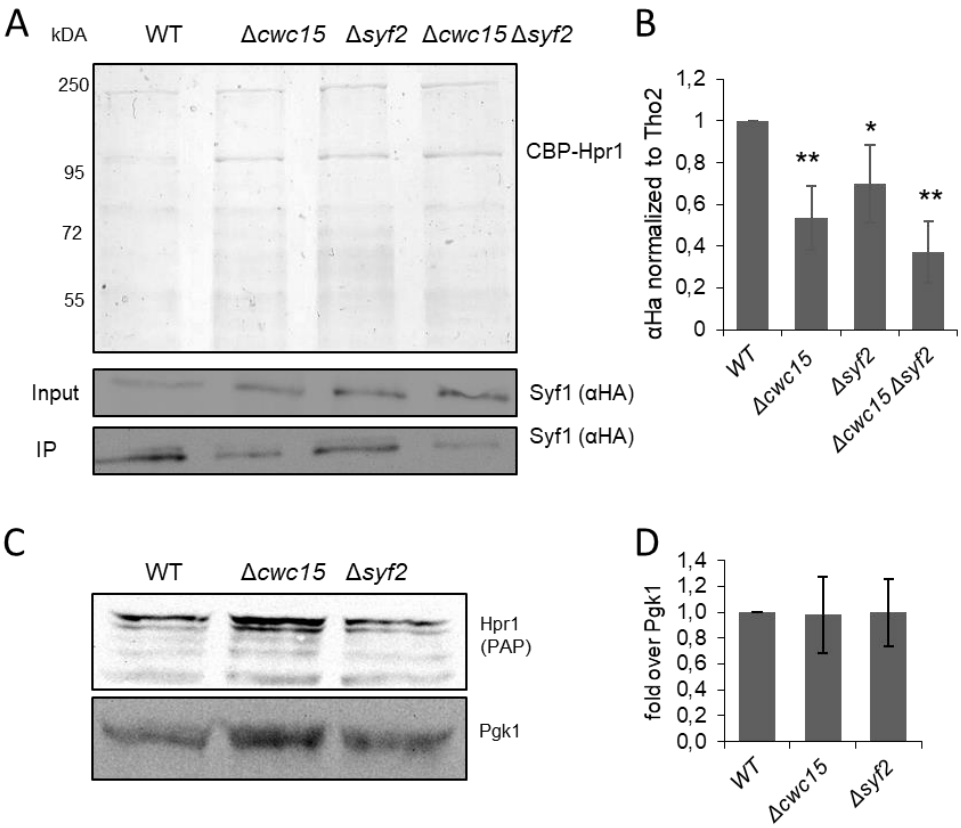

Figure 11: The interaction of TREX with Prp19C is reduced when Cwc15, Syf2 or both proteins are absent. (**A**) Coomassie-stained SDS-gel gel of eluates of purified, N-terminally TAP tagged Hpr1 from wild-type, *Δcwc15, Δsyf2* and *Δcwc15 Δsyf2* cells (upper panel). Syf1-HA levels of lysates and eluates were assessed by Western blotting using antibody against the HA-tag (lower panel). (**B**) Quantification of Syf1 co-purified with TREX of three independent experiments as shown in (A). (**C**) Western blots of whole cell lysate to determine the total levels of the N-terminal TAP-tagged Hpr1 in wild-type (WT), *Δcwc15* and *Δsyf2* cells using an antibody directed against protein A (PAP). Pgk1 levels served as loading control. (**D**) Quantification of Hpr1 levels normalized to Pgk1 of three independent experiments.

In the purification of the TREX complex, the faster migrating version of Hpr1 is no longer visible. However, the interaction of the Prp19C and TREX is still highly reduced (Figure 11A and B). In whole cell lysates of TAP-Hpr1-expressing Δ*cwc15* and Δ*syf2* cells, total levels of Hpr1 are not reduced (Figure 11C and D).

To find out whether the faster migrating band corresponds to a truncated version of Hpr1, Hpr1-CBP bands were cut from SDS-PAGE gels and analyzed by mass spectrometry to determine whether any part of Hpr1 is missing (Appendix Figure 2). In the double deletion strain as well as in the wild-type, the band corresponded to full-length Hpr1. Since it is known that Hpr1 can be ubiquitinylated (Babour, Dargemont, and Stutz 2012; Gwizdek et al. 2005), the difference in size could also be due to different modification of Hpr1 and in this case less ubiquitination.

In the lysate of wild-type and Δ*cwc15* Δ*syf2* cells, no difference in the ubiquitination pattern was visible using an antibody against ubiquitin (Figure 12A). However, the eluates of wild-type compared to Δ*cwc15* Δ*syf2* cells in Western blots, Hpr1 was less ubiquitinylated (Figure 12B). It has been reported that Hpr1 is ubiquitinylated at its C-terminus by the protein Rsp5 (Gwizdek et al. 2005). If Rsp5 is deleted Hpr1 is no longer ubiquitinylated, leading to increased protein stability at 37°C. Usually Hpr1 is rapidly degraded when cells are shifted to 37°C. In cells were Cwc15 and Syf2 are deleted, Hpr1 is more stable than in wild-type cells (Figure 12C). This is again evidence that in the double deletion mutant the ubiquitination of Hpr1 might be reduced.

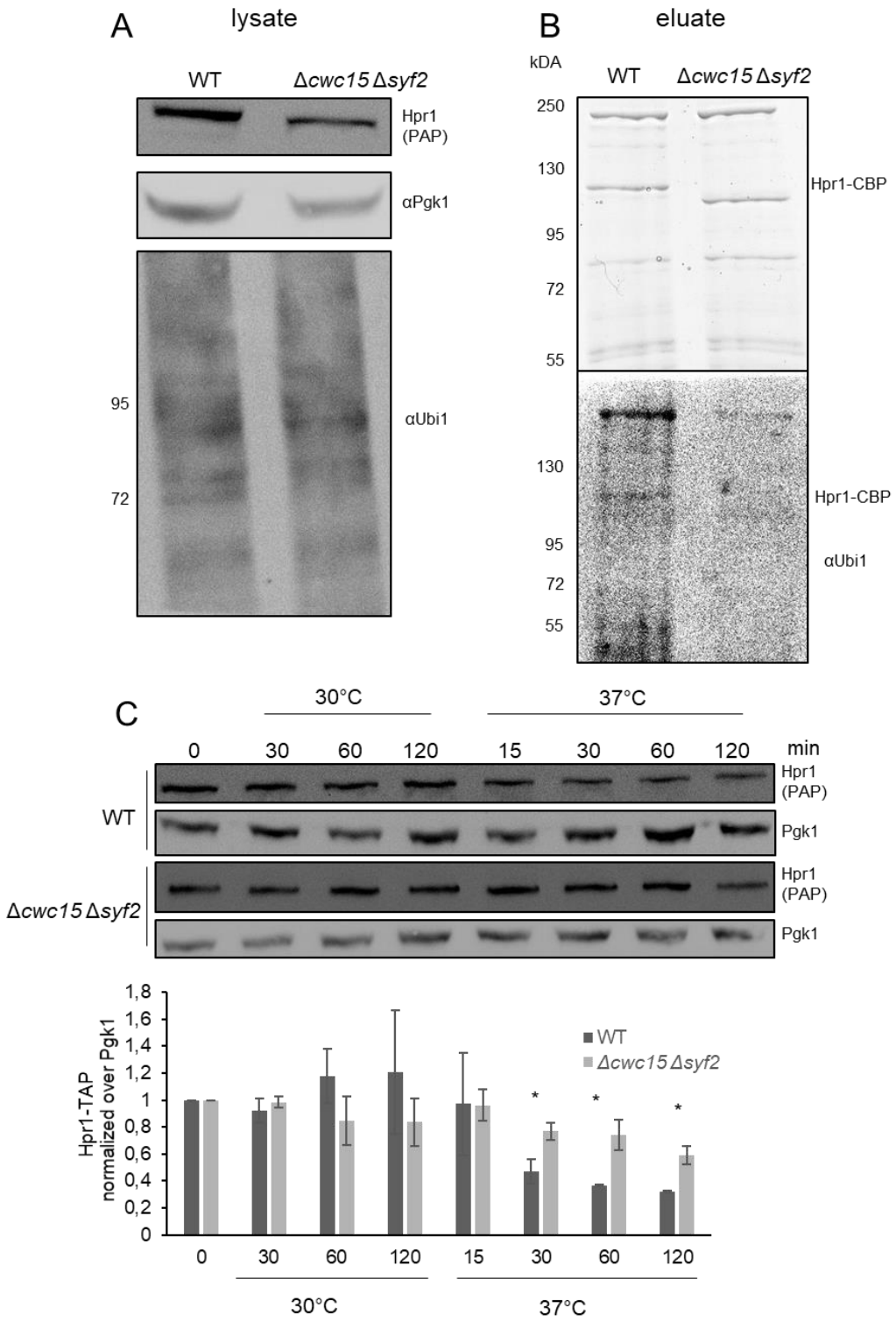

Figure 12: Double deletion of *CWC15* and *SYF2* causes de-ubiquitylation of Hpr1. (**A**) Western blot of lysates of cells C-terminally TAP-tagged from wild-type and *Δcwc15 Δsyf2* cells using antibodies against the TAP-tag (PAP), Pgk1 (αPgk1) and Ubiquitin (αUbi1). (**B**) Coomassie-stained SDS-PAGE gel of eluates of TAP purifications of C-terminally TAP-tagged Hpr1 from wild-type (WT) and *Δcwc15 Δsyf2* cells. Western blots of the eluates using an antibody against ubiquitin (αUbi1) (**C**) Hpr1 is more stable in the *Δcwc15 Δsyf2* double deletion mutant than in wild-type cells at 37°C. Cells were grown in YPD at 30°C and shifted to 37°C at an OD_{600} of 0.6 for the indicated time points. Quantification of three independent experiments using an antibody directed against protein A (PAP).

7.1.5 The double deletion of *CWC15* and *SYF2* does not cause an export defect

Since deletion of *CWC15* and/or *SYF2* has an effect on Hpr1 and Hpr1 is important for efficient mRNA export, it was interesting to investigate if deletion of *CWC15* and/or *SYF2* would affect mRNA export. To analyze nuclear mRNA export, poly(A)-RNA was visualized by fluorescence *in situ* hybridization (FISH) using an oligo(dT50) probe coupled to Cy3.

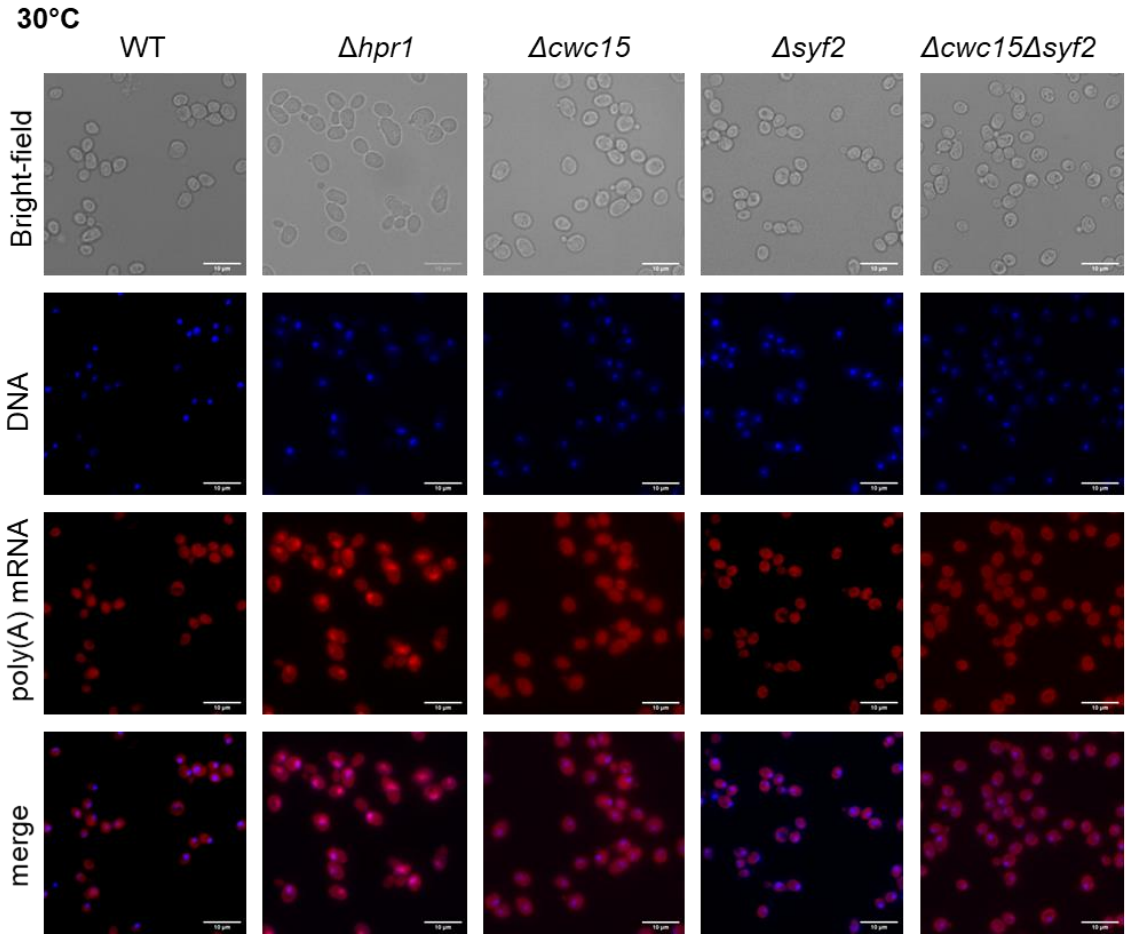

Figure 13: *Δcwc15, Δsyf2* and *Δcwc15 Δsyf2* cells do not show an mRNA export defect at 30°C. The poly(A)-tail of bulk mRNA was visualized by oligo(dT50) coupled to a Cy3-fluorecent dye. DNA was stained with DAPI to locate the nucleus. Cells were grown at 30°C. While *Δhpr1* cells show an export defect, *Δcwc15, Δsyf2* and *Δcwc15 Δsyf2* cells and wild-type cells show no export defect. The scale bar represents 10 µm.

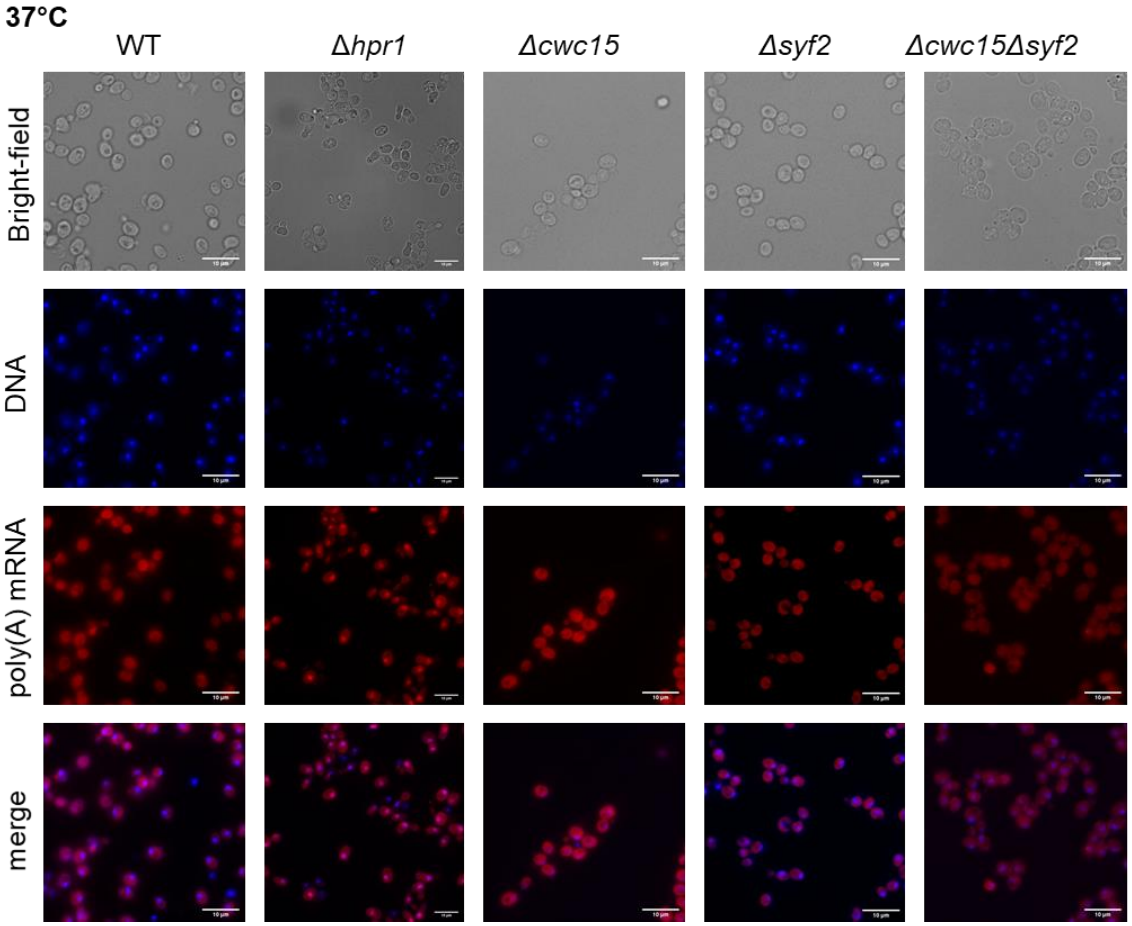

Figure 14: *Δcwc15, Δsyf2* and *Δcwc15 Δsyf2* cells do not show an mRNA export defect at 37°C. The poly(A)-tail of bulk mRNA was visualized by oligo(dT50) coupled to Cy3-fluorecent dye. DNA was stained with DAPI to locate the nucleus. Cells were grown at 30°C and shifted to 37°C 1 h before crosslinking the cells. While the *Δhpr1* cells show an export defect *the Δcwc15, Δsyf2* and *Δcwc15 Δsyf2* cells show no export defect. The scale bar represents 10 µm.

Deletion of *HPR1* leads to an export defect at 30°C (Figure 13) and an even stronger export defect at 37°C (Figure 14). The deletion of *CWC15* or *SYF2* does not lead to an mRNA export defect. The double deletion of *CWC15* and *SYF2* does not lead to a nuclear mRNA export defect, too (Figure 13 and Figure 14). This result suggests, that although the ubiquitinoylation of Hpr1 is no longer efficient, Hpr1 is still sufficient for effective mRNA export.

7.1.6 Non-essential Prp19C components function in the occupancy of Prp19C and TREX at transcribed genes

In *S. cerevisiae*, the TREX complex is recruited to transcribed genes and couples TRanscription to mRNA EXport (Katahira and Yoneda 2009). Furthermore, Prp19C also functions in transcription elongation by ensuring TREX occupancy at transcribed genes (Chanarat et al. 2012). The non-essential components of Prp19C are well studied in splicing (van Maldegem et al. 2015; Hogg, McGrail, and O'Keefe 2010; Chan and Cheng 2005). To elucidate if the non-essential components also affect the TREX occupancy chromatin immunoprecipitation (ChIP) experiments were performed at four highly expressed intronless (*PMA1*, *ILV5*, *CCW12* and *RPL9B*) and four highly expressed intron-containing (*DBP2*, *ACT1*, *RPS14B* and *RPL28*) genes (Figure 15).

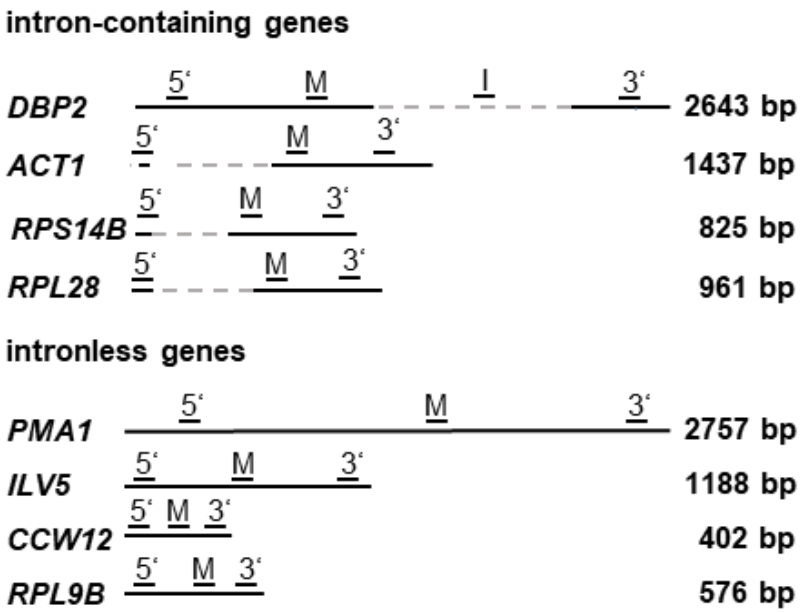

Figure 15: Figure 10. Schematic representation of four intron-containing and four intronless genes used for ChIP analysis. Solid black line represents an open reading frame (ORF) and the hatched grey line represents an intron. The bars above the solid line represent the position of primer pairs used for ChIP analysis. 5': 5' end of the gene, M: middle of the gene, 3': 3' end of the gene and I: within the intronic region.

First, RNAPII occupancy was determined to examine if RNAPII occupancy levels are changed. Subsequently, the Hpr1-TAP and Syf1-TAP ChIP signals were normalized to the RNAPII ChIP signal. The normalization over RNAPII is needed to exclude any false results which might be due to a change in transcription by RNAPII.

Surprisingly, in cells where *ISY1* or *SYF2* are deleted RNAPII occupancy was increased at all investigated genes. In *Δcwc15* (except at two positions) and *Δntc20* cells, RNAPII occupancy does not change. Deletion of *SNT309* leads to a reduced occupancy of RNAPII, the occupancy drops at all genes to around 50% of wild-type levels (Figure 16A).

To investigate if the occupancy of the Prp19C changes when any of the non-essential proteins are missing a Syf1-TAP ChIP was performed, Syf1 was used as representative protein of Prp19C. In all cells where one of the five non-essential proteins of the Prp19C is missing, the occupancy of Prp19C was decreased at intron-containing genes. This is not surprising since the main task of Prp19C is splicing. For intronless genes, Prp19C occupancy decreases specifically for *Δisy1* and *Δsyf2* at all gene positions. In *Δntc20* and *Δsnt309* cells, Prp19C occupancy is reduced at some genes but not at all genes. Only in cells in which *CWC15* has been deleted Prp19C occupancy is not changed compared to the wild-type (Figure 16B).

Next, the occupancy of TREX in the deletion mutants at transcribed genes was investigated. The occupancy of Hpr1 and thus most likely of the whole TREX complex at intronless and intron-containing genes is reduced in cells where *CWC15* and *ISY1* is deleted (Figure 16C).

Taken together, Isy1, Syf2 and Snt309 are needed for the fully occupancy of Prp19C at transcribed genes. Whereas for the fully occupancy of TREX at transcribed genes Cwc15 and Isy1 are needed.

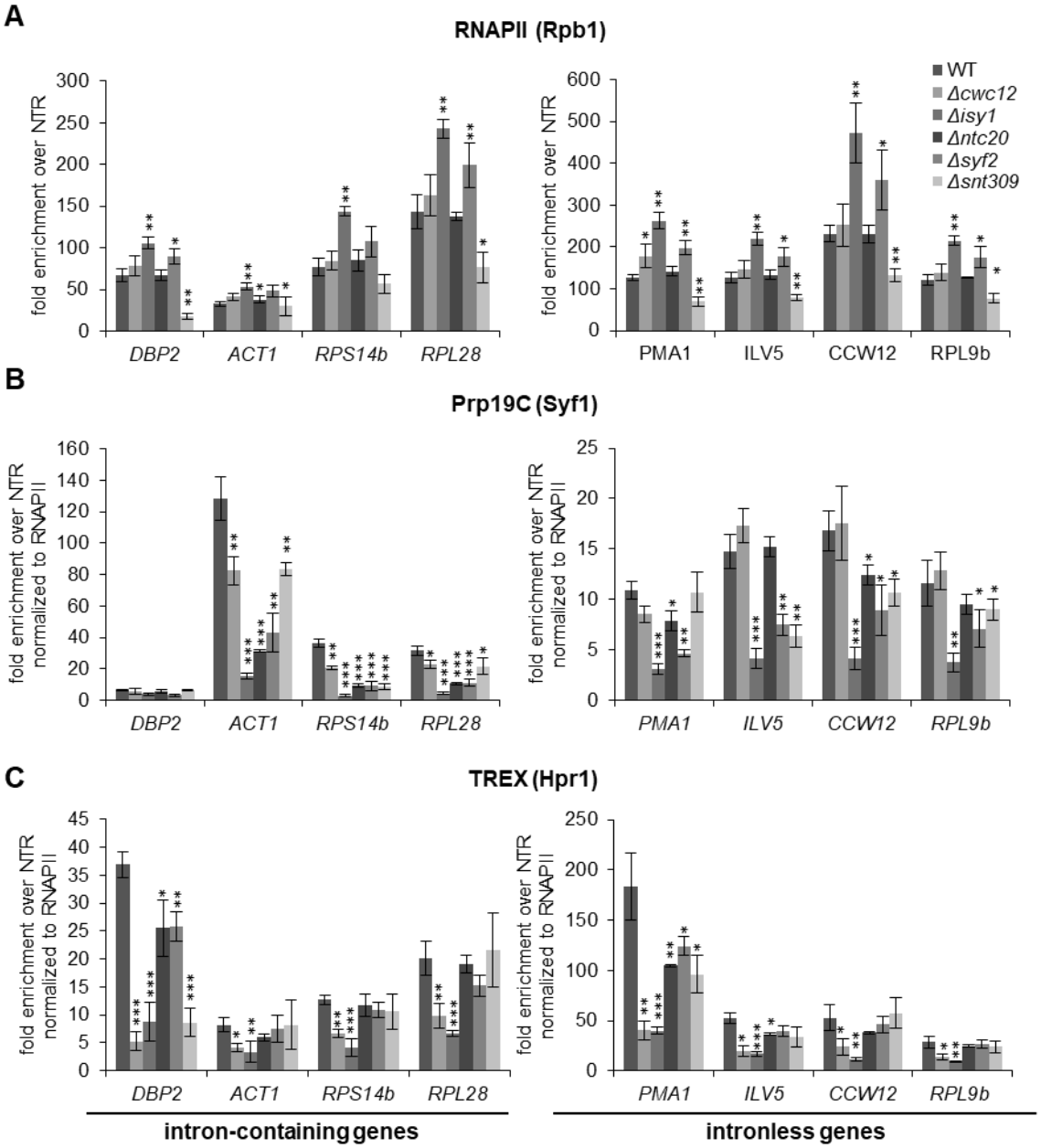

Figure 16: Syf2 and Isy1 function in the occupancy of Prp19C and Cwc15 and Isy1 functions in the occupancy of TREX to the genes. (**A**) RNAPII occupancy increases in Δ*syf2,* and Δ*isy1* mutant cells at both intron-containing and intronless genes and decreases in Δ*syf2* mutant cells. The occupancy of the RNAPII component Rpb1 was assessed in wild-type (WT), ***Δcwc15,*** Δ*isy1,* Δ*ntc20,* ***Δsyf2*** and Δ*snt309* mutant cells using chromatin immunoprecipitation (ChIP) at representative intron-containing (left panel) and intronless (right panel) genes. ChIPs were quantified by Real Time PCR using the primer pairs that bind at the 3' end of the gene as shown in Figure 15. (**B**) Prp19C occupancy normalized to RNAPII occupancy decreases in Δ*syf2* and Δ*isy1* mutant cells at intron-containing genes. The occupancy of Prp19C was assessed by ChIP using TAP-tagged Syf1. (**C**) TREX occupancy normalized to RNAPII decreases in ***Δcwc15*** and Δ*isy1* mutant cells. The occupancy of TREX was assessed by ChIP using TAP-tagged Hpr1. The raw data for the deletion mutants *CWC15, ISY1, NTC20, SYF2* were produced by Rashmi Minocha, the normalization to the RNAPII was performed by me, as well as the data for the WT and deletion mutant *SNT309*. (Non-normalized Prp19C and TREX ChIP can be found in Appendix Figure 1A and B).

7.1.7 Cwc15 is needed for efficient transcription *in vivo*

Prp19C is important for efficient transcription elongation (Chanarat, Seizl, and Strässer 2011). In this study, I wanted to determine whether the non-essential Prp19C components are involved in efficient transcription elongation. To test this, a yeast strain with deletion of *DST1*, a gene coding for the transcription elongation factor TFIIS, was used as a positive control for a defect in transcription elongation (Exinger and Lacroute 1992). This strain was used to see if any deletion mutant is synthetically lethal with Δ*dst1* or show a growth defect as the Δ*dst1* cells since this would be an indicator that these proteins might work in the same manner. To determine if the non-essential components of Prp19C are involved in transcription elongation, also double deletion mutant of *CWC15* and *SYF2* was studied, since the double deletion of *CWC15* and *SYF2* have an influence at Hpr1 which is needed for efficient transcription elongation.

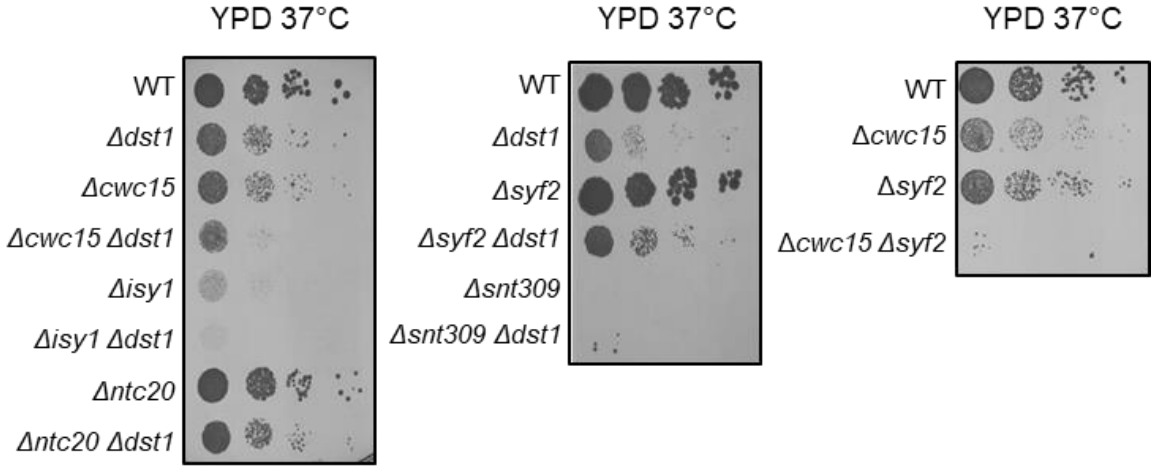

Figure 17: Isy1 and Snt309 are essential for growth at 37°C. Ten-fold serial dilutions of wild-type (WT), *Δcwc15*, *Δisy1, Δntc20, Δcwc15, Δsyf2, Δsnt309, Δdst1, Δcwc15 Δsyf2, Δdst1 Δcwc15, Δdst1 Δisy1, Δdst1 Δntc20, Δdst1 Δsyf2* and *Δdst1 Δsnt309* cells were spotted on YPD. The plates were incubated for 3 days at 37°C.

Cells in which either *ISY1* or *SNT309* is deleted cannot survive at 37°C (*Figure 17*). Cells lacking *CWC15* grow as poorly as Δ*dst1* cells. In the double deletion, Δ*cwc15* Δ*dst1*, there is an additive growth defect, which is a first hint that both proteins are involved in transcription elongation. Deletion of *NTC20* or *SYF2* does not lead to a growth defect at 37°C, and the double deletion of Δ*ntc20* Δ*dst1* do not show any additive effects. The double deletion of Δ*syf2* Δ*dst1* growth slightly faster than the single deletion of Δ*dst1* (Figure 17). For the double deletion of Δ*cwc15* Δ*syf2* a strong growth defect at 37°C was observed. This indicates that both proteins might have redundant functions and can compensate if the other protein is deleted. This is interesting because Cwc15 is only

known as a loosely attached protein of Prp19C and not even included in the core components.

To obtain a further indication if the non-essential Prp19C components are involved in transcription elongation the deletion mutants were spotted on plates containing 6-azauracil (6-AU). 6-AU leads to decreased intracellular GTP and UTP levels and therefore impairs transcription elongation (Exinger and Lacroute 1992). The growth of Δ*cwc15* cells on 6-AU-containing plates is not impaired compared to wild-type cells. However, in the Δ*cwc15* Δ*dst1* double mutant the growth is more impaired than in the Δ*dst1* mutant (Figure 18A). The additive effect of the double deletion indicates that Cwc15 and Dst1 might have overlapping function and therefore, Cwc15 might have a role in transcription elongation *in vivo*. The growth of Δ*isy1,* Δ*ntc20 and* Δ*syf2* cells is not impaired when compared to the wild-type. The same effect could be observed for the Δ*isy1* Δ*dst1,* Δ*ntc20* Δ*dst1 and* Δ*syf2* Δ*dst1* double deletion, which had no effect compared to either single mutant (Figure 18A). In cells where *SNT309* is deleted a growth defect was observed but not increased in the double deletion strain. This could be an indication that proteins Snt309 and Dst1 functions in different processes.

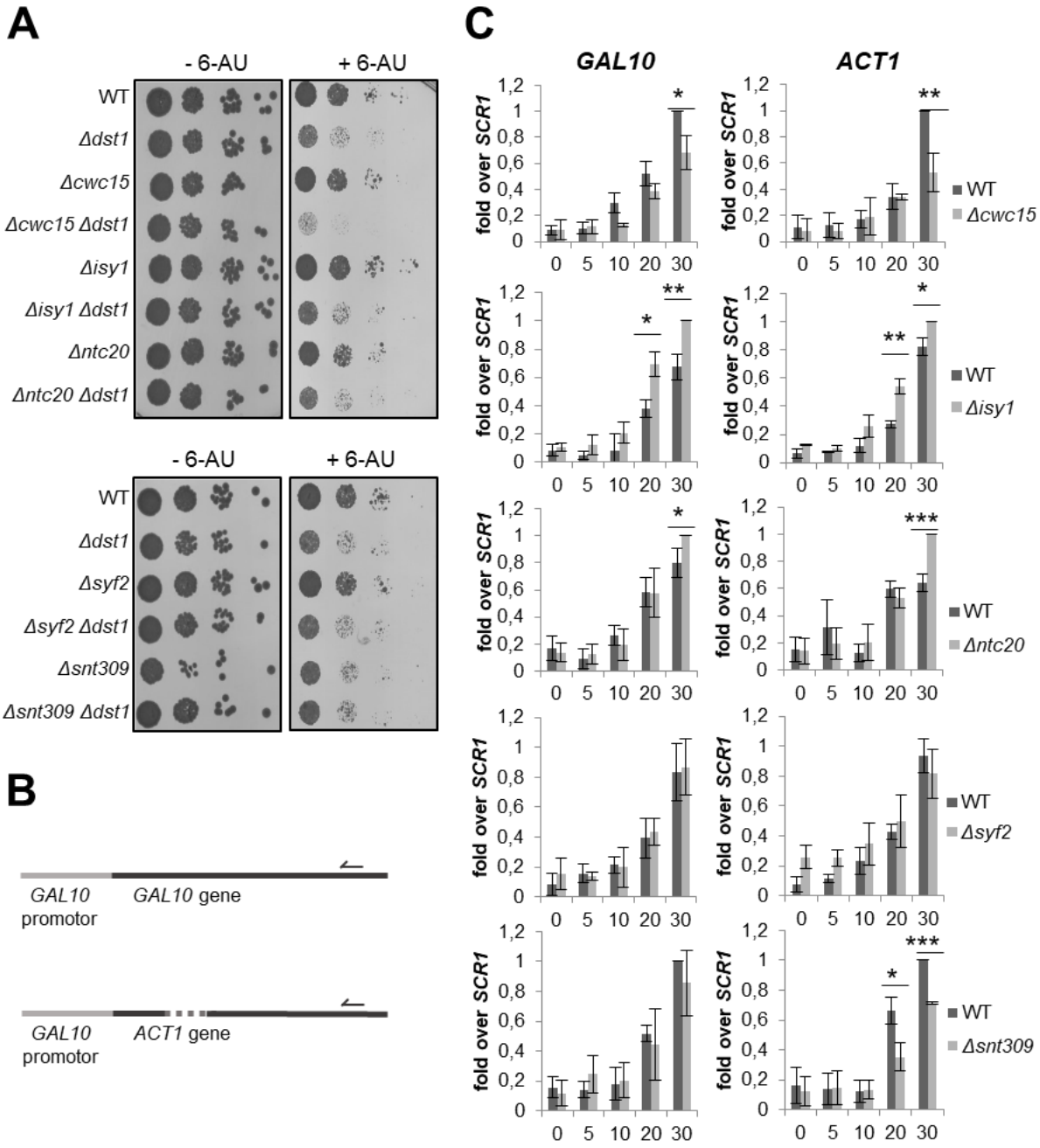

Figure 18: Cwc15 functions in transcription. (**A**) *Δcwc15* has an additive effect on growth when combined with *Δdst1* in the presence of 6-AU. Ten-fold serial dilutions of wild-type (WT), *Δcwc15*, *Δisy1, Δntc20, Δcwc15, Δsyf2, Δsnt309, Δdst1, Δdst1 Δcwc15, Δdst1 Δisy1, Δdst1 Δntc20, Δdst1 Δsyf2* and *Δdst1 Δsnt309* cells were spotted on SDC(-ura) plates containing solvent (-6AU) or 75 µg/ml 6AU (+6AU) and incubated for 2-3 days at 30°C. (**B**) Scheme of the oligonucleotides used in the primer extension assay. (**C**) Expression of the endogenous, intronless *GAL10* gene and the plasmid-encoded, intron-containing *ACT1* gene driven by the *GAL10* promoter was induced for 5, 10, 20 and 30 min by addition of galactose. Total RNA was extracted and the amount of *GAL10* and *ACT1* mRNA was determined by primer extension using 5'-Cy5-labeld reverse oligonucleotides as shown in C. The amount of *GAL10* and *ACT1* mRNA at the different time points of three independent experiments in wild-type (WT) and *Δcwc15, Δisy1, Δntc20, Δsyf2* and *Δsnt309* cells was quantified and normalized to the levels of the RNAPIII transcript *SCR1*. (Example UREA-SDS-Gels which were used for quantification can be found in Appendix Figure 3.)

To determine whether Cwc15 is indeed needed for efficient transcription *in vivo* transcription assays were performed. To do so two reporter genes were used: the endogenous, intronless *GAL10* gene and the intron-containing *ACT1* gene under the galactose-inducible *GAL10* promotor on a plasmid (Figure 18B). Expression from the *GAL10* promoter was induced, and cells were harvested after 0, 5, 10, 20 and 30 minutes of induction. After RNA isolation, the amount of synthesized *GAL10* and *ACT1* mRNA was quantified by primer extension (Figure 18C). In ∆*syf2* cells the same amount of mRNA is synthesized as in wild-type cells *in vivo*. In cells where either *Δisy1* or *Δntc20* are deleted more mRNA is synthesized than in wild-type cells. In ChIP experiments (Figure 16B) it was already detected that RNAPII occupancy increases in cells where *ISY1* is deleted. The deletion of *SNT309* leads to lower levels of synthesized *ACT1* but remains at wild-type levels for the *GAL10* gene. The lower levels of the intron-containing *ACT1* gene could be due to destabilization of Prp19C in cells were *SNT309* is deleted. For *Δcwc15* cells, *GAL10* and *ACT1* mRNA levels are significantly reduced compared to wild-type cells. For *Δcwc15* cells RNAPII occupancy after galactose induction were examined, to exclude that the lower mRNA synthesis might be due to reduced RNAPII occupancy at transcribed genes (Appendix Figure 1C). However, the RNAPII occupancy after galactose induction in cells where *CWC15* is deleted are as in wild-type cells. Consequently, Cwc15 is needed for efficient mRNA synthesis or mRNA stability for intron-containing and intronless genes *in vivo*.

7.2 The role of Msl5 in transcription and mRNP assembly

A previous study in our lab showed that Mud2 plays a role in transcription and is required for the occupancy of mRNA-binding proteins to the transcription machinery (Minocha et al. 2018). In this study they also re-analyzed PAR-CLIP data of Baejen et al. 2014 to compare binding intensities of intron-containing versus intronless mRNAs. From this relative binding intensities Mud2 (1,6) had a high ratio to intronless mRNAs compared to the analyzed splicing factors, however, Msl5 had the highest ratio with 9.3. From this we reasoned that – since Mud2 plays a role in splicing – Msl5, which is the direct interaction partner of Mud2, might also have a role in transcription, since it binds even more intronless mRNAs than Mud2.

7.2.1 Msl5 is recruited to intron-containing and intronless genes in a transcription-dependent manner

Since Msl5 is a known splicing factor the goal was to ascertain that Msl5 is not only recruited to intron-containing but also to intronless genes, to get a first indication if Msl5 has another role than splicing. To examine this a ChIP experiment, and occupancy of Msl5 was determined. Eight highly transcribed genes were examined, four intron-containing *(DBP2, ACT1, RSP14B and RPL28)* and four intronless genes *(PMA1, ILV5, CCW12 and RPL9)* using oligos binding to the 5', middle and 3' region of each gene (Figure 15).

Msl5 is not only recruited to intron-containing genes but also intronless genes (Figure 19). Different gene positions at these genes were tested, and indeed Msl5 is recruited to all tested positions of the gene (5', middle and 3'). This is an indication, that Msl5 has another role than just binding to the BP during splicing. For most of the genes the highest occupancy of Msl5 is at the middle or 3' position. These data show that Msl5 is recruited to genes whether or not an intron is present.

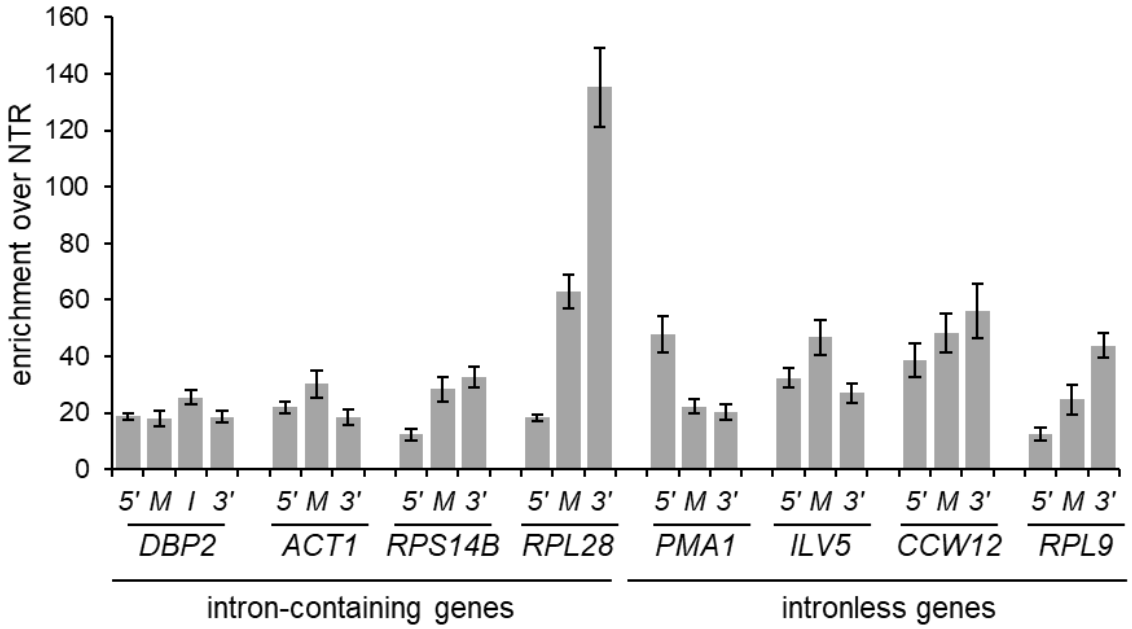

Figure 19: Msl5 is recruited to intronless and intron-containing genes. The determined occupancy of Msl5 was analyzed with ChIP followed by Real Time PCR using four intron-containing genes (*DBP2, ACT1, RSP14B and RPL28*) and four intronless genes (*PMA1, ILV5, CCW12 and RPL9*) as shown in Figure 15.

To determine, if Msl5 is binding to genes in a transcription-dependent manner ChIP was performed. For this, *GAL1* and *GAL10* were analyzed, which are under the control of galactose-inducible promotors. *GAL1* and *GAL10* are only transcribed if galactose is present in the media; if glucose is present in the media these two genes are repressed. A strain where Msl5 is endogenously TAP-tagged was either grown in glucose-containing media (YPD, glu) or galactose-containing media (YPG, gal).

In YPG media, the occupancy of Msl5 is highly increased at all examined positions (5', M and 3'), whereas in YPD media, under transcription-repressing conditions, the occupancy of Msl5 is close to background (Figure 20). This result demonstrates that the Msl5 occupancy at transcribed genes is transcription-dependent.

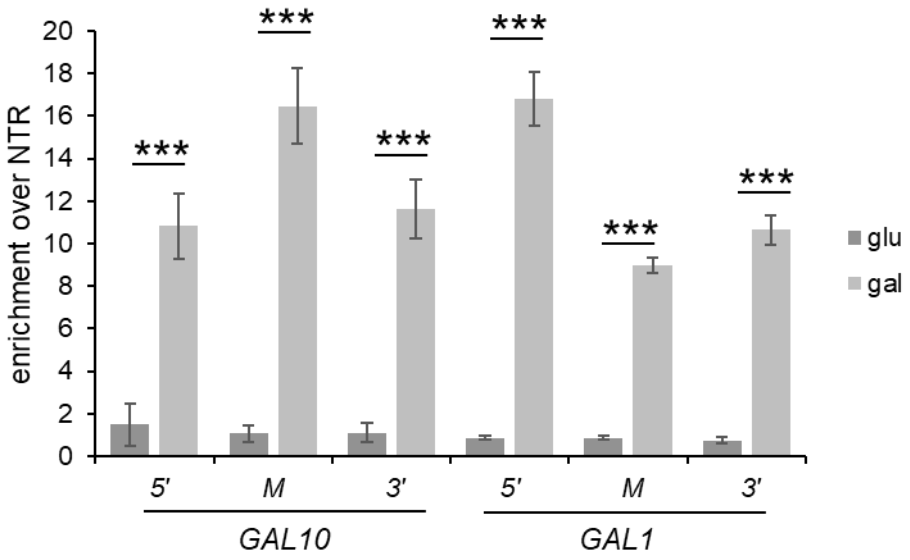

Figure 20: Msl5 is recited to the genes in a transcription-dependent manner. Occupancy of Msl5 at *GAL1* and *GAL10* using ChIP under repressed conditions (glucose-containing medium: glu), and induced conditions (galactose-containing medium: gal).

7.2.2 Depletion of Msl5

Msl5 is an essential gene and therefore a deletion of Msl5 would be lethal to the cells. However, to investigate the function of a protein it is often indispensable to investigate cells without this protein. Hence, a Msl5 depletion strain was generated, based on an auxin-inducible degron system, which is a plant hormone-induced system. In plants, auxin (indole-3-acetic acid; IAA; AU) induces the degradation of transcriptional repressors by mediating the interaction of a degron domain in the target protein with the substrate recognition domain of an F-box protein, Tir1 (Hayashi 2012). Upon interaction of Tir1 with the protein containing the degron domain, the protein with the degron domain is ubiquitylated by a ubiquitin ligase (E3) and subsequently degraded by the proteasome. The E3 ligase and therefore this pathway is highly conserved in eukaryotes. Through the constitutive expression of a Tir1 transgene, this system can also be used in yeast. The protein of interest needs the auxin induced degron-tag (AID-tag), which can be fused N- or C-terminally (Nishimura et al. 2009; Morawska and Ulrich 2013). The degradation of the tagged protein is quick, and 1 hour after addition of auxin Msl5 is no longer detectable.

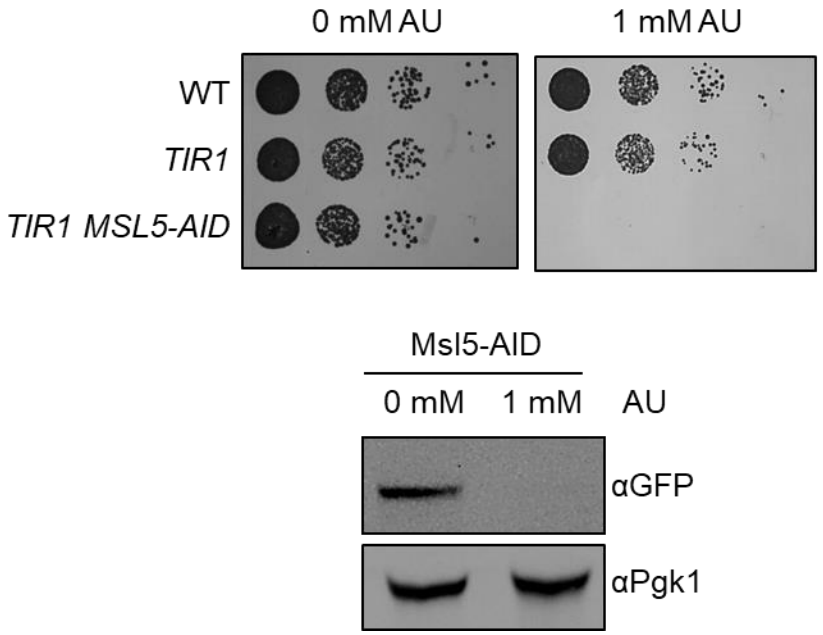

Figure 21: Depletion of Msl5 using the auxin degron system. Upper panel: Cells where Msl5 is depleted are dead. A ten-fold serial dilution of wild-type (WT) and indicated mutants on YPD plates with 0 mM of auxin and 1 mM of auxin. Lower panel: Msl5 is not detectable after incubation with 1 mM of AU for 1 h. The AID-tag contains besides the degron sequence a GFP therefore, Msl5 can be visualized by a GFP antibody. Pgk1 levels do not change.

On plates without auxin the strain containing the *TIR1* gene and the AID-tag on Msl5 are growing like the wild-type. Cells where Msl5 carries an AID-tag are not viable on plates containing 1 mM of auxin. The wild-type grows normal on plates containing auxin (Figure 21, upper panel). To examine if Msl5 is fully degraded 1h after addition of auxin a quantitative Western blot was performed (6.7), and Pgk1 was used as a loading control. Since the AID-tag also contains a GFP an antibody against GFP was used to determine the Msl5 levels. 1 h after adding 1 mM auxin Msl5 is not detectable anymore, whereas the levels of Pgk1 do not change compared to the control with 0 mM of auxin. Therefore, Msl5 is depleted and further investigations in the absence of Msl5 can be performed.

7.2.3 The absence of Msl5 and Mud2 leads to a decreased occupancy of RNAPII at transcribed genes

To elucidate, if Msl5 has a role during the recruitment of RNAPII an RNAPII ChIP was performed. Minocha et al. (2018) previously showed, that the deletion of Mud2 does not change the occupancy of RNAPII at transcribed genes. Since *MSL5* is an essential gene, the depletion system was used to investigate RNAPII occupancy in the cells if Msl5 is

missing. The cells were treated for 1 h with 1 mM auxin prior to crosslinking. For every experiment samples were taken before and after auxin treatment to verify the depletion of Msl5 as seen in Figure 21 (lower panel). RNAPII occupancy does not change if Msl5-AID is missing (Figure 22).

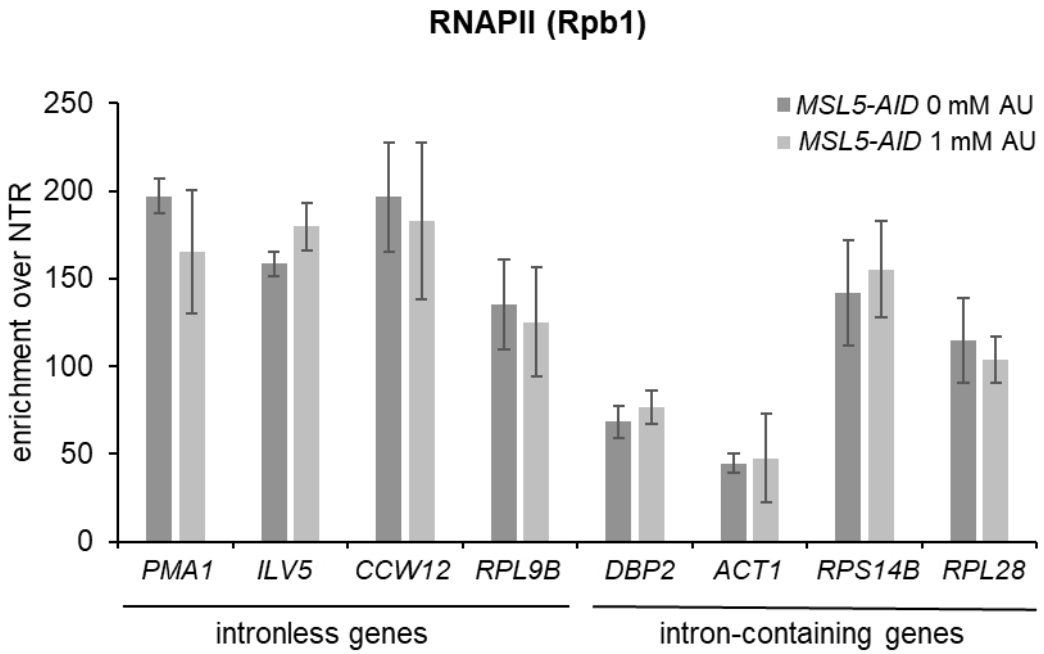

Figure 22: Depletion of Msl5 does not change the occupancy of RNAPII. RNAPII occupancy at both intron-containing and intronless genes do not change if Msl5-AID is depleted. The occupancy of the RNAPII component Rpb1 was assessed in an *MSL5*-AID strain after 0 mM and 1 mM auxin treatment for 1 h by chromatin immunoprecipitation (ChIP) at eight representative intron-containing and intronless genes at 3' position as shown in Figure 15. (AU control ChIP experiments can be found in Appendix Figure 4.)

Since neither the absence of Mud2 nor the absence of Msl5 show an effect on RNAPII occupancy, it was further interesting to investigate if it has an influence on the RNAPII occupancy when both proteins, Msl5 and Mud2, are missing. To investigate this, a strain in which *MUD2* was deleted and Msl5 can be depleted was produced. Before performing ChIP experiments with this strain, a growth assay on YPD without the addition of auxin was performed. This experiment was needed to exclude if any defects are occurring due to the modifications. Msl5-AID growth like the wild-type under permissive conditions (25°C and 30°C) (Figure 23). Even at condition of cold (16°C) or heat (37°C) stress the Msl5-AID strain grows like the wild-type, confirming that neither the insertion of *TIR1* gene nor the AID-tag on Msl5 have an influence on the growth of the cells. In cells where *MUD2* is deleted the cells grow like the wild-type under permissive (25°C and 30°C)

temperatures. However, at cold stress or heat stress (16°C and 37°C) the deletion of *MUD2* leads to a slight growth defect. In cells where Msl5 has an AID-tag and *MUD2* is deleted a growth defect is already visible at permissive temperatures (25°C and 30°C). Under heat stress the growth defect is stronger than the growth defect in cells were only *MUD2* is deleted. At 16°C the same effect can be observed; however, the growth defect is even stronger. These results show that the insertion of the AID-tag by itself has no effect on growth but leads to a strong growth defect under stress conditions if combined with the deletion of *MUD2*.

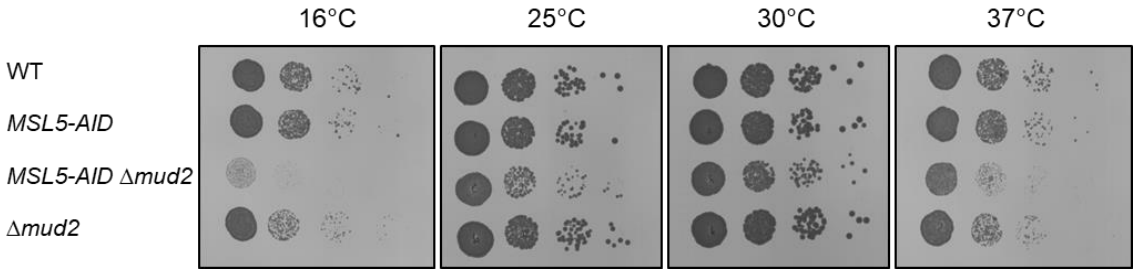

Figure 23: The strain *MSL5*-AID *Δmud2* has a growth defect in the absence of auxin. Deletion of *MUD2* leads to a growth defect at heat or cold stress (16°C and 37°C) *MSL5-AID* has no visible growth defect at all temperatures. Cells with an AID-tag on Msl5 and the deletion of *MUD2* show a growth defect at all temperatures. Ten-fold serial dilution of wild-type cells and indicated mutants were spotted on YPD plates (without auxin) and incubated for 2-4 day (25°C, 30°C and 37°C) or 7 day (16°C).

To investigate if the combined absence of Msl5 and Mud2 influences RNAPII occupancy a ChIP with a *Δmud2 MSL5-AID* strain with treatment of 0 mM and 1 mM of auxin.

RNAPII occupancy decreases to around 20-40% if Msl5 is depleted in the *Δmud2* background (Figure 24). **Figure *22***This effect can be detected at intron-containing and intronless genes. This reduction in RNAPII occupancy at transcribed genes in cells were Msl5 and Mud2 are absent suggests that mRNA transcription is impaired. This corresponds with the growth defect that can be detected at all examined temperatures.

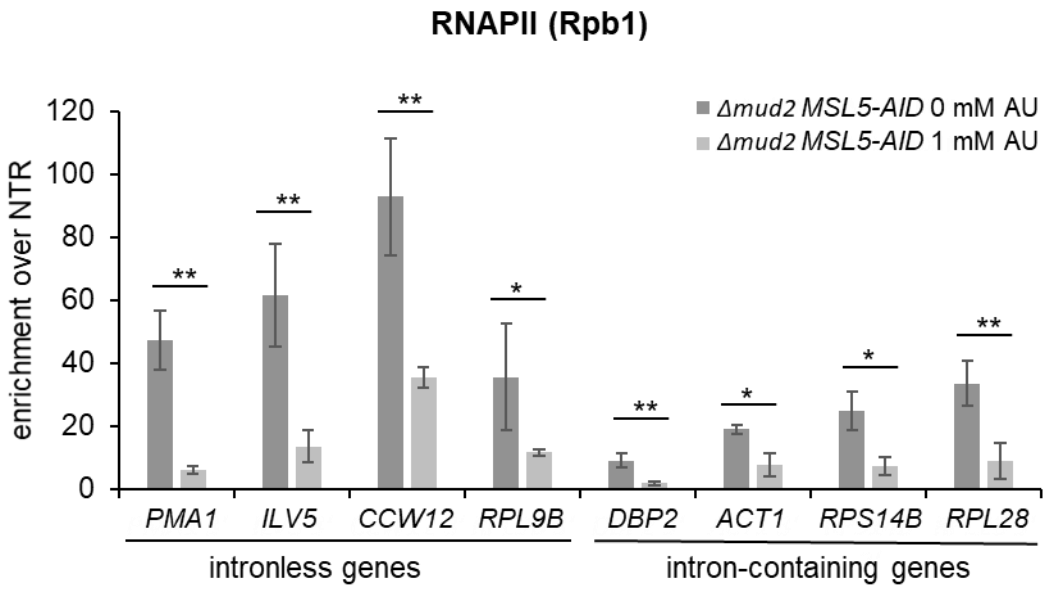

Figure 24: In the absence of Msl5 and Mud2 the occupancy of RNAPII is highly reduced. The occupancy of RNAPII is highly reduced when the Msl5 is depleted in a *Δmud2* mutant. The occupancy of the RNAPII component Rpb1 was assessed in an *Δmud2 MSL5-AID* strain after 0 mM and 1 mM auxin treatment for 1 h by chromatin immunoprecipitation (ChIP) at eight representative intron-containing and intronless genes at 3' position as shown in Figure 15.

7.2.4 Msl5 is needed for the fully occupancy of Mud2 at transcribed genes and *vice versa*

To determine if Msl5 or Mud2 are dependent on each other for their occupancy at transcribed genes a ChIP was performed.

If *MUD2* is deleted the occupancy of Msl5 is reduced to around 30% of wild-type levels at intron-containing and intronless genes (Figure 25A). This indicates that Mud2 is needed for a stable occupancy of Msl5 at transcribed genes.

Next, it was examind if Msl5 is needed for Mud2 occcupany at transcribed genes. Therefore, a ChIP was performed, and Msl5-depleted cells were compared to non-depleted cells. Here, almost the same effect could be detected: In the absence of Msl5, the occupancy of Mud2 drops to around 50% at intron-containing and intronless genes.

Taken together, Msl5 and Mud2 are important for the occupancy of each other at transcribed genes.

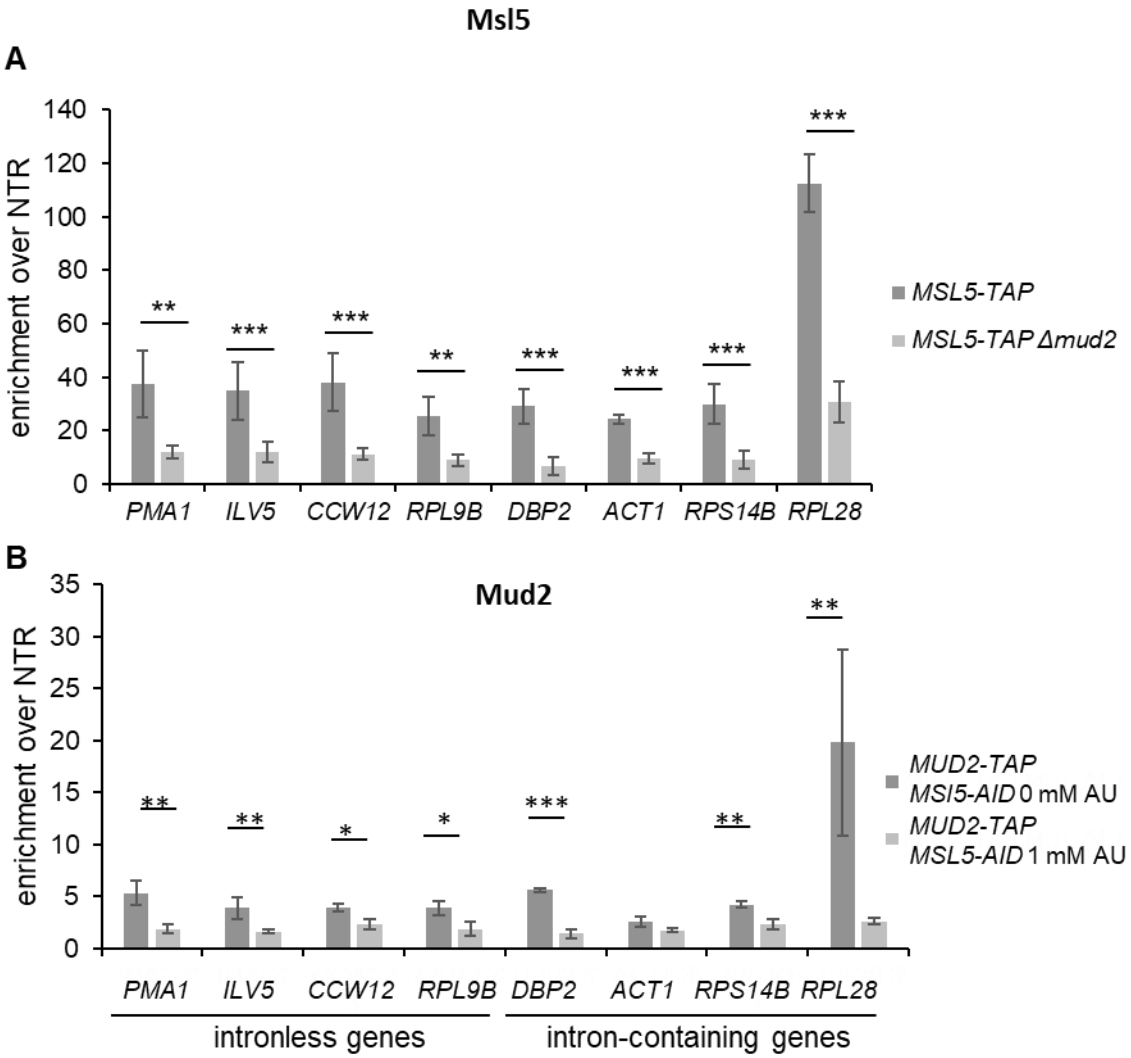

Figure 25: Msl5 and Mud2 are important for the occupancy of each other at transcribed genes. (**A**) Msl5 occupancy is reduced, if Mud2 is deleted at both intron-containing and intronless genes. The occupancy of Msl5 was assessed in *MSL5*-TAP and *MSL5*-TAP *Δmud2* cells using chromatin immunoprecipitation (ChIP) at eight representative intron-containing and intronless genes. ChIPs were quantified by Real Time PCR using the primer pairs at the 3' end of the gene as shown in Figure 15. (**B**) The occupancy of Mud2 is reduced if the *MSL5*-AID cells are treated with auxin. The experiment was performed as described in (A).

7.2.5 S5 CTD phosphorylation of RNAPII is required for the occupancy of Msl5 *in vivo*

The CTD of the largest subunit (Rpb1) of RNAPII is an important recruitment platform for mRNP biogenesis factors to the transcription machinery. The CTD consists of heptad repeats, which are phosphorylated at different time points during the transcription cycle. During transcription initiation, S5 is phosphorylated (Mayer et al. 2010). In *S. cerevisiae,* Mud2 is recruited to transcribed genes through the S2 phosphorylation, a marker for

elongating RNAPII, and the occupancy of the TREX complex also depends on S2 phosphorylation (Meinel et al. 2013; Minocha et al. 2018).

Since Mud2 is recruited to the transcription site by S2 phosphorylation it would be interesting to investigate, if Msl5 is, recruited in the same manner. Therefore, the Msl5 occupancy at transcribed genes was assessed in Rpb1-CTD mutants. A strain with a Rpb1-CTD truncated to 14 wild-type repeats served as control. The S2A mutant Rpb1-CTD carried 8 wild-type repeats and 6 repeats with Ser2 to Ala substitutions (West and Corden 1995).

To examine if the occupancy of Msl5 changes when S2 is no longer properly phosphorylated, a ChIP experiment was performed. Interestingly, the Msl5 occupancy is not reduced; at some genes it even increases significantly (Figure 26). Therefore, it can be concluded that while Msl5 occupancy at transcribed genes depends on Mud2, Msl5 also requires an additional recruitment protein/platform for binding to transcribed genes beyond Mud2.

Next, it was interesting to investigate, if Msl5 might be recruited to transcribed genes by the S5 phosphorylation. This would suggest that Msl5 is recruited to transcribed genes before Mud2 and during transcription initiation. To do so another Rpb1-CTD mutant was used. The S5A mutant Rpb1-CTD carried 7 wild-type repeats and 7 repeats with Ser2 to Ala substitutions (West and Corden 1995).

The occupancy of Msl5 decreases significantly in the *rbp1-S5A* mutant strain at both intron-containing and intronless genes (Figure 27). From this it can be concluded that S5 phosphorylation is important for the efficient recruitment of Msl5 to transcribed genes.

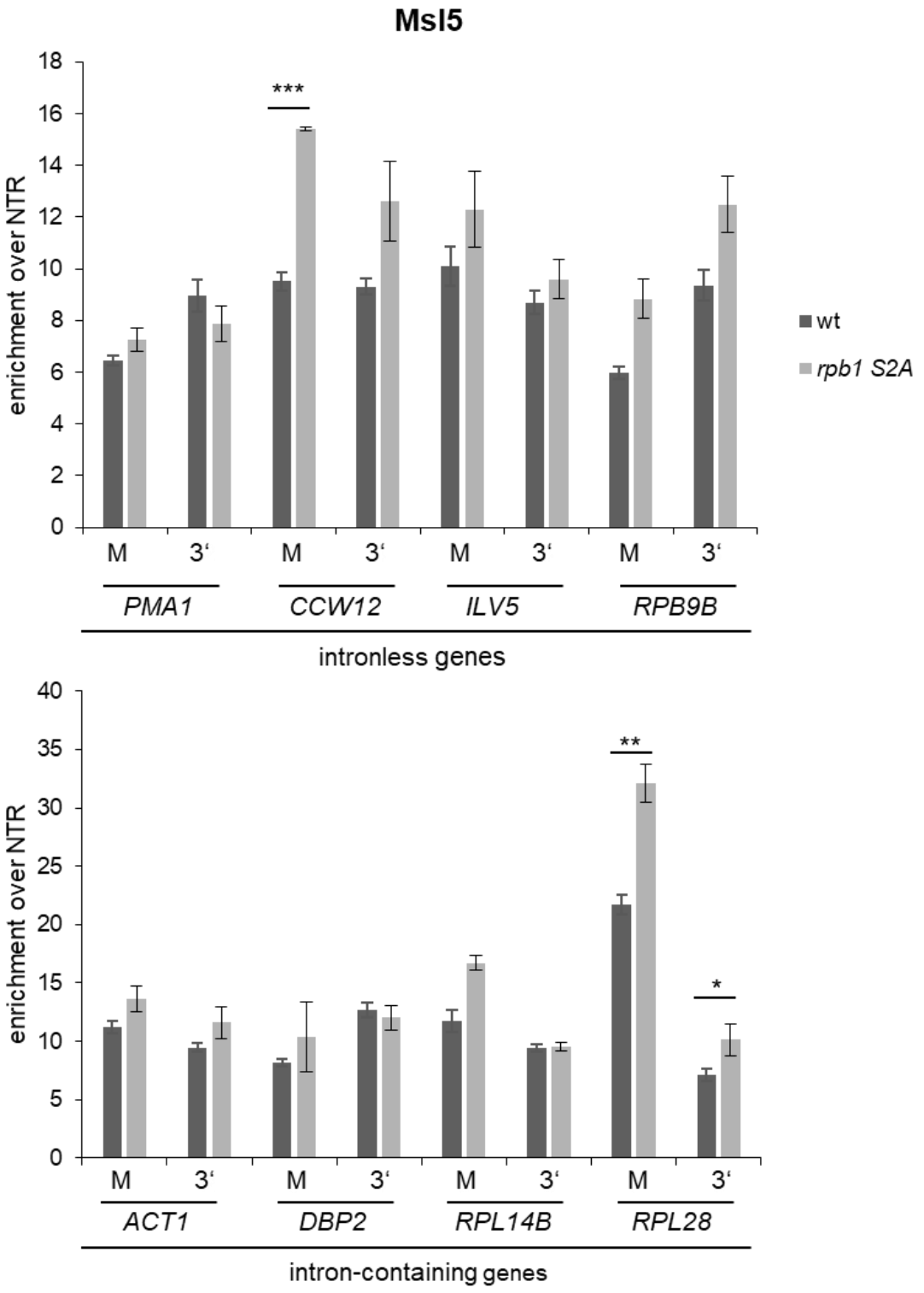

Figure 26: S2 phosphorylation is not required for Msl5 occupancy. Msl5 does not change if S2 cannot be fully phosphorylated. *RPB1* shuffle strain with endogenously TAP-tagged Msl5, with either a plasmid with 14 wild-type heptapeptide repeats or 6 S2 were mutated to A was used. Chromatin immunoprecipitation (ChIP) at exemplary intron-containing and intronless genes was performed. ChIPs were quantified by Real Time PCR using the primer pairs which bind at the 3', M end of the gene as shown in Figure 15.

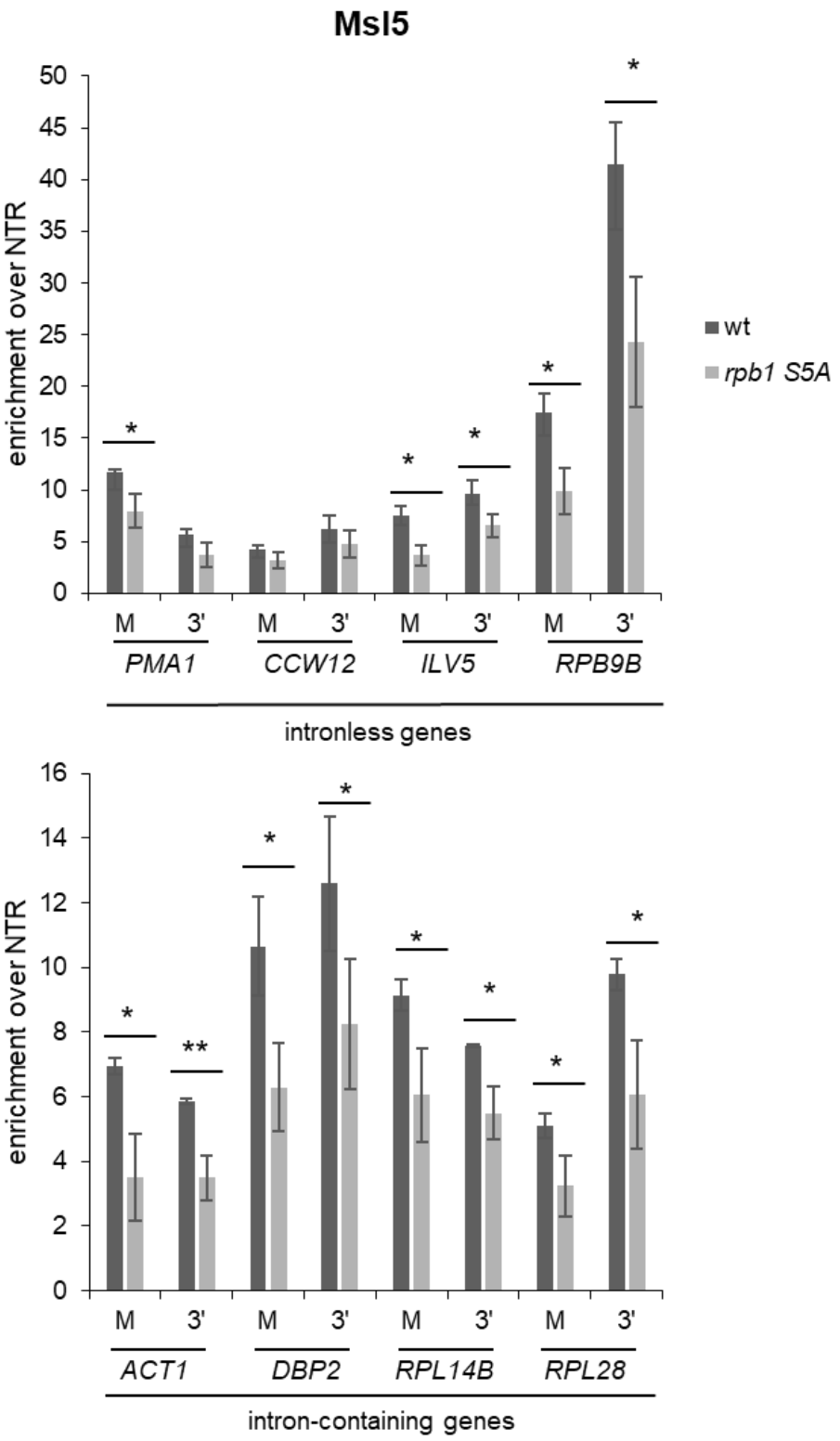

Figure 27: S5 phosphorylation of the CTD is needed for occupancy of Msl5. Msl5 occupancy is reduced if S5 cannot be fully phosphorylated. *RPB1* shuffle strain with endogenously TAP-tagged Msl5 in which either a plasmid with 14 wild-type heptapeptide repeats or 7 S2 were mutated to A was transformed. Chromatin immunoprecipitation (ChIP) at eight representative intron-containing and intronless genes was performed. ChIPs were quantified by Real Time PCR using the primer pairs which bind at the 3', M end of the gene as shown in Figure 15.

7.2.6 The occupancy of Msl5, Mud2 and Syf1 is RNA-dependent

To investigate if a protein is recruited to the transcription elongation complex through direct interaction with the mRNA, a hepatitis δ ribozyme-based ChIP assay was performed. For this assay two strains were used. One with a silent (mutated), which serves as a control or with an active hepatitis δ ribozyme inserted at the 5' end of the non-essential gene *YCT1* placed under the control of a *GAL1* promoter. The protein examined needs to be endogenously TAP-tagged or an antibody which is directed against the protein of interest is needed. The strains with the with a silent or active ribozyme were grown in medium with galactose as carbon source to activate transcription of the ribozyme-containing reporter. During the transcription of the modified *YCT1* mRNA the ribozyme inside the mRNA folds to an active ribozyme and initiates self-cleavage. Upon transcript cleavage, the 5' end of the nascent mRNA and the proteins that are bound to it are released from the transcription site. A ChIP of the protein of interest at the reporter gene carrying the silent or active ribozyme was performed and relative occupancies were calculated (Fong, Ohman, and Bentley 2009).

The protein Rbp3, which is a subunit of the RNAPII and therefore not RNA-dependent, served as a negative control. Hpr1 is RNA-dependent and served as a positive control (Meinel et al. 2013).

For Msl5, the ChIP signal after cleavage drops to 70% (Figure 28). This is comparable to Hpr1, proving that the occupancy of Msl5 is RNA-dependent. The same effect can be seen for Mud2 and Syf1, with ChIP signal after cleavage dropping to 50% and 60% (Figure 28), respectively. Taken together these results show that Msl5, Mud2 and Syf1 are recruited to the genes in an RNA-dependent manner.

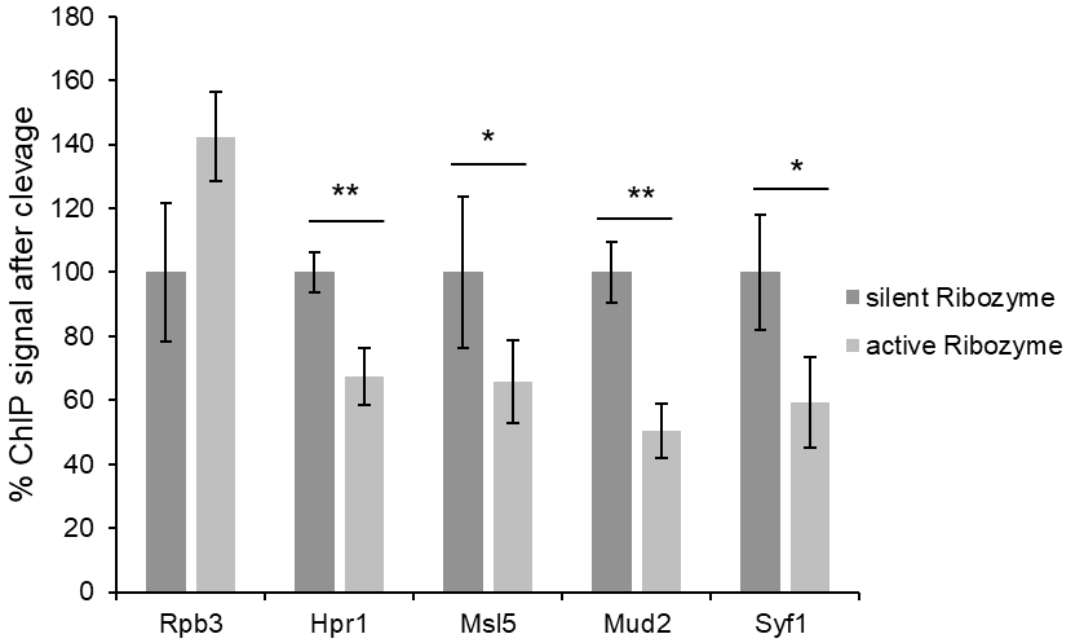

Figure 28: Msl5, Mud2 and Syf1 are recruited to the nascent mRNA in an RNA-dependent manner. Ribozyme assay followed by a ChIP and Real Time PCR. The ChIP signals of the reporter carrying the silent ribozyme were set to 100%. Rpb3, a subunit of the RNAPII, served as a negative control, and Hpr1 served as a positive control.

7.2.7 Prp19C and TREX are not required for Msl5 occupancy

To elucidate if in addition to RNA and S5 phosphorylation also protein-protein interaction facilitate the occupancy of Msl5, it needed to be investigated if either the Prp19 or the TREX complex are needed for the Msl5 occupancy at transcribed genes. To determine whether Prp19C is needed for the occupancy at transcribed genes a *syf1* mutant, *syf1-37*, was used. The mutated Syf1 lacks part of its C-terminus and the occupancy of Prp19C at transcribed genes is reduced (Chanarat, Seizl, and Strässer 2011).

Msl5 was endogenously TAP-tagged in a *SYF1* shuffle strain. After that, either a plasmid encoding the wild-type *SYF1* or *syf1-37* was transformed into the *SYF1* shuffle strain. The occupancy of Msl5 does not change in the *syf1-37* mutant when compared to the wild-type *SYF1* (Figure 29). Therefore, Syf1 and the whole Prp19C complex is not needed for the occupancy of Msl5 at transcribed genes.

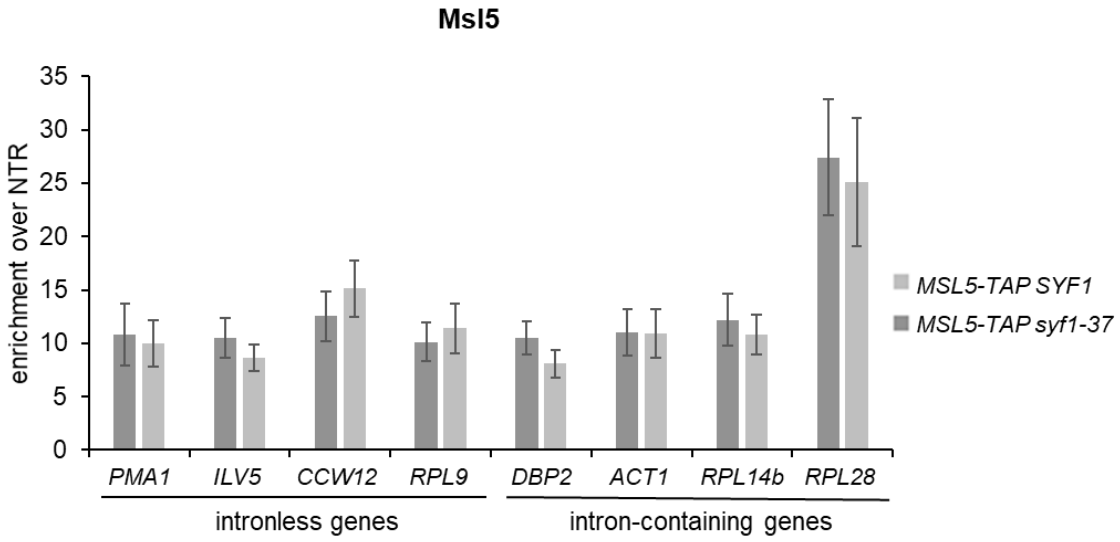

Figure 29: Msl5 occupancy does not depend on Prp19C. Occupancy of Msl5 was determined in *syf1-37* mutant cells compared to *SYF1* wild-type cells. A ChIP experiment followed by Real Time PCR sing the primer pairs that bind at the 3' end of the gene as shown in Figure 15.

To investigate if TREX is needed for the occupancy of Msl5 at transcribed genes, a ChIP was performed in a strain where Msl5 is endogenously TAP-tagged. A wild-type strain was compared to a *Δhpr1* strain. If *HPR1* is deleted, THO and the TREX complex are absent from transcribed genes (Strässer et al. 2002).

Deletion of *HPR1* does not alter the occupancy of Msl5, indicating that TREX is not needed for the occupancy of Msl5 at transcribed genes either at intron-containing genes or at intronless genes. Taken together, occupancy of Msl5 to the transcription site does not dependent on Prp19C or the TREX complex.

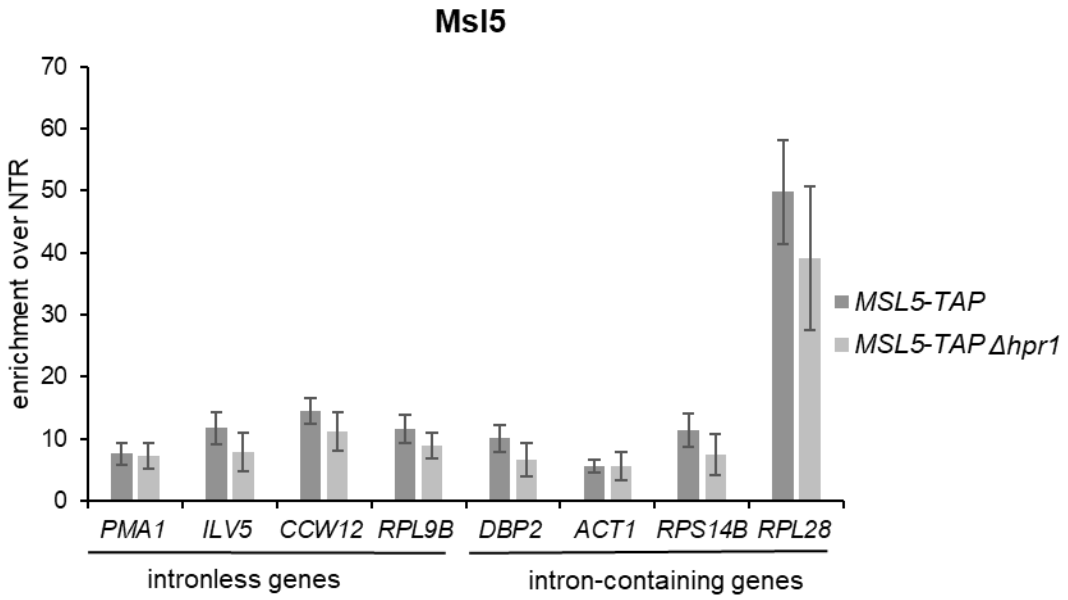

Figure 30: Msl5 does not require the TREX complex for its occupancy. Msl5 occupancy of Msl5 was determined in *Δhpr1* cells compared to wild-type cells. A ChIP experiment followed by Real Time PCR using primer pairs at four representative intron-containing (*DBP2, ACT1, RSP14B and RPL28*) and intronless genes (*PMA1, ILV5, CCW12 and RPL9B*) which bind at the 3' end of the gene as shown in Figure 15.

7.2.8 Depletion of Msl5 leads to reduced occupancy of Prp19C and TREX at transcribed genes

Deletion of *MUD2* leads to reduced occupancy of Prp19C and thus TREX (Minocha et al. 2018). Therefore, it was interesting if depletion of Msl5 has a similar effect. Because, depletion of Msl5 has no influence on the RNAPII occupancy at transcribed genes (Figure 22), normalization to RNAPII occupancy is not necessary.

Depletion of Msl5 reduces Syf1 occupancy and therefore presumably the whole Prp19C to around 50% at all tested intron-containing and intronless genes (Figure 31A).

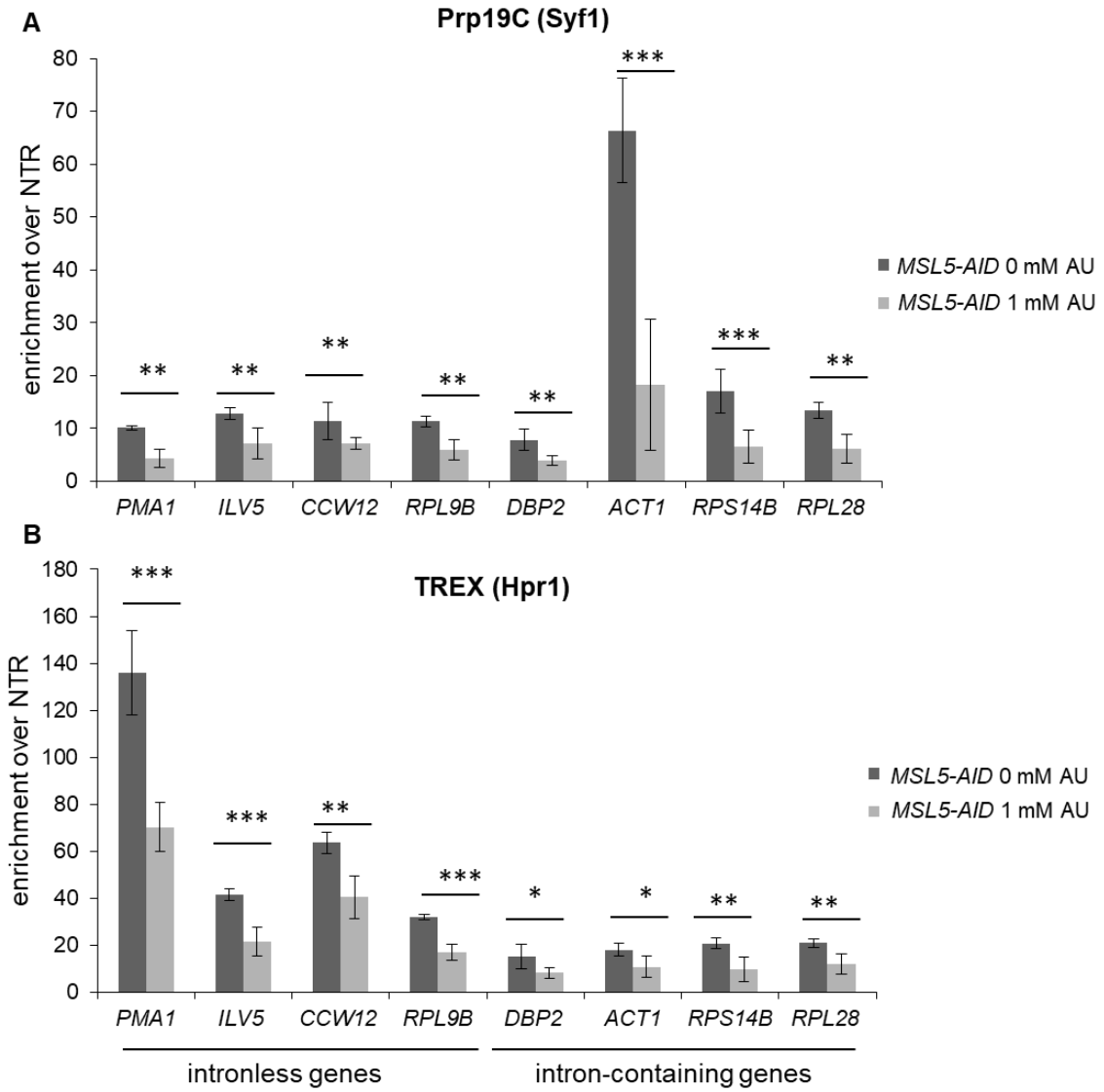

Figure 31: Prp19C and TREX have a reduced occupancy at intron-containing and intronless genes if Msl5 is depleted. (**A**) Syf1 occupancy is reduced if Msl5 is depleted at both intron-containing and intronless genes. The occupancy of Syf1 was assessed in a *MSL*5-AID *SYF1-TAP* strain treated with 0 mM or 1 mM of auxin using chromatin immunoprecipitation (ChIP) at eight representative intron-containing (*DBP2, ACT1, RSP14B and RPL28*) and intronless genes (*PMA1, ILV5, CCW12 and RPL9B*). ChIPs were quantified by Real Time PCR using primer pairs that bind at the 3' end of the gene as shown in Figure 15. (**B**) The occupancy of TREX is reduced if *MSL5*-AID cells are treated with auxin. The experiment was performed as described in (A). Instead of Syf1 the protein Hpr1 was TAP-tagged. (AU control ChIP can be found in Appendix Figure 4.)

For the TREX complex a similar pattern can be observed (Figure 31B). The loss of Msl5 reduces occupancy of Hpr1 and therefore, presumably the whole TREX at intron-containing and intronless genes.

Considering that the occupancies of Prp19C and TREX decreased at transcribed genes if Msl5 is depleted it was interesting to investigate if the protein levels of Syf1 and Hpr1

are influenced by the depletion of Msl5. To do so equal amounts of cells in which either Syf1 or Hpr1 were endogenously TAP-tagged were harvested. After cell lysis, protein amounts were analyzed by Western blot (Appendix Figure 5). The depletion of Msl5 has no influence on either Syf1 or Hpr1 levels in the cells. Therefore, the reduced occupancy of Prp19C or TREX cannot be due to reduced protein levels of Syf1 or Hpr1.

7.2.9 Msl5 is needed for the stability of Mud2

The depletion of Msl5 leads to an even stronger reduction of Prp19C and TREX than the deletion of *MUD2.* To elucidate if the recruitment of Prp19C and therefore TREX is dependent on the interaction of Mud2 and Msl5, a mutant is required where Mud2 and Msl5 are not able to interact with each other.

Deletion of the amino acids 2-56 (Wang et al. 2008) or 34-56 (Chang, Schwer, and Shuman 2012) of Msl5 abolishes the interaction with Mud2. First, a *MSL5* shuffle strain with a Mud2-FTpA tag, was transformed with pRS315_*MSL5-HA*, pRS315_*msl5 Δ2-56-HA* or pRS315_*msl5 Δ34-56-HA*.

To get an indication of whether the alterations of Msl5 have a global impact on cells Dot spots were performed. None of the truncated Msl5 versions led to a growth defect at any of the tested temperatures (Figure 32).

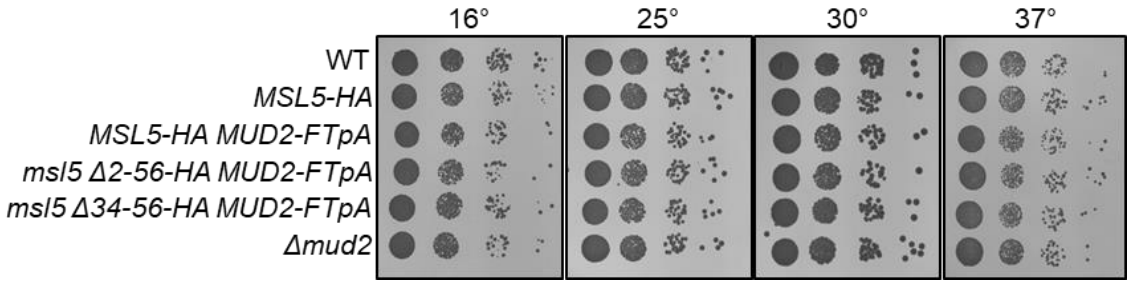

Figure 32: Truncations in Msl5 do not induce a growth defect. A 10-fold serial dilution of WT and the indicated mutants were spotted onto YPD plates. The plates were incubated for 2-4 day (25°C, 30°C, 37°C) or 7 days (16°C).

To investigate if Msl5 levels change when Msl5 is mutated or on a plasmid the protein levels were determined by Western blot. Msl5 expression from the plasmid is slightly lower if compared to endogenously expressed Msl5 (Figure 33A).

In strains transformed with either pRS315_*msl5 Δ2-56-HA* or pRS315_*msl5 Δ34-56-HA*, no decrease in Msl5 levels is detectable compared to either the endogenous strain or to the strain with the plasmid expressing wild-type Msl5.

Next, it was necessary to investigate if the alterations on Msl5 have an influence on Mud2. In the strains expressing a shortened version of Msl5, the protein amount of Mud2 drops significantly, with only 20-30% of the original amount of Mud2 still detectable. This result suggests that the interaction of Msl5 with Mud2 might stabilize Mud2 (Figure 33B).

Since Mud2 levels are strongly reduced in cells expressing the Msl5-Mud2 interaction mutant *msl5 Δ34-56*, it was interesting to know if RNA levels are changing. It was specifically interesting if the RNA levels of *MSL5* and *MUD2* change, and it was further analyzed if *PGK1* and *ACT1* do change, examples of an intronless and an intron-containing gene, respectively (Figure 33C).

Strains expressing full-length *MSL5-HA*, *msl5 Δ2-56-HA*, or *msl5 Δ34-56-HA* were compared. The mRNA levels of *MSL5* and *MUD2* did not change. There was also no detectable difference in the mRNA levels of the example genes for intronless and intron-containing genes, *PGK1* and *ACT1*. Therefore, the deletions in Msl5 do not lead in any change in the mRNA levels.

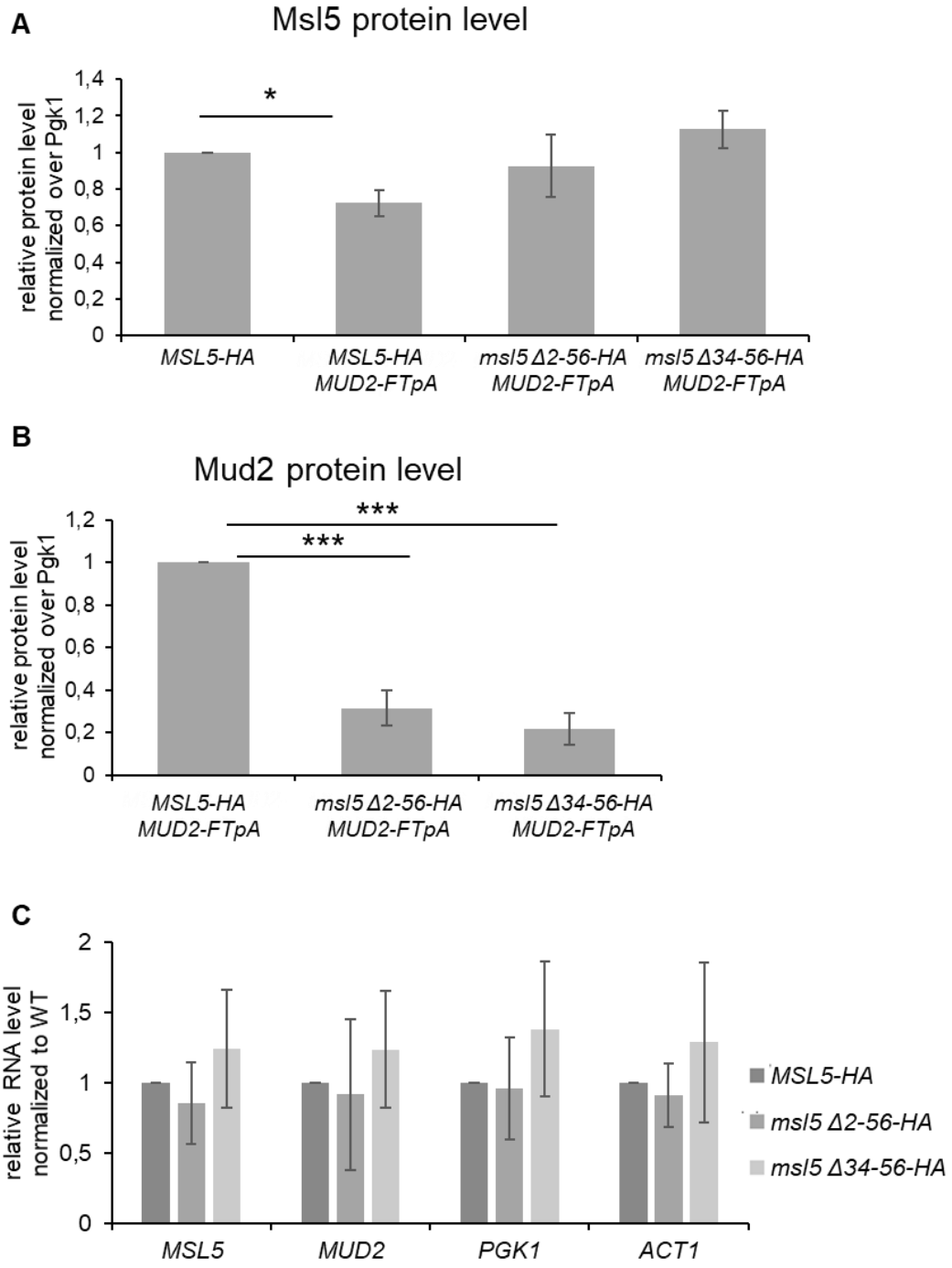

Figure 33: Deletions in Msl5 affect Mud2 protein levels. (A) Analysis of Msl5 protein levels. Neither deletion (*msl5 Δ2-56 HA*, *msl5 Δ34-56-HA*) leads to a change in Msl5 protein levels. To quantify the protein levels of Msl5, equal amounts of cells were harvested and followed by a quantitative Western blot analysis using PAP antibody against the FTpA-tag, Pgk1 was used as a loading control and an antibody against HA was used to determine the protein levels of Msl5. The Western blots were quantified by FIJI (ImageJ). **(B)** Truncations of *MSL5* lead to decreased levels of Mud2. The experiment was performed as described in (A), to determine the Msl5 protein levels an antibody against HA was used. Mud2 was quantified using the PAP antibody. **(C)** In truncated *MSL5* strains mRNA levels do not change. Equal amount of yeast cells was harvested during their exponential growth phase followed by RNA isolation. 100 ng of RNA was used for the synthesis of cDNA and the amount of cDNA was determined by qPCR.

Since the deletion of amino acids 2-56 or 34-56 of Msl5 leads to reduced levels of Mud2 it was interesting to investigate if this effect is also detectable after a one-hour depletion of Msl5. Indeed, already after the one-hour depletion of Msl5 a reduction of Mud2 protein levels is visible (Figure 34A). The protein levels of Mud2 are reduced to around 40%, which is comparable to the Mud2 amounts in the deletion mutants of *MSL5* where either the amino acids 2-56 or 34-56 are deleted.

To investigate if Mud2 is also important for the stabilization of Msl5. *MUD2* was deleted in a *MSL5-TAP* strain. Then equal amounts of cells in the different strains were harvested. Deletion of *MUD2* does not lead to reduced levels of Msl5, indicating that Mud2 is not important for Msl5 stability (Figure 34B).

Since the reduced Mud2 protein levels are not due to reduced mRNA levels (Figure 33C), the reduced protein levels might be due to the destabilization of Mud2. Therefore, a cycloheximide assay was performed. 125 µg/ml of cycloheximide was added to the cultures to stop mRNA translation. Samples were taken 0, 10, 30, 60 and 90 min after the addition of cycloheximide and the protein half-live was analyzed by a quantitative Western blot for Mud2. Pgk1 was used as a loading control. In *S. cerevisiae*, the protein Pgk1 has a half-life of 16.4 h (Christiano et al. 2014), which is longer than most proteins in *S. cerevisiae*. The results of the cycloheximide assay shows that the protein stability of Mud2 deceases significantly if Msl5 is depleted. In cells where Msl5 is not depleted the protein half-life of Mud2 is 149.5±41.7 min. In cells where Msl5 is depleted the half-life drops to 48.05±6.9 min.

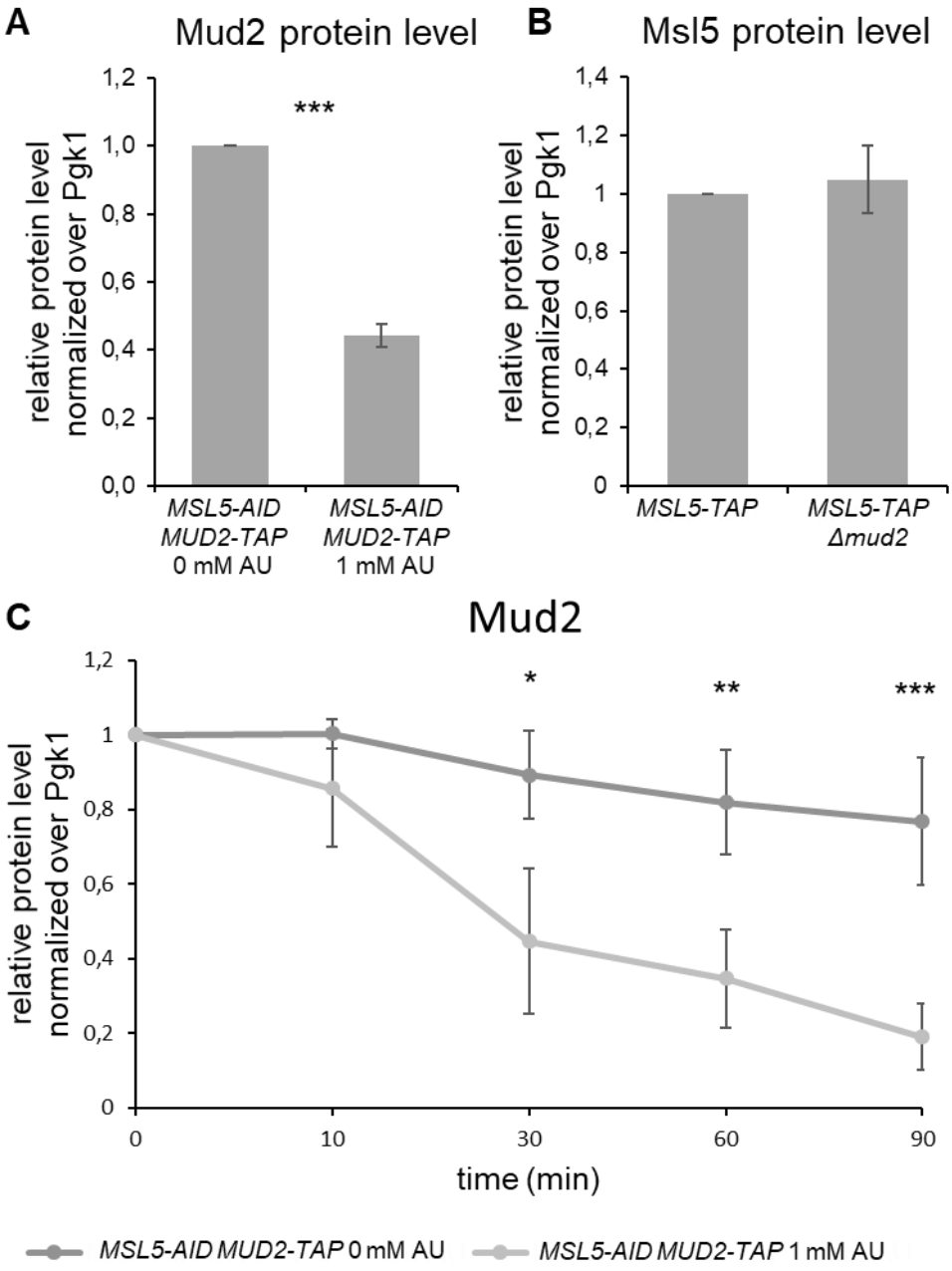

Figure 34: Depletion of Msl5 leads to reduced Mud2 levels. (A) Analyses of Msl5 in a Mud2 deletion strain compared to the wild-type strain. To quantify the protein levels of Msl5 equal amounts of cells were harvested and followed by a quantitative Western Blot analysis. Pgk1 was used as a loading control and antibody against protein A (PAP) was used to determine the protein levels of Msl5. The Western blots were quantified by FIJI (ImageJ). **(B)** Analyses of Mud2 protein levels in Msl5-depleted cells. Experiment was performed as described in A. **(C)** The protein half-live of Mud2 is decreased if Msl5 is depleted compared to the non-depleted cells. The level of Mud2-TAP was assessed by quantitative Western blot 0, 10, 30, 60 and 90 min after the addition of 125 µg/ml cycloheximide and quantified by ImageJ. Pgk1 served as a loading control.

7.2.10 In a strain with Mud2 overexpression the depletion of Msl5 leads to a reduced occupancy of Prp19C and TREX at transcribed genes

Since the depletion of Msl5 leads to reduced levels of Mud2 a strain was needed where Mud2 expression can be maintained when Msl5 is depleted. To do so *MUD2* was cloned into pRS425, a plasmid that is “high copy” in *S. cerevisiae*. Indeed, if Mud2 is overexpressed in *MSL5*-AID cells, levels of Mud2 stay high, comparable to wild-type after depletion of Msl5.

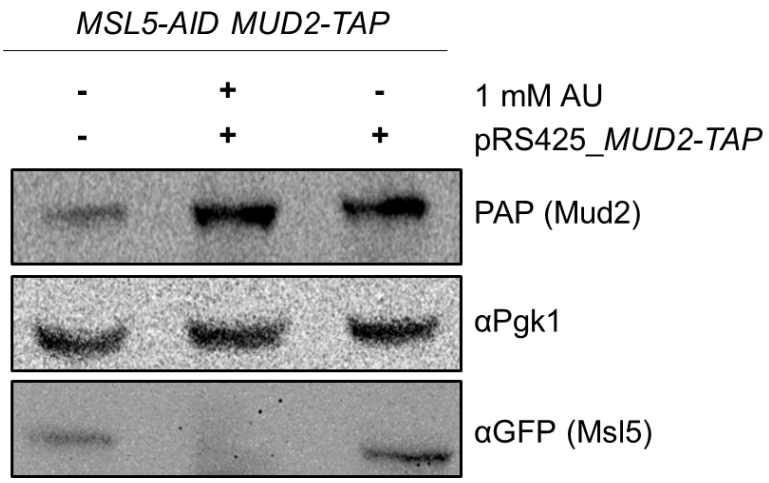

Figure 35: Overexpressen of Mud2 can rescue the loss of Mud2 if Msl5 is depleted. To detect Mud2, Mud2 were endogenously TAP-taggged in a *MSL5-AID* strain and *MUD2-TAP* on a pRS425 plasmid were transforment into a *MSL5-AID MUD2-TAP* strain. To identify the proteins the PAP antibody (*MUD2-TAP*), αPgk1 antibody (Pgk1) or αGFP antibody (Msl5) was used.

Depletion of Msl5 leads to a reduced occupancy of Prp19C and TREX at transcribed genes (Figure 31). However, depletion of Msl5 also leads to a drop of the Mud2 protein level to around 40%. As Minocha at al. (2018) showed that deletion of Mud2 leads to a reduced occupancy of Prp19C and TREX, therefore it cannot be excluded that the results are due to the loss Mud2 and not Msl5. For that reason, the ChIP in the Msl5 depletion strain was repeated with the pRS425-*MUD*2 plasmid. Changes in recruitment observed in this ChIP can be attributed to the loss of Msl5 and not to the loss of Mud2.

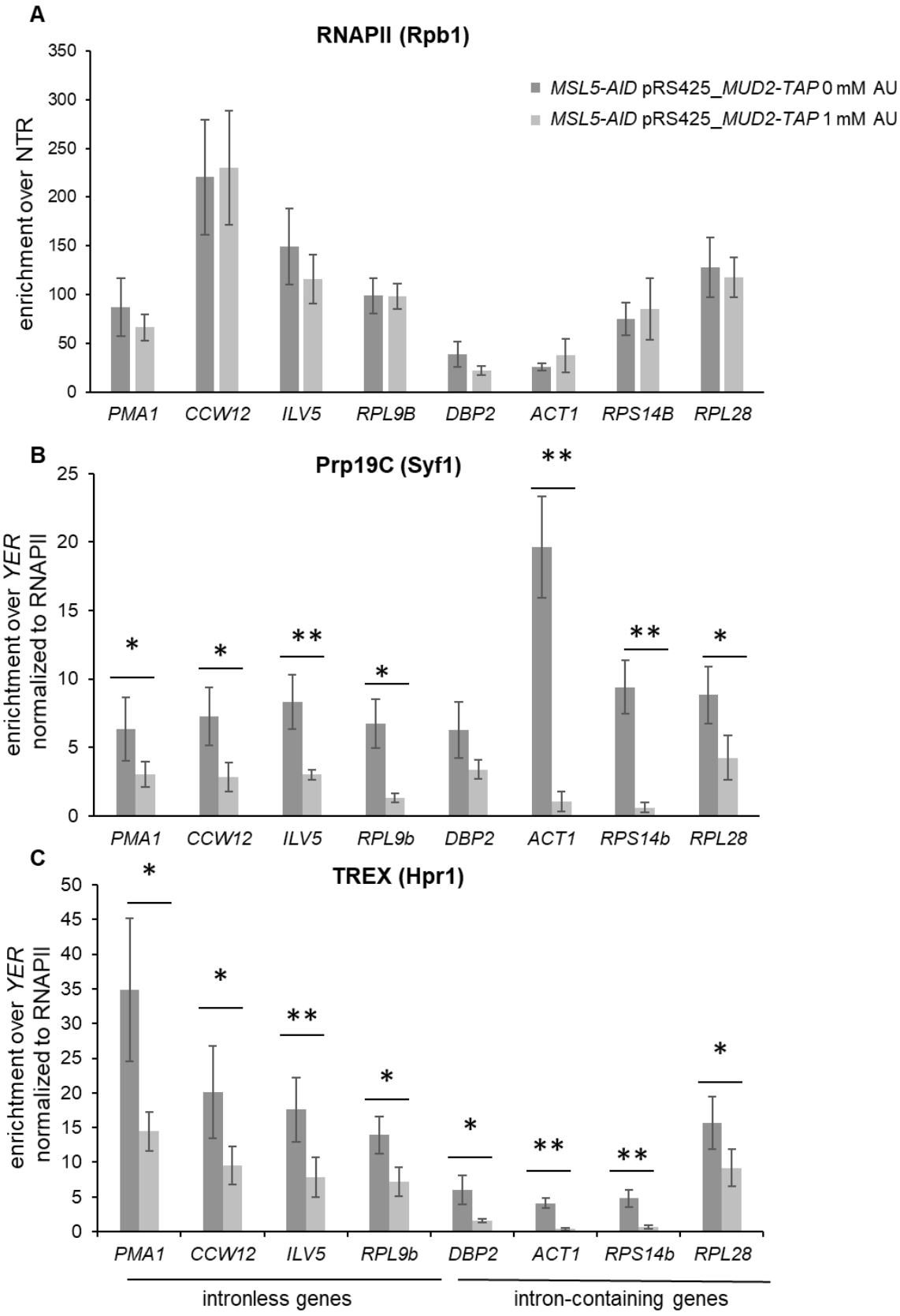

Figure 36: Msl5 is needed for full Prp19C and TREX occupancy. (**A**) RNAPII occupancy does not change when Msl5 is depleted. The occupancy of the RNAPII subunit Rpb1 was assessed in *MSL5*-AID pRS425-*MUD2* cells using chromatin immunoprecipitation (ChIP) at exemplary intron-containing (left panel) and intronless (right panel) genes. ChIPs were quantified by Real Time

PCR using the primer pairs which that bind at the 3' end of the genes as shown in Figure 15. (**B**) Prp19C occupancy normalized to RNAPII occupancy decreases in *MSL5-AID* pRS425_*MUD2* treated with 1 mM auxin at both intron-containing and intronless genes. The occupancy of Prp19C was assessed by ChIP using TAP-tagged Syf1. (**C**) TREX occupancy normalized to RNAPII decreases in *MSL5-AID* pRS425_ *MUD2* treated with 1 mM auxin. The occupancy of TREX was assessed by ChIP using TAP-tagged Hpr1.

After depletion of the Msl5 in the strain with a high copy plasmid containing Mud2, the RNAPII occupancy does not change at either intron-containing or at intronless genes (Figure 36A). This result is not surprising since the depletion of Msl5 without Mud2 overexpression also showed no difference in the occupancy of RNAPII.

In the strain in which Mud2 had wild-type protein levels and depleted Msl5 occupancy of Syf1 and presumably the whole Prp19C was still decreased at the tested transcribed genes (Figure 36B). At almost all tested genes around 50% of Prp19C is lost.

A similar pattern was observed for the TREX complex (Figure 36C). The loss of Msl5 leads to a decreased occupancy of TREX at intron-containing and intronless genes.

From these results it can be concluded that depletion of Msl5 reduces the occupancy of Prp19C and TREX. Any indirect effects due to decreased Mud2 levels can be ruled out, since Mud2 had wild-type like protein levels in these experiments. Therefore, Mud2 and Msl5 are both important for full occupancy of Prp19C and TREX.

7.2.11 mRNP composition does not change when Msl5 is depleted

Since depletion of Msl5 has an influence on the occupancy of Prp19C and TREX it was interesting to investigate, if it would also have an influence on the composition of nuclear mRNPs. To do so, a TAP purification (6.11) until TEV elution was performed. For the purification the Cbc20 was used, to purify nuclear mRNPs. After the purification some co-purified proteins including Npl3, TREX components (Hpr1, Sub2, Yra1), the mRNA exporter subunit Mex67, Tho1 and the poly(A)-binding protein Nab2 were analyzed by Western blot. Further, the lysate (after ultracentrifugation) was quantified to examine if there might be a change in proteins levels of the investigated proteins caused by depletion of Msl5.

At 30°C and depletion of Msl5 total levels of the examined proteins do not change, suggesting that Msl5 is not needed for maintaining the protein levels of Npl3, Syf1, Nab2, Tho1, Mex67, Hpr1, Sub2 or Yra1 (Figure 37A). Next, the mRNP composition were examined in a strain in which Msl5 is depleted versus a strain in which Msl5 is not depleted. Here, no change in the composition of the mRNP could be detected (Figure 37B).

From this it can be conclude that although the occupancy of Prp19C and TREX are partially impaired, the composition of the mRNP does not change.

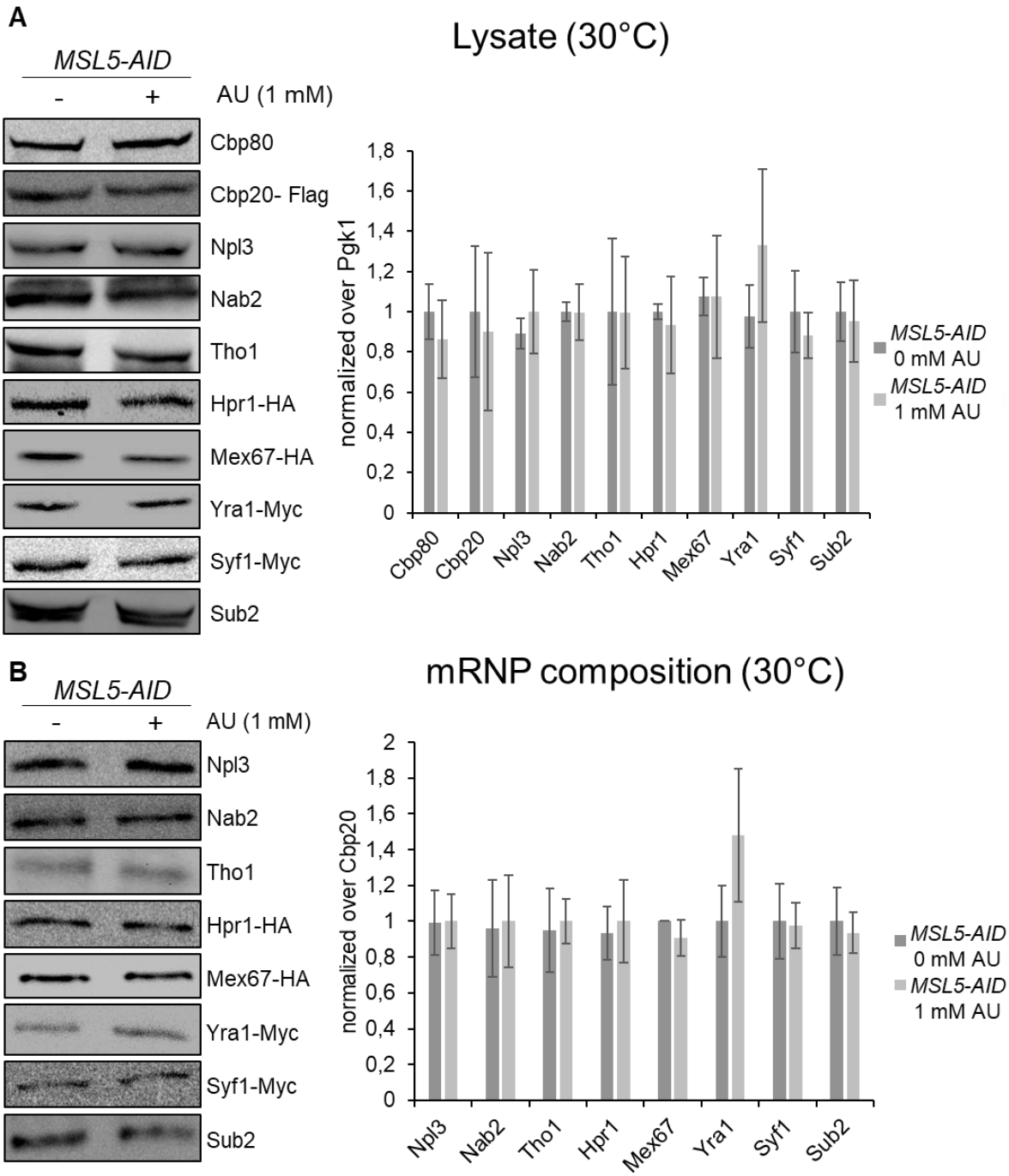

Figure 37: Depletion of Msl5 has no influence on mRNP composition at 30°C. (A) Depletion of *MSL5-AID* does not lead to a change in the examined proteins. The selected proteins were determined by Western blot and normalized to Pgk1. **(B)** Nuclear mRNPs were purified by endogenously TAP-tagged Cbp20 until the TEV eluate from *MSL5-AID* cells treated with 0 and 1 mM of AU and selected co-purifiers were determined by Western blot and quantified of at least three biological independent replicates. The quantified amounts were normalized to Cbp20.

Since there is no change of the mRNP composition at 30°C, it was interesting to investigate if there might be a change at 37°C when Msl5 is depleted. 37°C induces heat stress in *S. cerevisiae*; which forces the cell to turn on several mechanisms to compensate the heat stress.

The examined proteins do not show any changes in total levels at 37°C if Msl5 if depleted, which is the same result as at 30°C. This also suggests that Msl5 is not needed for maintaining the protein levels of Npl3, Syf1, Nab2, Tho1, Mex67, Hpr1, Sub2 or Yra1 (Figure 38A). However, the mRNP composition in a strain in which Msl5 was depleted at 37°C, the levels of Syf1 are significantly reduced. Suggesting that less Syf1 is present in the mRNP. This fits to the ChIP results, which showed that reduced occupancy of Prp19C also leads to reduced occupancy of the TREX complex.

Depletion of Msl5 leads to significantly more Mex67 and Yra1 in the mRNP composition. Indicating, that Mex67 and Yra1 somehow accumulated at the mRNP in the absence of Msl5.

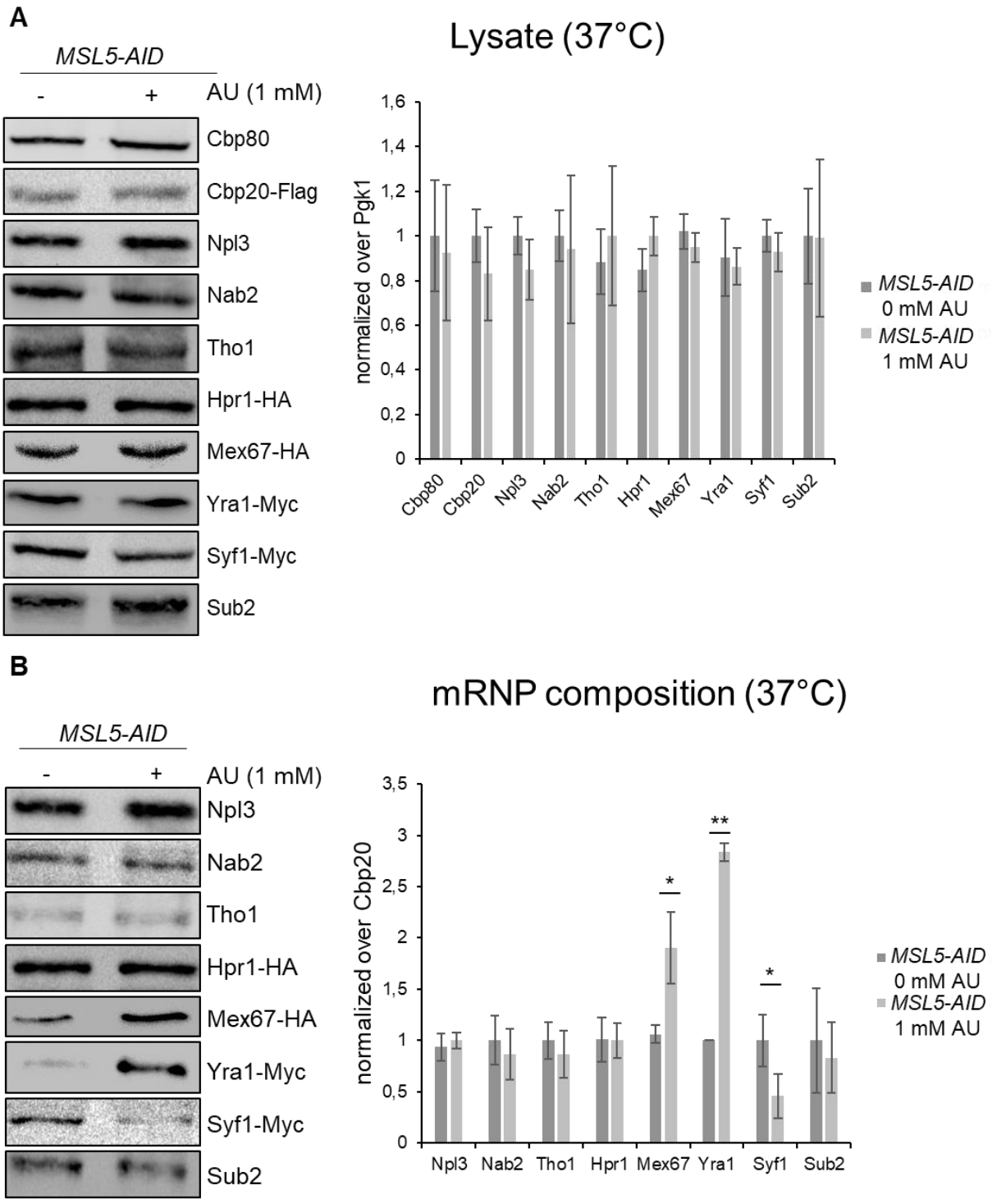

Figure 38: Depletion of Msl5 reduces Syf1 levels in the mRNP at 37°C. (A) Depletion of *MSL5-AID* does not lead to a change in the examined proteins at 37°C. The selected proteins were determined by Western blot and normalized to Pgk1. **(B)** Nuclear mRNPs were purified by endogenously TAP-tagged Cbp20 until the TEV eluate from *MSL5-AID* cells treated with 0 mM and 1 mM of AU and selected co-purifiers were determined by Western blot and quantified of at least three biological independent replicates. The quantified amounts were normalized to Cbp20.

7.2.12 Msl5 has no influence on the mRNA level or protein stability of Syf1

Next, the Syf1 mRNA levels and protein stability was examined in the absent of Msl5. Neither at 30°C nor at 37°C did the mRNA level of Syf1 change in the cells where Msl5 is depleted compared to the cells in which Msl5 is not depleted (Figure 39A). Therefore, Msl5 does not influence the mRNA level of Syf1.

To investigate if the stability of Syf1 is dependent on Msl5 a protein stability assay was performed. The depletion has neither at 30°C (Figure 39B) nor at 37°C (Figure 39C) an influence on the protein stability of Syf1.

This data show that Msl5 has no influence on Syf1 mRNA levels or Syf1 protein stability.

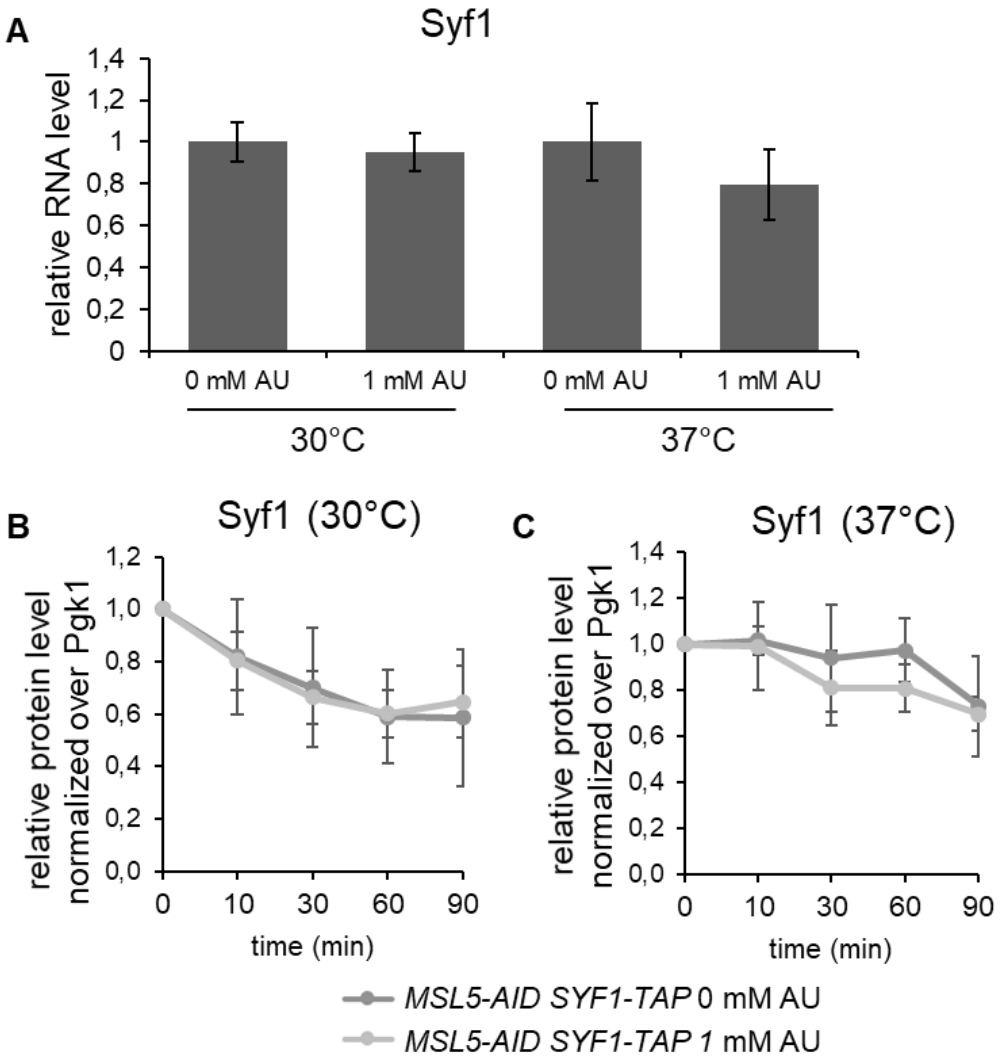

Figure 39: Syf1 protein and mRNA levels are not dependent on Msl5. (A) The mRNA levels of Syf1 are not dependent on Msl5 at 30°C or 37°C. Equal amounts of yeast cells were harvested during their exponential growth phase followed by RNA isolation. 100 ng of RNA was used for the

synthesis of cDNA and the amount of cDNA was determined by qPCR. **(B&C)** The protein half-life of Syf1 is not influenced if Msl5 is depleted when compared to the non-depleted cells at 30°C (B) and 37°C (C). The level of *SYF1-TAP* was assessed by quantitative Western blot analysis at different time points 0, 10, 30, 60 and 90 min after the addition of 125 µg/ml cycloheximide and quantified by ImageJ. Msl5 was depleted 1 h before the addition of cycloheximide. Pgk1 served as a loading control.

7.2.13 Depletion of Msl5 leads to nuclear poly(A) RNA dots in the nucleus at 37°C

Since the depletion of Msl5 leads to a reduced occupancy of Prp19C and TREX at transcribed genes, it was interesting to investigate if the depletion of Msl5 would lead to functional consequences during mRNA export. To visualize the poly(A) RNA, a fluorescence *in situ* hybridization (FISH) using an oligo(dT50) probe coupled to Cy3 at 30°C and 37°C was performed.

At 30°C no accumulation in the nucleus neither in the non-depleted cells nor in the depleted cell (Figure 40).

However, at 37°C poly(A) RNA dots accumulate in the nucleus when Msl5 is depleted. In cells where Msl5 is not depleted, no effect is visible at 37°C (Figure 40). Therefore, the accumulated dots in the nucleus are due to the depletion of Msl5.

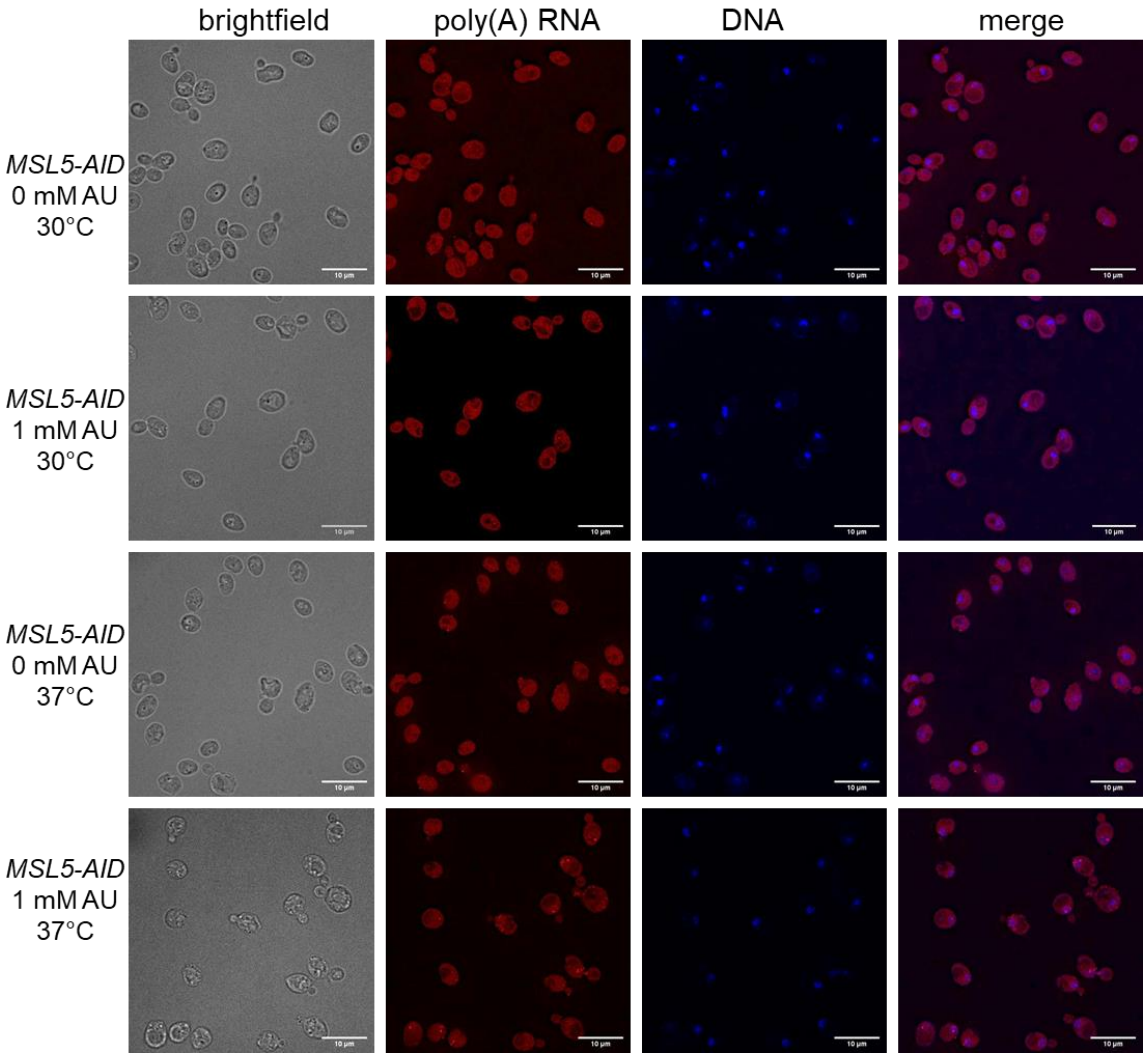

Figure 40: Depletion of Msl5 induces formation of nuclear poly(A) RNA dots at 37°C. Poly(A) RNA was visualized by oligo(dT50) coupled to Cy3-fluorecent dye in red. DNA was stained with DAPI in blue to locate the nucleus. Cells were either grown at 30°C or shifted to 37°C for one hour, the depletion of Msl5 was performed for one hour during the incubation at 30°C or 37°C.

7.2.14 Depletion of Msl5 leads to a change of Mex67 localization

Since the depletion of Msl5 leads to an accumulation of poly(A) RNA in in the nucleus it was interesting to investigate how this is occurring. Mex67 is the export receptor during the export of nuclear mRNA. Therefore, localization of Mex67 might be altered if Msl5 is depleted.

To analyze localization of Mex67, I deleted the endogenous gene and inserted a plasmid fluorescently tagged Mex67.

At 30°C the non-depleted cells had the typical rim staining for Mex67. If Msl5 was depleted the Mex67 rim staining was lost in many cells (Figure 41A). In the non-depleted cells, 82.8±3.8 % cells showed rim staining, whereas only 32.6±9.5 % of the cells had Mex67 rim staining (Figure 41B).

As a control wild-type cells were examined as well at 30°C there is no detectable difference depending on the treatment (0 mM or 1 mM AU), with 81.0±3.9 % of control cells having rim staining and 75.9±10.1 % under 1 mM AU conditions (Figure 41C).

At 37° the same effects appear for *MSL5-AID* and wild-type cells. *MSL5-AID* cells with 0 mM of AU show 86.5±1.5 % of Mex67 rim staining and with 1 mM of AU only 35.8±8.8 % of the cells have Mex67 rim staining (Figure 41D).

In wild-type cells at 37°C 82.1±2.1% have Mex67 rim staining, after addition of 0 mM AU and after the addition of 1 mM of AU 80.0±3.5 % of the cells have Mex67 rim staining (Figure 41E).

From this data it can be concluded that the depletion of Msl5 leads to a miss-localization of Mex67 in the cells.

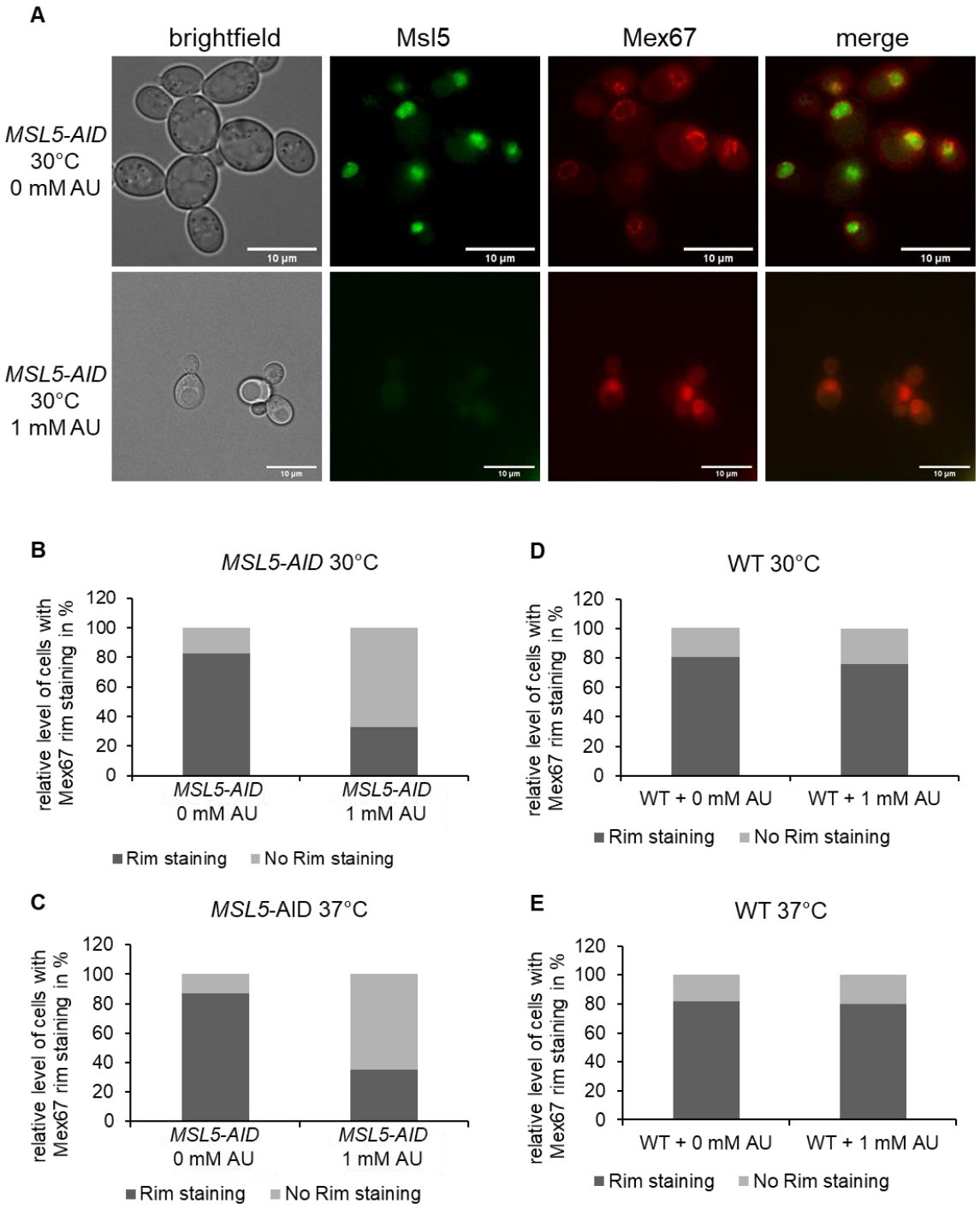

Figure 41: Mex67 miss-localizes in cells when Msl5 is depleted. (A) Representative microscopy images of cells treated with 0 mM AU or 1 mM AU. Mex67 is tagged with mCherry and therefore appears in red. Msl5 is endogenously tagged with a GFP and therefore appears green, after the treatment with 1 mM AU Msl5 is depleted and not detectable. (**B**) Analysis of at least 3 independent experiments of Msl5-AID cells at 30°C. From each experiment, at least 30 cells where counted and rim staining was determined. For 0 mM AU 82.8±3.8 % of cells showed rim staining and 17.3±3.8 % of cells showed no rim staining. After the treatment with 1 mM AU 32.6±9.5 % of the cells showed rim staining and 67,5±9,5 % of the cells showed no rim staining. (**C-E**) Calculations of the rim staining were calculated as described in B. (**C**) In wild-type cells at 30°C and treatment with 0 mM AU 81.8±3.9 % of cells showed rim staining and 19.7±3.1 % of cells showed no rim staining. After treatment with 1 mM AU 75.9±10.1 % of the cells showed rim staining and 24.1±10.1 % of the cells showed no rim staining. (**D**) In *MSL5*-AID cells at 37°C for

treatment with 0 mM AU 86.8±1.5 % of cells had rim staining and 13.2±1.5 % of cells showed no rim staining. After the treatment with 1 mM AU 35.0±8.8 % of the cells had rim staining and 65.0±8.8 % of the cells showed no rim staining. (**E**) In wild-type cells for treatment with 0 mM AU 82.0±2.1 % of cells showed rim staining and 18.3±1.7 % of cells showed no rim staining at 37°C. After the treatment with 1 mM AU 80.0±3.5 % of the cells had rim staining and 20.0±3.5 % of the cells showed no rim staining.

7.2.15 Depletion of Msl5 does not affect the mRNA levels and protein stability of Mex67 and Yra1

Since the depletion of Msl5 influences the localization of Mex67 the question arose if the depletion of Msl5 changes the mRNA level or protein stability of Mex67. Since Yra1 interacts with Mex67 and is important for the recruitment of Mex67-Mtr2 dimer to the mRNP Yra1 and Mtr2 were further investigated regarding a change in the mRNA level or protein stability as well.

The mRNA level of *YRA1* does not change in cells were Msl5 is depleted compared to non-depleted cells at 30°C or 37°C (Figure 42A). Therefore, it can be excluded that the Mex67 localization is changed due to reduced Yra1. Further Yra1 was especially interesting since it contains an intron, therefore it was important to rule out a change in mRNA levels due to a depletion of Msl5.

The mRNA level of Mex67 also does not change if Msl5 is depleted. The temperature shift to 37°C has no influence on the mRNA level of Mex67 (Figure 42B).

Further, the mRNA level of Mtr2 were interesting to investigate since Mtr2 has an intron in its 5’ UTR which could influence the mRNA level of Mtr2 when Msl5 is depleted. Another reason why Mtr2 was investigated is that Mex67 and Mtr2 built a dimer and therefore a change in Mtr2 could affect Mex67. However, the depletion of Msl5 has no influence on the mRNA level of Mtr2 at neither 30°C nor at 37°C (Figure 42C).

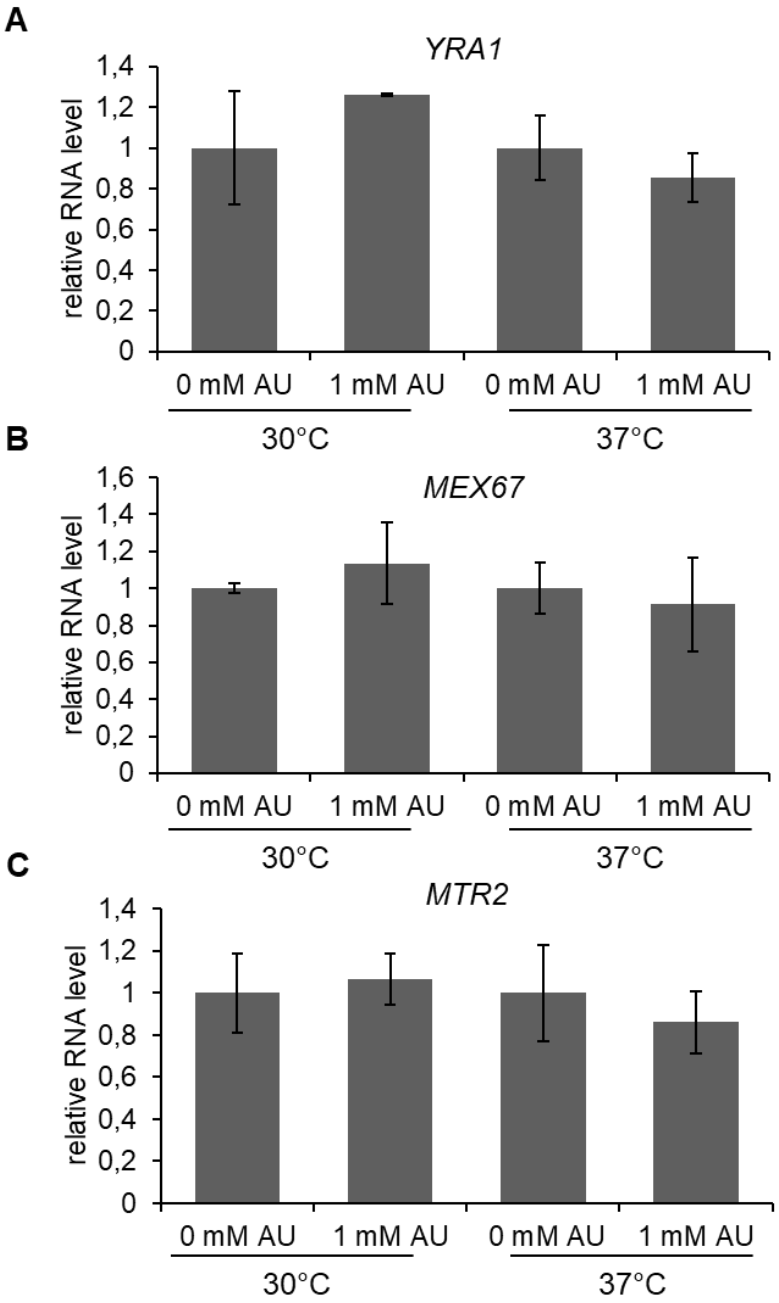

Figure 42: Depletion of Msl5 has no influence at the mRNA level of Yra1, Mex67 or Mtr2. Equal amounts of yeast cells were harvested during their exponential growth phase followed by RNA isolation. 100 ng of RNA was used for the synthesis of cDNA using oligo(dT) and the amount of cDNA was determined by qPCR using primers against the 3' region of Yra1 (**A**), Mex67 (**B**) and Mtr2 (**C**).

Whereas the mRNA of Mex67, Yra1 and Mtr2 are not influenced by the depletion of Msl5 It was interesting to investigate if the protein stability of Yra1 or Mex67 changes when Msl5 is depleted.

To measure protein half-lives, a cycloheximide assay was performed at 30°C and 37°C.

At 30°C, the protein stability of Mex67 and Yra1 is not influenced by the depletion of Msl5. The same was observed at 37°C, with no difference in the protein stability of Mex67 or Yra1 detectable.

Taken together the change in the Mex67 localization is not due to a change of mRNA level of Yra1, Mex67 or Mtr2. In addition, the depletion of Msl5 does not influence the protein stability of Mex67 or Yra1.

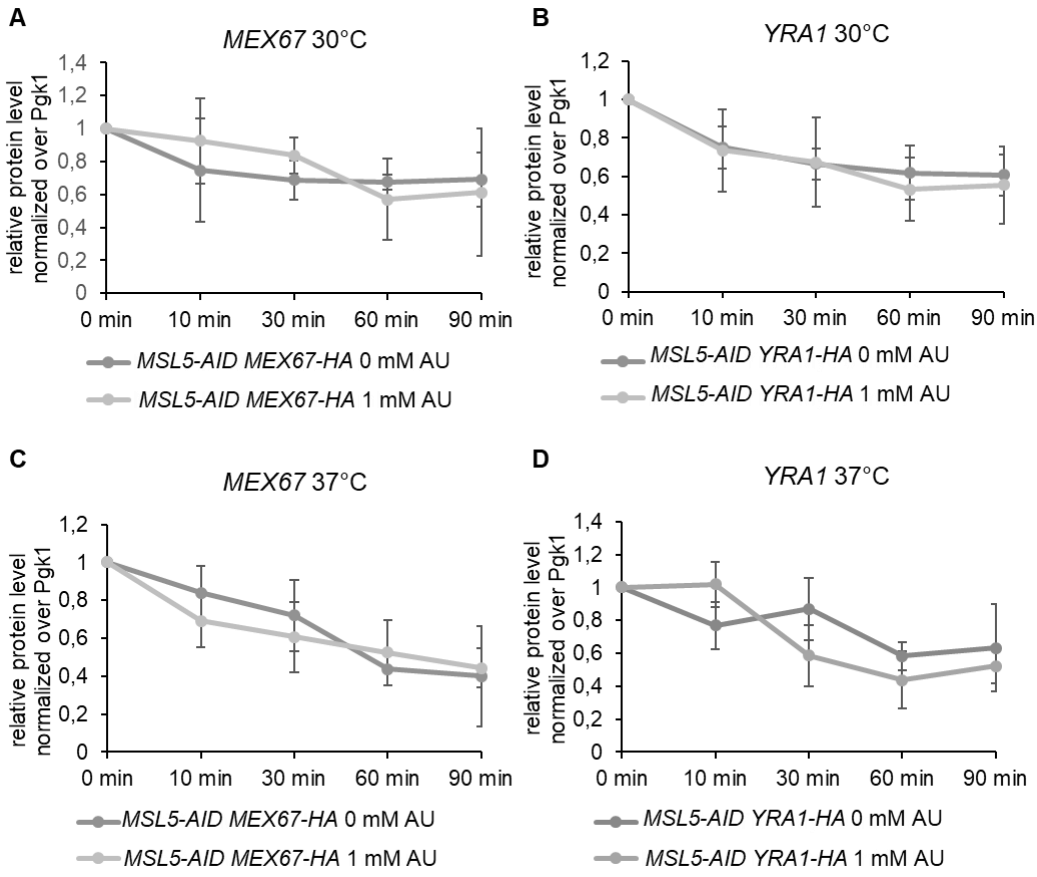

Figure 43: The protein half-lives of Mex67 or Yra1 are not influenced if Msl5 is depleted. Yra1 was examined at 30°C (**A**) and 37°C (**C**) and Mex67 at 30°C (**B**) and 37°C (**D**). The level of *MEX67-HA* and *YRA1-HA* was assessed by quantitative Western blot analysis at timepoints 0, 10, 30, 60 and 90 min after the addition of 125 µg/ml cycloheximide and quantified by ImageJ. Pgk1 served as a loading control.

8 Discussion

8.1 The non-essential proteins of the Prp19C have various roles in the cells

In *S. cerevisiae*, Prp19C is mostly known for its role during splicing. It is known that the Prp19 and TREX complexes interact with each other but the molecular details of the interaction are not understood. Prp19C interacts with THO *in vivo* in an RNA-independent manner (Chanarat, Seizl, and Strässer 2011), further it could be shown that THO and Prp19C also interact directly *in vitro* with each other (Minocha 2018).

In this study, I investigated the role of the non-essential proteins of Prp19C, namely Cwc15, Isy1, Ntc20, Syf2 and Snt309 during transcription elongation. Additionally, I investigated if deletion of any of those non-essential proteins lead to a change of RNAPII, Prp19C and TREX occupancy at transcribed genes. Furthermore, I wanted to examine if any of the non-essential proteins are important for the stable interaction of Prp19C-TREX, Prp19C-Mud2 and Prp19C-RNAPII.

8.1.1 Ntc20 has no function during transcription elongation

Ntc20 is a non-essential protein of the Prp19C but the deletion of *NTC20* combined with the deletion of *ISY1* leads to impaired cellular growth. This indicates that *ISY1* and *NTC20* might be functionally redundant (Chen et al. 2001). Ntc20 also forms a subcomplex within the Prp19C with Syf1, Isy1 and Syf2. This is an indication that one protein of the subcomplex might compensate if another protein of the subcomplex is missing (Chen et al. 2002). Deletion of *NTC20* leads to more transcription *in vivo*, the same effect can be observed if *ISY1* is deleted (Figure 18C). This shows again that the proteins may have overlapping functions in the cells. Surprisingly the whole cell levels of Rbp1 decrease slightly but significantly in cells were *NTC20* is deleted (Figure 7C), but this has no influence on the occupancy of Rbp1 at transcribed genes. Further the deletion has no influence on TREX occupancy (Figure 16) or the interaction of Prp19C with the TREX complex (Figure 9).

Taken together, Ntc20 appears to have no direct impact on transcription elongation. However, the observed enhanced rate of transcription elongation *in vivo* could potentially be attributed to its overlapping functions with Isy1.

8.1.2 The non-essential protein Snt309 is important for the stability of Prp19C

Snt309 is a known splicing factor as deletion of *SNT309* leads to an accumulation of pre-mRNA (Chen et al. 1999). Although this protein is not needed for the vegetative growth of *S. cerevisiae* at 30°C, however, a deletion of *SNT309* leads to death of the cells at 37°C (Figure 17). Knockdown of Spf27, the human orthologue of Snt309, destabilizes the entire Prp19C and leads to specific mitotic defects in human cells (Hofmann et al. 2013). Interestingly, Snt309 only directly binds to Prp19, it plays a crucial role in stabilizing the entire Prp19C complex (Chen et al. 1998).

In this study I could show that the deletion of *SNT309* leads to several severe effects that can be explained by a destabilization of the whole Prp19C. The deletion of *SNT309* leads to a decreased interaction of the Prp19C with Mud2, RNAPII and TREX (Figure 8 and Figure 9). In addition, RNAPII and Prp19C occupancy at transcribed genes is reduced in *SNT309*-deleted cells which can be also due to a destabilized Prp19C (Figure 16).

In summary, deletion of *SNT309* elicits many effects, which in the end can be explained by a destabilization of the Prp19C. Therefore, my hypothesis would suggest that Snt309 does not possess a role in transcription elongation, but instead serves an important function within the Prp19C itself.

8.1.3 Isy1 is needed for the full occupancy of Prp19C and TREX at transcribed genes

Deletion of *ISY1* has no influence on the vegetative growth of *S. cerevisiae* but leads to a lower splicing efficiency (Dix et al. 1999; Villa and Guthrie 2005).

In the absence of Isy1 occupancy of RNAPII is increased (Figure 16B). This could be due to different reasons; more initiation events are possible or due to RNAPII stalling the occupancy of RNAPII is higher. However, the *in vivo* experiment where the efficient

transcription was determined (Figure 18C) showed that two galactose-induced genes (*GAL10* and *ACT1*) are transcribed in higher amounts (Figure 18C), this result rules out RNAPII stalling, since this would lead to lower levels of mRNA levels in cells where *ISY1* is deleted compared to wild-type cells. Despite the increased occupancy of RNAPII in the absence of Isy1, the occupancy of Prp19C at transcribed genes decreases significantly (Figure 16C). The question arises why the occupancy of Prp19C decreases even though the occupancy of RNAPII increases, which is an important recruitment platform for Prp19C. Therefore, Isy1 is needed for the occupancy of Prp19C at transcribed genes. In addition to RNAPII, the occupancy of Prp19C at transcribed genes is depended on Mud2. However, when Prp19C is purified in the absence of Isy1, more Mud2 co-purified with Prp19C than in wild-type cells, indicating that the deletion of *ISY1* leads to a stronger interaction with Mud2 (Figure 8B). The reason for this could be that there might be a third protein which is important for the occupancy of Prp19C and the deletion of *ISY1* disturbs this interaction and/or since Isy1, Ntc20, Syf2 and Syf1 form a subcomplex within the Prp19C, the complex might be destabilized (Chen et al. 2002). To investigate this further it would be important to design mutants of Isy1. Since Isy1 interacts with Syf1 directly it would be interesting to investigate what happens if this interaction is disturbed by mutating Isy1. If the interaction of Syf1 to Isy1 is disrupted, it would not be unexpected to observe a decrease in the occupancy of Prp19C at transcribed genes. Thus, any disturbance in the interaction of Isy1 with Syf1 could potentially affect the stable association of Prp19C with the transcription machinery, leading to a decrease in Prp19C occupancy at transcribed genes (Chanarat, Seizl, and Strässer 2011; Vincent et al. 2003).

It is not surprising that the occupancy of TREX is also highly reduced in cells where *ISY1* is deleted, since Prp19C is important for the stabilization of TREX at transcribed genes (Figure 16D).

Taken together, *ISY1* has an additional function in the gene expression, namely in maintaining Prp19C and TREX occupancies at transcribed genes. The exact mechanism behind this function is still unclear and needs to be found out.

8.1.4 Cwc15 and Syf2 have a role in transcription elongation and Prp19C / TREX occupancy

Syf2 forms a subcomplex within the Prp19C with Isy1, Ntc20 and Syf1. These four proteins have redundant functions: If one of them is missing the other proteins can compensate for its absence to a certain degree (Chen et al. 2001; Chen et al. 2002). Cwc15 is not a core component in *S. cerevisiae* Prp19C but rather loosely associated. However, the human orthologue of Cwc15, AD002, is a core component of Prp19C (Grote et al. 2010). To unravel if the deletion of *Δcwc15* and/or *Δsyf2* affects the interaction between the Prp19C and TREX I investigated this interaction further.

Deletion of *CWC15* or *SYF2* lead to a decrease in the whole cell levels of Hpr1, if Hpr1 contains a C-terminal TAP-tag (Figure 9C and D). This effect was unexpected, and is not seen if any of the other non-essential proteins of the Prp19C are deleted. It is a rare phenomenon that the deletion of a protein has such a high influence on a protein from another protein complex.

Deletion of either *CWC15* or *SYF2* leads to weaker interaction (*Δcwc15*: 40%; *Δsyf2*: 80%) between Prp19C and TREX compared to wild-type (Figure 9A and B). In a double deletion strain of *Δcwc15 Δsyf2*, the interaction of Prp19C and TREX is reduced to around 30% compared to wild-type levels (Figure 10A and B). This additive effect of the deletion of *CWC15* and *SYF2* on the interaction of Prp19C and TREX suggests that these proteins both contribute to this interaction. At 37°C a double deletion of *CWC15* and *SYF2* lead to synthetic lethality (Figure 17), this again indicated a genetic interaction of Cwc15 and Syf2. In addition, Hpr1-TAP migrates faster in an SDS gel in the absence of Cwc15 or Syf2. In the double deletion strain *Δcwc15 Δsyf2*, only the faster migrating version of Hpr1-CBP was detectable (Figure 10A). In strains where Hpr1 was N-terminally TAP-tagged the faster migrating signal was not detectable; however, the weaker interaction between Prp19C and TREX was the same (Figure 11).

Since mass spectrometry data showed that the faster migrating variant of Hpr1 is still full-length Hpr1, the divergent migration of Hpr1 was likely to come from a modification of Hpr1. Hpr1 is polyubiquitylated by Rsp5 and then degraded by the 26S proteasome (Gwizdek et al. 2005). The polyubiquitylation of Hpr1 interacts with the ubiquitin-associated (UBA) domain of the mRNA exporter Mex67 and therefore promotes the co-transcriptional recruitment of Mex67. At 37°C Hpr1 is not stable due to its polyubiquitylation by Rsp5, whereas in a *Δrsp5* strain Hpr1 is much more stable (Gwizdek et al. 2005). In a *Δcwc15 Δsyf2* strain, Hpr1 is significantly more stable at 37°C,

suggesting that the deletion of *CWC15* and/or *SYF1* leads to less polyubiquitylation of Hpr1. This could be confirmed in the Western blot analysis of the purified THO complex using an antibody against ubiquitin (Figure 12A-C). However, it is still unclear why the protein amount of *HPR1-CBP* is reduced at 30°C in the single mutants and double mutant of *Δcwc15* and *Δsyf2*. It could be shown that at 30°C the protein amount of *HPR1-TAP* is in the *Δcwc15 Δsyf2* strain at the same level as in the wild-type (Figure 12), indicating that at 30°C *HPR1-TAP* does not get ubiquitinylated as at 37°C. The lower protein levels in the *Δcwc15* and *Δsyf2* deletion strains are presumably not due to less ubiquitination of *HPR1-TAP* and therefore still need to be investigated.

Deletion of *HPR1* leads to a nuclear mRNA export defect (Strässer et al. 2002). Since its interaction with the mRNA exporter Mex67 depends on polyubiquitylation of Hpr1, it was interesting to investigate if the deletion of *CWC15* and *SYF2* would evoke an mRNA export defect. However, the double deletion of *CWC15* and *SYF2* does not induce an export defect neither at 30°C nor at 37°C, indicating that the export defect in *Δhpr1* cells is not caused by the missing or weaker interaction of Hpr1 and Mex67, but indeed by the disturbed THO complex.

Moreover, I found that Syf2 is required for the full occupancy of Prp19C at transcribed genes (Figure 16C). This could be due to the fact that Syf2 is part of a subcomplex within the Prp19C (Syf2, Isy1, Ntc20 and Syf1). For Isy1, and at most genes also for Ntc20, the occupancy of the Prp19C is also reduced if one of these proteins is missing. Consequently, Syf2 is needed for full Prp19C occupancy.

In the *Δcwc15* strain neither the RNAPII nor the Prp19C occupancy changes (Figure 16B and C), whereas the occupancy of TREX is reduced. Therefore, Cwc15 is needed for the full occupancy of TREX (Figure 16D). Cells in which *CWC15* is deleted are also slightly more sensitive to 6-azaurcil than wild-type cells. Combined with the deletion of *DST1,* the cells are almost dead on 6-azaurcil (Figure 18A). mRNA synthesis is also impaired in cells where *CWC15* is deleted if compared to wild-type cells in an *in vivo* transcription assay (Figure 18C).

In summary, I found that Syf2 and Cwc15 have an overlapping function in ensuring efficient transcription elongation. Both proteins are needed for normal polyubiquitylation levels of Hpr1. In the future, it will be interesting to investigate if Cwc15 and Syf2 directly interact with each other, and whether they interact directly with Hpr1. To investigate this, these three proteins need to be purified independently and the interaction tested *in vitro* to exclude an involvement of other proteins.

8.2 The role of Msl5

Msl5 is a well-known splicing factor. In human cells, its orthologue is *SF1* (Abovich and Rosbash 1997; Berglund, Abovich, and Rosbash 1998). Mud2 has a role in transcription elongation and binds directly to Msl5 (Chang, Schwer, and Shuman 2012; Minocha et al. 2018). PAR-CLIP analysis showed that Msl5 also interacts with intronless mRNAs, raising the question why Msl5 binds to intronless mRNAs and what role it fulfils at intronless genes (Baejen et al. 2014).

8.2.1 The interaction of Msl5 and Mud2

The interaction of Msl5 and Mud2 is conserved form yeast to man (Abovich and Rosbash 1997). In early spliceosome assembly, the U1 snRNP binds to the 5' splice site of the pre-mRNA whereupon U1 interacts with the branchpoint-binding protein Msl5. Msl5 binds to Mud2 and Mud2 is bound to the 3' splice site (Wang et al. 2008). Msl5 and Mud2 form a heterodimer in stoichiometry 1:1 (Wang et al. 2008).

Msl5 is an essential protein whereas Mud2 is not essential. From this it is clear that the interaction between Msl5 and Mud2 is not necessary for their involvement in splicing. The interaction domain of Msl5 with Mud2 in Msl5 (*msl5 Δ34-56*) is not an essential part of Msl5 (Chang, Schwer, and Shuman 2012). However, the deletion of this domain leads to a destabilization of Mud2 (Figure 33). The deletion of Mud2 has no influence on Msl5 levels (Figure 33). This suggests that Mud2 has an auxiliary role for Msl5.

To investigate how important the interaction of Mud2-Msl5 is, a mutant would be needed where this interaction cannot longer be formed. Since the mutation of Msl5 leads to lower protein levels of Mud2, a mutation in Mud2 would be needed. Chang et al. (2012) solved a crystal structure of Msl5 and Mud2 that implicates the RRM3 domain of Mud2 in the interaction with Msl5. However, by using a mutant of Mud2 where the RRM3 domain is missing further defects could occur besides the loss of the interaction between Msl5 and Mud2. Therefore, it is important to use appropriate controls when using a *mud2-ΔRRM3* mutant. This needs to be examined in Mud2's role in splicing and also in transcription elongation.

The occupancy of Msl5 and Mud2 is dependent on each other (Figure 25). For Mud2 this is not surprising since the protein levels and protein stability of Mud2 depended on Msl5 (Figure 34B). However, the protein levels of Msl5 are not dependent on Mud2. Therefore,

it would be interesting to investigate if the occupancy of Msl5 also decreases at transcribed genes if Mud2 and Msl5 are not able to interact with each other. From this data it could be concluded if Mud2 or Msl5 recruits the other protein to the transcribed genes or the mRNA itself recruits Msl5 or Mud2 to the transcribed gens (Figure 28).

It is also interesting to note that a strain where Mud2 is deleted and Msl5 is mutated by addition of the AID-tag has a growth defect even if the deletion of Mud2 or the mutation of Msl5 by itself does not (Figure 23). Further, in a strain where Msl5 is depleted and Mud2 is deleted RNAPII occupancy is reduced (Figure 22B), therefore mRNA is presumably less synthesized. Thus, Msl5 and Mud2 can compensate this effect since if Msl5 or Mud2 are lacking no effect on RNAPII occupancy is detectable (Minocha et al. 2018 and Figure 22A).

8.2.2 Msl5 has a function in transcription

For nearly three decades, the role of Msl5 and Mud2 in splicing has been known. The heterodimer is known for the interaction with the branchpoint of the intron, and therefore they have an important role in the activation of splicing. Moreover, it was found that Msl5 and Mud2 interact with the CTD of RNAPII to facilitate the recruitment of Prp19C to the spliceosome (David et al. 2011; Abovich and Rosbash 1997).

Minocha et al. (2018) showed that Mud2 has a function in transcription by maintaining Prp19C and TREX occupancies at transcribed genes. The analysis of PAR-CLIP data revealed that Msl5 is more abundant at intronless genes than Mud2 (Baejen et al. 2014). For this reason, it was interesting to elucidate if Msl5 has a role in transcription. If that is the case, it would be intriguing to investigate whether Msl5 shares similar functions as Mud2 or if it has additional roles yet to be discovered. The first evidence is that Msl5 binds to intronless and intron-containing genes in a transcription-dependent manner (Figure 19 and Figure 20).

The recruitment of TREX is mediated by the direct binding of the THO subcomplex to the S2/S5 di-phosphorylated CTD (Meinel et al. 2013). Mud2 is recruited to transcribed genes through S2 phosphorylation (Minocha et al. 2018). However, Mud2 and Msl5 are also recruited to the RNA in an RNA-dependent manner (Figure 28). Msl5 is recruited to the DNA in an S5P-dependent manner (Figure 27), which is interesting since it suggests that Msl5 is recruited to the nascent mRNA before Mud2 since the S5 phosphorylation occurs during transcription initiation and S2 phosphorylation occurs and increases during

transcription elongation (Zhang et al. 2012). It is already known that the S5-phosphorylated CTD interacts with the spliceosome; however, it is the U5 snRNP that is enriched by the S5 phosphorylation, whereas the U1 snRNP is only detected at low levels in mammalian native elongating transcript sequencing (mNET-seq) of S5 phosphorylation (Nojima et al. 2018). At the time the U5 snRNP enters the spliceosome, Msl5 has already left the spliceosome, therefore the recruitment of Msl5 *via* the S5 phosphorylation is presumably due to another purpose than for Msl5's purpose during splicing.

In *S. cerevisiae*, Prp19C is needed for full transcription activity and it ensures the full occupancy of TREX at transcribed genes (Chanarat et al. 2012). The loss of Mud2 leads to a loss of Prp19C and also a loss of TREX from transcribed genes (Minocha et al. 2018). Thus, it was interesting to investigate if Msl5 has a similar role by the stabilization of Prp19C and TREX at transcribed genes. Depletion of Msl5 leads to a reduced occupancy of Prp19C/TREX, even when Mud2 levels are constant (Figure 36A). It could also be shown that in cells where Msl5 is depleted at 37°C the level of Syf1 and therefore presumably the whole Prp19C are reduced in the mRNP (Figure 38B). This also indicates that Msl5 and Prp19C interact with each other in a direct or indirect manner. In the Msl5 depletion strain the occupancy of TREX is, as expected, also reduced.

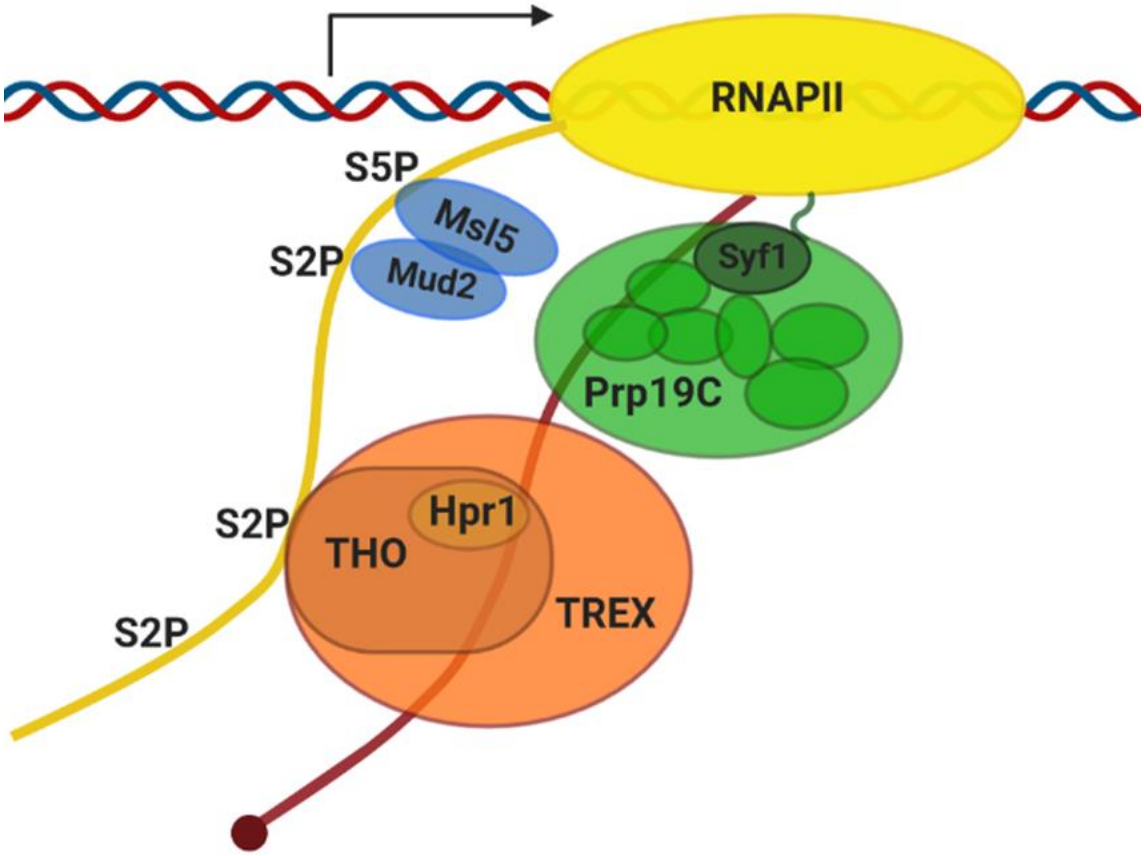

Figure 44: Schematic model of Msl5's involvement in transcription elongation. Msl5 interacts with the S5-phosphorylated CTD, and Mud2 interacts with the S2-phosphorylated CTD of RNAPII. Mud2 and Msl5 interact with Prp19C and are required to maintain Prp19C at transcribed genes. Prp19C in turn is necessary to maintain TREX occupancy, which also interacts with the S2-phosphorylated CTD.

From these results it can be concluded that Msl5 recruits/stabilizes Mud2, Prp19C and therefore TREX at transcribed genes. Thus, Msl5 has an additional function in transcription elongation.

8.2.3 Msl5 and its role in mRNA export

In this study, a first indication could be made that Msl5 seems to have a role in transcription in addition to its role in splicing (8.2.2). Further, the question arises if the loss of Msl5 impairs mRNA export and whether this depends on its role in splicing or in transcription. Minocha et al. (2018) showed that although Mud2 has a role in transcription elongation the deletion of Mud2 does not lead to an mRNA export defect. Also, a mutant of Syf1, which also has a role in transcription elongation, does not show an mRNA export defect (Chanarat 2011). The depletion of Msl5 leads to an mRNA export defect in form

of nuclear dots at 37°C (Figure 40). These dots appear to be mostly at the nuclear rim. To investigate this further it is necessary to identify the proteins that co-localize with the nuclear dots. If this question is answered it is easier to identify if these dots appear due to the role of Msl5 in splicing or to its role in transcription. To investigate this, I would propose Immunofluorescence (IF), to look either at splicing factors or at transcription factors.

Two different models have been proposed to explain how the cells retain intron-containing mRNA at nuclear pores. The “selection model” and the “retention model”, with Msl5 playing a role in the retention model. In the retention model, proteins specifically bind to faulty mRNPs and are recognized by the nuclear basket. This interaction would then trigger their retention in the nucleus (Bonnet and Palancade 2015). Since Mlp1 has been reported to interact with Msl5 in an RNA-dependent manner, it is possible that Msl5 has a role in mRNA retention (Galy et al. 2004). Pml1, which is a subunit of the Retention and Splicing (RES) complex, was shown to contribute to Mlp1/Pml39-mediated pre-mRNA retention (Palancade et al. 2005; Dziembowski et al. 2004). Therefore, I would also suggest to perform IF of Pml1. If Pml1 co-localized with the nuclear mRNA dots, this would be a strong indication that the dots emerge from unspliced mRNAs.

The depletion of Msl5 changes the mRNP composition at 37°C. It leads to higher levels of Mex67 and Yra1 (Figure 38). Since it is reported that the SR-proteins Gbp2 and Hrb1 recruit Mex67 upon completion of splicing (Hackmann et al. 2014), the increased levels of Mex67 and Yra1 in the mRNP during the absence of Msl5 is presumably not due to unspliced mRNAs. The depletion of Msl5 leads to a mislocalization of Mex67. In the presence of Msl5, Mex67 is located around the nuclear rim; however, if Msl5 is depleted the Mex67 rim staining vanishes and Mex67 is located throughout the nucleus (Figure 41). To investigate if these effects are due to the role of Msl5 in splicing, other splicing factors could be deleted/depleted. If Mex67 stayed within the “typical” rim-staining and the mRNP composition remained the same, this would be a first indication that these effects are due to the role of Msl5 in transcription. On the other hand, a mutant of Msl5 could be designed that is unable to bind to the branchpoint within the mRNA. If Mex67 and Yra1 levels in the mRNP remain the same and Mex67 does not mislocalize, it could be concluded that Msl5 has another role during mRNA export.

Taken together, the depletion of Msl5 leads to an mRNA export defect at 37°C. It still needs to be elucidated whether Msl5 has a direct role in mRNA export or if the depletion of Msl5 leads mRNA retention of unspliced mRNA inside the nucleus.

9 References

Abovich, N., and M. Rosbash. 1997. 'Cross-intron bridging interactions in the yeast commitment complex are conserved in mammals', *Cell*, 89: 403-12.

Adams, R. L., and S. R. Wente. 2020. 'Dbp5 associates with RNA-bound Mex67 and Nab2 and its localization at the nuclear pore complex is sufficient for mRNP export and cell viability', *PLoS Genet*, 16: e1009033.

Amrani, N., M. Minet, F. Wyers, M. E. Dufour, L. P. Aggerbeck, and F. Lacroute. 1997. 'PCF11 encodes a third protein component of yeast cleavage and polyadenylation factor I', *Mol Cell Biol*, 17: 1102-9.

Aoi, Y., Y. H. Takahashi, A. P. Shah, M. Iwanaszko, E. J. Rendleman, N. H. Khan, B. K. Cho, Y. A. Goo, S. Ganesan, N. L. Kelleher, and A. Shilatifard. 2021. 'SPT5 stabilization of promoter-proximal RNA polymerase II', *Mol Cell*, 81: 4413-24.e5.

Ares, M., Jr., L. Grate, and M. H. Pauling. 1999. 'A handful of intron-containing genes produces the lion's share of yeast mRNA', *Rna*, 5: 1138-9.

Arning, S., P. Grüter, G. Bilbe, and A. Krämer. 1996. 'Mammalian splicing factor SF1 is encoded by variant cDNAs and binds to RNA', *Rna*, 2: 794-810.

Ashkenazy-Titelman, A., M. K. Atrash, A. Boocholez, N. Kinor, and Y. Shav-Tal. 2022. 'RNA export through the nuclear pore complex is directional', *Nat Commun*, 13: 5881.

Babour, A., C. Dargemont, and F. Stutz. 2012. 'Ubiquitin and assembly of export competent mRNP', *Biochim Biophys Acta*, 1819: 521-30.

Baejen, C., P. Torkler, S. Gressel, K. Essig, J. Söding, and P. Cramer. 2014. 'Transcriptome maps of mRNP biogenesis factors define pre-mRNA recognition', *Mol Cell*, 55: 745-57.

Beck, M., and E. Hurt. 2017. 'The nuclear pore complex: understanding its function through structural insight', *Nat Rev Mol Cell Biol*, 18: 73-89.

Berglund, J. A., N. Abovich, and M. Rosbash. 1998. 'A cooperative interaction between U2AF65 and mBBP/SF1 facilitates branchpoint region recognition', *Genes Dev*, 12: 858-67.

Bonnet, A., and B. Palancade. 2015. 'Intron or no intron: a matter for nuclear pore complexes', *Nucleus*, 6: 455-61.

Brambilla, M., F. Martani, S. Bertacchi, I. Vitangeli, and P. Branduardi. 2019. 'The Saccharomyces cerevisiae poly (A) binding protein (Pab1): Master regulator of mRNA metabolism and cell physiology', *Yeast*, 36: 23-34.

Buchanan, B. W., M. E. Lloyd, S. M. Engle, and E. M. Rubenstein. 2016. 'Cycloheximide Chase Analysis of Protein Degradation in Saccharomyces cerevisiae', *J Vis Exp*.

Casañal, A., A. Kumar, C. H. Hill, A. D. Easter, P. Emsley, G. Degliesposti, Y. Gordiyenko, B. Santhanam, J. Wolf, K. Wiederhold, G. L. Dornan, M. Skehel, C. V. Robinson, and L. A. Passmore. 2017. 'Architecture of eukaryotic mRNA 3'-end processing machinery', *Science*, 358: 1056-59.

Chan, S. P., and S. C. Cheng. 2005. 'The Prp19-associated complex is required for specifying interactions of U5 and U6 with pre-mRNA during spliceosome activation', *J Biol Chem*, 280: 31190-9.

Chan, S. P., D. I. Kao, W. Y. Tsai, and S. C. Cheng. 2003. 'The Prp19p-associated complex in spliceosome activation', *Science*, 302: 279-82.

Chanarat, S. 2011. The Prp19 complex is a novel transcription elongation factor required for TREX occupancy at transcribed genes. Dissertation, LMU München, Fakultät für Chemie und Pharmazie

Chanarat, S., C. Burkert-Kautzsch, D. M. Meinel, and K. Sträßer. 2012. 'Prp19C and TREX: interacting to promote transcription elongation and mRNA export', *Transcription*, 3: 8-12.

Chanarat, S., M. Seizl, and K. Strässer. 2011. 'The Prp19 complex is a novel transcription elongation factor required for TREX occupancy at transcribed genes', *Genes Dev*, 25: 1147-58.

Chanarat, S., and K. Sträßer. 2013. 'Splicing and beyond: the many faces of the Prp19 complex', *Biochim Biophys Acta*, 1833: 2126-34.

Chang, J., B. Schwer, and S. Shuman. 2012. 'Structure-function analysis and genetic interactions of the yeast branchpoint binding protein Msl5', *Nucleic Acids Res*, 40: 4539-52.

Chávez, S., and A. Aguilera. 1997. 'The yeast HPR1 gene has a functional role in transcriptional elongation that uncovers a novel source of genome instability', *Genes Dev*, 11: 3459-70.

Chen, C. H., W. Y. Tsai, H. R. Chen, C. H. Wang, and S. C. Cheng. 2001. 'Identification and characterization of two novel components of the Prp19p-associated complex, Ntc30p and Ntc20p', *J Biol Chem*, 276: 488-94.

Chen, C. H., W. C. Yu, T. Y. Tsao, L. Y. Wang, H. R. Chen, J. Y. Lin, W. Y. Tsai, and S. C. Cheng. 2002. 'Functional and physical interactions between components of the Prp19p-associated complex', *Nucleic Acids Res*, 30: 1029-37.

Chen, H. R., S. P. Jan, T. Y. Tsao, Y. J. Sheu, J. Banroques, and S. C. Cheng. 1998. 'Snt309p, a component of the Prp19p-associated complex that interacts with Prp19p and associates with the spliceosome simultaneously with or immediately after dissociation of U4 in the same manner as Prp19p', *Mol Cell Biol*, 18: 2196-204.

Chen, H. R., T. Y. Tsao, C. H. Chen, W. Y. Tsai, L. S. Her, M. M. Hsu, and S. C. Cheng. 1999. 'Snt309p modulates interactions of Prp19p with its associated components to stabilize the Prp19p-associated complex essential for pre-mRNA splicing', *Proc Natl Acad Sci U S A*, 96: 5406-11.

Cheng, S. C., W. Y. Tarn, T. Y. Tsao, and J. Abelson. 1993. 'PRP19: a novel spliceosomal component', *Mol Cell Biol*, 13: 1876-82.

Cho, S. Y., E. S. Shin, P. J. Park, D. W. Shin, H. K. Chang, D. Kim, H. H. Lee, J. H. Lee, S. H. Kim, M. J. Song, I. S. Chang, O. S. Lee, and T. R. Lee. 2007. 'Identification of mouse Prp19p as a lipid droplet-associated protein and its possible involvement in the biogenesis of lipid droplets', *J Biol Chem*, 282: 2456-65.

Christiano, R., N. Nagaraj, F. Fröhlich, and T. C. Walther. 2014. 'Global proteome turnover analyses of the Yeasts S. cerevisiae and S. pombe', *Cell Rep*, 9: 1959-65.

Crick, F. 1970. 'Central dogma of molecular biology', *Nature*, 227: 561-3.

Dahmus, M. E. 1995. 'Phosphorylation of the C-terminal domain of RNA polymerase II', *Biochim Biophys Acta*, 1261: 171-82.

David, C. J., A. R. Boyne, S. R. Millhouse, and J. L. Manley. 2011. 'The RNA polymerase II C-terminal domain promotes splicing activation through recruitment of a U2AF65-Prp19 complex', *Genes Dev*, 25: 972-83.

Dix, I., C. Russell, S. B. Yehuda, M. Kupiec, and J. D. Beggs. 1999. 'The identification and characterization of a novel splicing protein, Isy1p, of Saccharomyces cerevisiae', *Rna*, 5: 360-8.

Doherty, J. P., R. Lindeman, R. J. Trent, M. W. Graham, and D. M. Woodcock. 1993. 'Escherichia coli host strains SURE and SRB fail to preserve a palindrome cloned in lambda phage: improved alternate host strains', *Gene*, 124: 29-35.

Dziembowski, A., A. P. Ventura, B. Rutz, F. Caspary, C. Faux, F. Halgand, O. Laprévote, and B. Séraphin. 2004. 'Proteomic analysis identifies a new complex required for nuclear pre-mRNA retention and splicing', *Embo j*, 23: 4847-56.

Ehara, H., and S. I. Sekine. 2018. 'Architecture of the RNA polymerase II elongation complex: new insights into Spt4/5 and Elf1', *Transcription*, 9: 286-91.

Exinger, F., and F. Lacroute. 1992. '6-Azauracil inhibition of GTP biosynthesis in Saccharomyces cerevisiae', *Curr Genet*, 22: 9-11.

Fabrizio, P., J. Dannenberg, P. Dube, B. Kastner, H. Stark, H. Urlaub, and R. Lührmann. 2009. 'The evolutionarily conserved core design of the catalytic activation step of the yeast spliceosome', *Mol Cell*, 36: 593-608.

Fairbanks, G., T. L. Steck, and D. F. Wallach. 1971. 'Electrophoretic analysis of the major polypeptides of the human erythrocyte membrane', *Biochemistry*, 10: 2606-17.

Fasken, M. B., M. Stewart, and A. H. Corbett. 2008. 'Functional significance of the interaction between the mRNA-binding protein, Nab2, and the nuclear pore-associated protein, Mlp1, in mRNA export', *J Biol Chem*, 283: 27130-43.

Flaherty, S. M., P. Fortes, E. Izaurralde, I. W. Mattaj, and G. M. Gilmartin. 1997. 'Participation of the nuclear cap binding complex in pre-mRNA 3' processing', *Proc Natl Acad Sci U S A*, 94: 11893-8.

Fong, N., M. Ohman, and D. L. Bentley. 2009. 'Fast ribozyme cleavage releases transcripts from RNA polymerase II and aborts co-transcriptional pre-mRNA processing', *Nat Struct Mol Biol*, 16: 916-22.

Galy, V., O. Gadal, M. Fromont-Racine, A. Romano, A. Jacquier, and U. Nehrbass. 2004. 'Nuclear retention of unspliced mRNAs in yeast is mediated by perinuclear Mlp1', *Cell*, 116: 63-73.

Gibson, D. G., L. Young, R. Y. Chuang, J. C. Venter, C. A. Hutchison, 3rd, and H. O. Smith. 2009. 'Enzymatic assembly of DNA molecules up to several hundred kilobases', *Nat Methods*, 6: 343-5.

Gilbert, W. 1978. 'Why genes in pieces?', *Nature*, 271: 501.

Gilbert, W., and C. Guthrie. 2004. 'The Glc7p nuclear phosphatase promotes mRNA export by facilitating association of Mex67p with mRNA', *Mol Cell*, 13: 201-12.

Grote, M., E. Wolf, C. L. Will, I. Lemm, D. E. Agafonov, A. Schomburg, W. Fischle, H. Urlaub, and R. Lührmann. 2010. 'Molecular architecture of the human Prp19/CDC5L complex', *Mol Cell Biol*, 30: 2105-19.

Gwizdek, C., M. Hobeika, B. Kus, B. Ossareh-Nazari, C. Dargemont, and M. S. Rodriguez. 2005. 'The mRNA nuclear export factor Hpr1 is regulated by Rsp5-mediated ubiquitylation', *J Biol Chem*, 280: 13401-5.

Hackmann, A., H. Wu, U. M. Schneider, K. Meyer, K. Jung, and H. Krebber. 2014. 'Quality control of spliced mRNAs requires the shuttling SR proteins Gbp2 and Hrb1', *Nat Commun*, 5: 3123.

Hahn, S. 2004. 'Structure and mechanism of the RNA polymerase II transcription machinery', *Nat Struct Mol Biol*, 11: 394-403.

Hayashi, K. 2012. 'The interaction and integration of auxin signaling components', *Plant Cell Physiol*, 53: 965-75.

Hector, R. E., K. R. Nykamp, S. Dheur, J. T. Anderson, P. J. Non, C. R. Urbinati, S. M. Wilson, L. Minvielle-Sebastia, and M. S. Swanson. 2002. 'Dual requirement for yeast hnRNP Nab2p in mRNA poly(A) tail length control and nuclear export', *Embo j*, 21: 1800-10.

Herzel, L., D. S. M. Ottoz, T. Alpert, and K. M. Neugebauer. 2017. 'Splicing and transcription touch base: co-transcriptional spliceosome assembly and function', *Nat Rev Mol Cell Biol*, 18: 637-50.

Hirtreiter, A., G. E. Damsma, A. C. Cheung, D. Klose, D. Grohmann, E. Vojnic, A. C. Martin, P. Cramer, and F. Werner. 2010. 'Spt4/5 stimulates transcription elongation through the RNA polymerase clamp coiled-coil motif', *Nucleic Acids Res*, 38: 4040-51.

Hobeika, M., C. Brockmann, F. Gruessing, D. Neuhaus, G. Divita, M. Stewart, and C. Dargemont. 2009. 'Structural requirements for the ubiquitin-associated domain of the mRNA export factor Mex67 to bind its specific targets, the transcription elongation THO complex component Hpr1 and nucleoporin FXFG repeats', *J Biol Chem*, 284: 17575-83.

Hobeika, M., C. Brockmann, N. Iglesias, C. Gwizdek, D. Neuhaus, F. Stutz, M. Stewart, G. Divita, and C. Dargemont. 2007. 'Coordination of Hpr1 and ubiquitin binding by the UBA domain of the mRNA export factor Mex67', *Mol Biol Cell*, 18: 2561-8.

Hofmann, J. C., J. Tegha-Dunghu, S. Dräger, C. L. Will, R. Lührmann, and O. J. Gruss. 2013. 'The Prp19 complex directly functions in mitotic spindle assembly', *PLoS One*, 8: e74851.

Hogg, R., J. C. McGrail, and R. T. O'Keefe. 2010. 'The function of the NineTeen Complex (NTC) in regulating spliceosome conformations and fidelity during pre-mRNA splicing', *Biochem Soc Trans*, 38: 1110-5.

Holstege, F. C., and H. T. Timmers. 1997. 'Analysis of open complex formation during RNA polymerase II transcription initiation using heteroduplex templates and potassium permanganate probing', *Methods*, 12: 203-11.

Hossain, M. A., and T. L. Johnson. 2014. 'Using yeast genetics to study splicing mechanisms', *Methods Mol Biol*, 1126: 285-98.

Hsin, J. P., and J. L. Manley. 2012. 'The RNA polymerase II CTD coordinates transcription and RNA processing', *Genes Dev*, 26: 2119-37.

Hu, S., L. Peng, C. Xu, Z. Wang, A. Song, and F. X. Chen. 2021. 'SPT5 stabilizes RNA polymerase II, orchestrates transcription cycles, and maintains the enhancer landscape', *Mol Cell*, 81: 4425-39.e6.

Idrissou, M., and A. Maréchal. 2022. 'The PRP19 Ubiquitin Ligase, Standing at the Cross-Roads of mRNA Processing and Genome Stability', *Cancers (Basel)*, 14.

Iglesias, N., E. Tutucci, C. Gwizdek, P. Vinciguerra, E. Von Dach, A. H. Corbett, C. Dargemont, and F. Stutz. 2010. 'Ubiquitin-mediated mRNP dynamics and surveillance prior to budding yeast mRNA export', *Genes Dev*, 24: 1927-38.

Jaehning, J. A. 2010. 'The Paf1 complex: platform or player in RNA polymerase II transcription?', *Biochim Biophys Acta*, 1799: 379-88.

Jimeno, S., A. G. Rondón, R. Luna, and A. Aguilera. 2002. 'The yeast THO complex and mRNA export factors link RNA metabolism with transcription and genome instability', *Embo j*, 21: 3526-35.

Katahira, J. 2012. 'mRNA export and the TREX complex', *Biochim Biophys Acta*, 1819: 507-13.

Katahira, J., K. Strässer, A. Podtelejnikov, M. Mann, J. U. Jung, and E. Hurt. 1999. 'The Mex67p-mediated nuclear mRNA export pathway is conserved from yeast to human', *Embo j*, 18: 2593-609.

Katahira, J., and Y. Yoneda. 2009. 'Roles of the TREX complex in nuclear export of mRNA', *RNA Biol*, 6: 149-52.

Kelly, S. M., S. W. Leung, L. H. Apponi, A. M. Bramley, E. J. Tran, J. A. Chekanova, S. R. Wente, and A. H. Corbett. 2010. 'Recognition of polyadenosine RNA by the zinc finger domain of nuclear poly(A) RNA-binding protein 2 (Nab2) is required for correct mRNA 3'-end formation', *J Biol Chem*, 285: 26022-32.

Keogh, M. C., V. Podolny, and S. Buratowski. 2003. 'Bur1 kinase is required for efficient transcription elongation by RNA polymerase II', *Mol Cell Biol*, 23: 7005-18.

Kim, M., N. J. Krogan, L. Vasiljeva, O. J. Rando, E. Nedea, J. F. Greenblatt, and S. Buratowski. 2004. 'The yeast Rat1 exonuclease promotes transcription termination by RNA polymerase II', *Nature*, 432: 517-22.

Kim, S. J., J. Fernandez-Martinez, I. Nudelman, Y. Shi, W. Zhang, B. Raveh, T. Herricks, B. D. Slaughter, J. A. Hogan, P. Upla, I. E. Chemmama, R. Pellarin, I. Echeverria, M. Shivaraju, A. S. Chaudhury, J. Wang, R. Williams, J. R. Unruh, C. H. Greenberg, E. Y. Jacobs, Z. Yu, M. J. de la Cruz, R. Mironska, D. L. Stokes, J. D. Aitchison, M. F. Jarrold, J. L. Gerton, S. J. Ludtke, C. W. Akey, B. T. Chait, A. Sali, and M. P. Rout. 2018. 'Integrative structure and functional anatomy of a nuclear pore complex', *Nature*, 555: 475-82.

Komarnitsky, P., E. J. Cho, and S. Buratowski. 2000. 'Different phosphorylated forms of RNA polymerase II and associated mRNA processing factors during transcription', *Genes Dev*, 14: 2452-60.

Kressler, D., G. Bange, Y. Ogawa, G. Stjepanovic, B. Bradatsch, D. Pratte, S. Amlacher, D. Strauß, Y. Yoneda, J. Katahira, I. Sinning, and E. Hurt. 2012. 'Synchronizing nuclear import of ribosomal proteins with ribosome assembly', *Science*, 338: 666-71.

Laemmli, U. K. 1970. 'Cleavage of structural proteins during the assembly of the head of bacteriophage T4', *Nature*, 227: 680-5.

Lee, J. M., and A. L. Greenleaf. 1989. 'A protein kinase that phosphorylates the C-terminal repeat domain of the largest subunit of RNA polymerase II', *Proc Natl Acad Sci U S A*, 86: 3624-8.

Legrain, P., B. Seraphin, and M. Rosbash. 1988. 'Early commitment of yeast pre-mRNA to the spliceosome pathway', *Mol Cell Biol*, 8: 3755-60.

Linder, P., and E. Jankowsky. 2011. 'From unwinding to clamping - the DEAD box RNA helicase family', *Nat Rev Mol Cell Biol*, 12: 505-16.

Liu, X., D. A. Bushnell, and R. D. Kornberg. 2013. 'RNA polymerase II transcription: structure and mechanism', *Biochim Biophys Acta*, 1829: 2-8.

Lund, M. K., and C. Guthrie. 2005. 'The DEAD-box protein Dbp5p is required to dissociate Mex67p from exported mRNPs at the nuclear rim', *Mol Cell*, 20: 645-51.

Martinez-Rucobo, F. W., R. Kohler, M. van de Waterbeemd, A. J. Heck, M. Hemann, F. Herzog, H. Stark, and P. Cramer. 2015. 'Molecular Basis of Transcription-Coupled Pre-mRNA Capping', *Mol Cell*, 58: 1079-89.

Mayer, A., M. Heidemann, M. Lidschreiber, A. Schreieck, M. Sun, C. Hintermair, E. Kremmer, D. Eick, and P. Cramer. 2012. 'CTD tyrosine phosphorylation impairs termination factor recruitment to RNA polymerase II', *Science*, 336: 1723-5.

Mayer, A., M. Lidschreiber, M. Siebert, K. Leike, J. Söding, and P. Cramer. 2010. 'Uniform transitions of the general RNA polymerase II transcription complex', *Nat Struct Mol Biol*, 17: 1272-8.

Meinel, D. M. 2013 Genome wide recruitment of TREX reveals a direct interaction with the Rpb1 CTD. Dissertation, LMU München, Fakultät für Chemie und Pharmazie

Meinel, D. M., C. Burkert-Kautzsch, A. Kieser, E. O'Duibhir, M. Siebert, A. Mayer, P. Cramer, J. Söding, F. C. Holstege, and K. Sträßer. 2013. 'Recruitment of TREX to the transcription machinery by its direct binding to the phospho-CTD of RNA polymerase II', *PLoS Genet*, 9: e1003914.

Meinel, D. M., and K. Sträßer. 2015. 'Co-transcriptional mRNP formation is coordinated within a molecular mRNP packaging station in S. cerevisiae', *Bioessays*, 37: 666-77.

Mermelstein, F. H., O. Flores, and D. Reinberg. 1989. 'Initiation of transcription by RNA polymerase II', *Biochim Biophys Acta*, 1009: 1-10.

Minocha R. 2018. The functions of Mud2 and Prp19C components in transcription and TREX occupancy. Dissertation, LMU München, Fakultät für Chemie und Pharmazie

Minocha, R., V. Popova, D. Kopytova, D. Misiak, S. Huttelmaier, S. Georgieva, and K. Strasser. 2018. 'Mud2 functions in transcription by recruiting the Prp19 and TREX complexes to transcribed genes', *Nucleic Acids Res*, 46: 9749-63.

Minvielle-Sebastia, L., B. Winsor, N. Bonneaud, and F. Lacroute. 1991. 'Mutations in the yeast RNA14 and RNA15 genes result in an abnormal mRNA decay rate; sequence analysis reveals an RNA-binding domain in the RNA15 protein', *Mol Cell Biol*, 11: 3075-87.

Moore, M. J., and N. J. Proudfoot. 2009. 'Pre-mRNA processing reaches back to transcription and ahead to translation', *Cell*, 136: 688-700.

Morawska, M., and H. D. Ulrich. 2013. 'An expanded tool kit for the auxin-inducible degron system in budding yeast', *Yeast*, 30: 341-51.

Mosley, A. L., S. G. Pattenden, M. Carey, S. Venkatesh, J. M. Gilmore, L. Florens, J. L. Workman, and M. P. Washburn. 2009. 'Rtr1 is a CTD phosphatase that regulates RNA polymerase II during the transition from serine 5 to serine 2 phosphorylation', *Mol Cell*, 34: 168-78.

Narain, A., P. Bhandare, B. Adhikari, S. Backes, M. Eilers, L. Dölken, A. Schlosser, F. Erhard, A. Baluapuri, and E. Wolf. 2021. 'Targeted protein degradation reveals a direct role of SPT6 in RNAPII elongation and termination', *Mol Cell*, 81: 3110-27.e14.

Nishimura, K., T. Fukagawa, H. Takisawa, T. Kakimoto, and M. Kanemaki. 2009. 'An auxin-based degron system for the rapid depletion of proteins in nonplant cells', *Nat Methods*, 6: 917-22.

Nojima, T., T. Hirose, H. Kimura, and M. Hagiwara. 2007. 'The interaction between cap-binding complex and RNA export factor is required for intronless mRNA export', *J Biol Chem*, 282: 15645-51.

Nojima, T., K. Rebelo, T. Gomes, A. R. Grosso, N. J. Proudfoot, and M. Carmo-Fonseca. 2018. 'RNA Polymerase II Phosphorylated on CTD Serine 5 Interacts with the Spliceosome during Co-transcriptional Splicing', *Mol Cell*, 72: 369-79.e4.

Ohi, M. D., A. J. Link, L. Ren, J. L. Jennings, W. H. McDonald, and K. L. Gould. 2002. 'Proteomics analysis reveals stable multiprotein complexes in both fission and budding yeasts containing Myb-related Cdc5p/Cef1p, novel pre-mRNA splicing factors, and snRNAs', *Mol Cell Biol*, 22: 2011-24.

Ohi, M. D., C. W. Vander Kooi, J. A. Rosenberg, L. Ren, J. P. Hirsch, W. J. Chazin, T. Walz, and K. L. Gould. 2005. 'Structural and functional analysis of essential pre-mRNA splicing factor Prp19p', *Mol Cell Biol*, 25: 451-60.

Palancade, B., M. Zuccolo, S. Loeillet, A. Nicolas, and V. Doye. 2005. 'Pml39, a novel protein of the nuclear periphery required for nuclear retention of improper messenger ribonucleoparticles', *Mol Biol Cell*, 16: 5258-68.

Parenteau, J., M. Durand, G. Morin, J. Gagnon, J. F. Lucier, R. J. Wellinger, B. Chabot, and S. A. Elela. 2011. 'Introns within ribosomal protein genes regulate the production and function of yeast ribosomes', *Cell*, 147: 320-31.

Puig, O., F. Caspary, G. Rigaut, B. Rutz, E. Bouveret, E. Bragado-Nilsson, M. Wilm, and B. Séraphin. 2001. 'The tandem affinity purification (TAP) method: a general procedure of protein complex purification', *Methods*, 24: 218-29.

Ramanathan, A., G. B. Robb, and S. H. Chan. 2016. 'mRNA capping: biological functions and applications', *Nucleic Acids Res*, 44: 7511-26.

Reed, R. 2003. 'Coupling transcription, splicing and mRNA export', *Curr Opin Cell Biol*, 15: 326-31.

Reuter, L. M., D. M. Meinel, and K. Sträßer. 2015. 'The poly(A)-binding protein Nab2 functions in RNA polymerase III transcription', *Genes Dev*, 29: 1565-75.

Richard, P., and J. L. Manley. 2009. 'Transcription termination by nuclear RNA polymerases', *Genes Dev*, 23: 1247-69.

Rodriguez, C. R., T. Takagi, E. J. Cho, and S. Buratowski. 1999. 'A Saccharomyces cerevisiae RNA 5'-triphosphatase related to mRNA capping enzyme', *Nucleic Acids Res*, 27: 2181-8.

Rosado-Lugo, J. D., and M. Hampsey. 2014. 'The Ssu72 phosphatase mediates the RNA polymerase II initiation-elongation transition', *J Biol Chem*, 289: 33916-26.

Rosonina, E., S. Kaneko, and J. L. Manley. 2006. 'Terminating the transcript: breaking up is hard to do', *Genes Dev*, 20: 1050-6.

Röther, S., and K. Strässer. 2007. 'The RNA polymerase II CTD kinase Ctk1 functions in translation elongation', *Genes Dev*, 21: 1409-21.

Rout, M. P., J. D. Aitchison, A. Suprapto, K. Hjertaas, Y. Zhao, and B. T. Chait. 2000. 'The yeast nuclear pore complex: composition, architecture, and transport mechanism', *J Cell Biol*, 148: 635-51.

Rutz, B., and B. Séraphin. 1999. 'Transient interaction of BBP/ScSF1 and Mud2 with the splicing machinery affects the kinetics of spliceosome assembly', *Rna*, 5: 819-31.

Rutz B., and B. Séraphin. 2000. 'A dual role for BBP/ScSF1 in nuclear pre-mRNA retention and splicing', *Embo j*, 19: 1873-86.

Sambrook, J., and D.W. Russell. 2001. *Molecular Cloning: A Laboratory Manual* (Cold Spring Harbor Laboratory Press).

Santos-Rosa, H., H. Moreno, G. Simos, A. Segref, B. Fahrenkrog, N. Panté, and E. Hurt. 1998. 'Nuclear mRNA export requires complex formation between Mex67p and Mtr2p at the nuclear pores', *Mol Cell Biol*, 18: 6826-38.

Schier, A. C., and D. J. Taatjes. 2020. 'Structure and mechanism of the RNA polymerase II transcription machinery', *Genes Dev*, 34: 465-88.

Séraphin, B., and M. Rosbash. 1991. 'The yeast branchpoint sequence is not required for the formation of a stable U1 snRNA-pre-mRNA complex and is recognized in the absence of U2 snRNA', *Embo j*, 10: 1209-16.

Shatkin, A. J., and J. L. Manley. 2000. 'The ends of the affair: capping and polyadenylation', *Nat Struct Biol*, 7: 838-42.

Sikorski, R. S., and P. Hieter. 1989. 'A system of shuttle vectors and yeast host strains designed for efficient manipulation of DNA in Saccharomyces cerevisiae', *Genetics*, 122: 19-27.

Soucek, S., A. H. Corbett, and M. B. Fasken. 2012. 'The long and the short of it: the role of the zinc finger polyadenosine RNA binding protein, Nab2, in control of poly(A) tail length', *Biochim Biophys Acta*, 1819: 546-54.

Strässer, K., and E. Hurt. 2000. 'Yra1p, a conserved nuclear RNA-binding protein, interacts directly with Mex67p and is required for mRNA export', *Embo j*, 19: 410-20.

Strässer K, Hurt E. 2001. 'Splicing factor Sub2p is required for nuclear mRNA export through its interaction with Yra1p', *Nature*, 413: 648-52.

Strässer, K., S. Masuda, P. Mason, J. Pfannstiel, M. Oppizzi, S. Rodriguez-Navarro, A. G. Rondón, A. Aguilera, K. Struhl, R. Reed, and E. Hurt. 2002. 'TREX is a conserved complex coupling transcription with messenger RNA export', *Nature*, 417: 304-8.

Tarn, W. Y., C. H. Hsu, K. T. Huang, H. R. Chen, H. Y. Kao, K. R. Lee, and S. C. Cheng. 1994. 'Functional association of essential splicing factor(s) with PRP19 in a protein complex', *Embo j*, 13: 2421-31.

Thomas, B. J., and R. Rothstein. 1989. 'Elevated recombination rates in transcriptionally active DNA', *Cell*, 56: 619-30.

Thomas, M. C., and C. M. Chiang. 2006. 'The general transcription machinery and general cofactors', *Crit Rev Biochem Mol Biol*, 41: 105-78.

Topisirovic, I., Y. V. Svitkin, N. Sonenberg, and A. J. Shatkin. 2011. 'Cap and cap-binding proteins in the control of gene expression', *Wiley Interdiscip Rev RNA*, 2: 277-98.

Towbin, H., T. Staehelin, and J. Gordon. 1979. 'Electrophoretic transfer of proteins from polyacrylamide gels to nitrocellulose sheets: procedure and some applications', *Proc Natl Acad Sci U S A*, 76: 4350-4.

Tran, E. J., Y. Zhou, A. H. Corbett, and S. R. Wente. 2007. 'The DEAD-box protein Dbp5 controls mRNA export by triggering specific RNA:protein remodeling events', *Mol Cell*, 28: 850-9.

van Maldegem, F., S. Maslen, C. M. Johnson, A. Chandra, K. Ganesh, M. Skehel, and C. Rada. 2015. 'CTNNBL1 facilitates the association of CWC15 with CDC5L and is required to maintain the abundance of the Prp19 spliceosomal complex', *Nucleic Acids Res*, 43: 7058-69.

Villa, T., and C. Guthrie. 2005. 'The Isy1p component of the NineTeen complex interacts with the ATPase Prp16p to regulate the fidelity of pre-mRNA splicing', *Genes Dev*, 19: 1894-904.

Vincent, K., Q. Wang, S. Jay, K. Hobbs, and B. C. Rymond. 2003. 'Genetic interactions with CLF1 identify additional pre-mRNA splicing factors and a link between activators of yeast vesicular transport and splicing', *Genetics*, 164: 895-907.

Wade, P. A., W. Werel, R. C. Fentzke, N. E. Thompson, J. F. Leykam, R. R. Burgess, J. A. Jaehning, and Z. F. Burton. 1996. 'A novel collection of accessory factors associated with yeast RNA polymerase II', *Protein Expr Purif*, 8: 85-90.

Wahl, M. C., C. L. Will, and R. Lührmann. 2009. 'The spliceosome: design principles of a dynamic RNP machine', *Cell*, 136: 701-18.

Wang, Q., L. Zhang, B. Lynn, and B. C. Rymond. 2008. 'A BBP-Mud2p heterodimer mediates branchpoint recognition and influences splicing substrate abundance in budding yeast', *Nucleic Acids Res*, 36: 2787-98.

Wegener, M., and M. Müller-McNicoll. 2019. 'View from an mRNP: The Roles of SR Proteins in Assembly, Maturation and Turnover', *Adv Exp Med Biol*, 1203: 83-112.

West, M. L., and J. L. Corden. 1995. 'Construction and analysis of yeast RNA polymerase II CTD deletion and substitution mutations', *Genetics*, 140: 1223-33.

Will, C. L., and R. Lührmann. 2011. 'Spliceosome structure and function', *Cold Spring Harb Perspect Biol*, 3.

Wong, C., S. Sridhara, J. C. Bardwell, and U. Jakob. 2000. 'Heating greatly speeds Coomassie blue staining and destaining', *Biotechniques*, 28: 426-8, 30, 32.

Xie, Y., B. P. Clarke, Y. J. Kim, A. L. Ivey, P. S. Hill, Y. Shi, and Y. Ren. 2021. 'Cryo-EM structure of the yeast TREX complex and coordination with the SR-like protein Gbp2', *Elife*, 10.

Xie, Y., and Y. Ren. 2019. 'Mechanisms of nuclear mRNA export: A structural perspective', *Traffic*, 20: 829-40.

Zhai, L. T., and S. Xiang. 2014. 'mRNA quality control at the 5' end', *J Zhejiang Univ Sci B*, 15: 438-43.

Zhang, D. W., J. B. Rodríguez-Molina, J. R. Tietjen, C. M. Nemec, and A. Z. Ansari. 2012. 'Emerging Views on the CTD Code', *Genet Res Int*, 2012: 347214.

Zhao, J., M. M. Kessler, and C. L. Moore. 1997. 'Cleavage factor II of Saccharomyces cerevisiae contains homologues to subunits of the mammalian Cleavage/ polyadenylation specificity factor and exhibits sequence-specific, ATP-dependent interaction with precursor RNA', *J Biol Chem*, 272: 10831-8.

10 Lists of figures

11 Lists of tables

12 Abbreviation

Table 15:Abbreviations

Abbreviation	Description
3'SS	3' splice site
5'SS	5' splice site
6-AU	6-azauracil
A	Alanine
aa	amino acids
ATP	adenosintriphosphat
AU	indole-3-acetic acid; IAA
BBP	branchpoint binding protein
BP	branch point
CBC	cap binding complex
CC1	Commitment complex 1
CC2	Commitment complex 2
ChIP	Chromatin Immunoprecipitation
CPSF	cleavage and polyadenylation specify factor
CSTF	cleavage stimulation factor
CTD	C-terminal domain
E. coli	*Escherichia coli*
EtOH	Ethanol
FG repeats	phenylalanine and glycine repeats
FISH	Fluorescence in situ hybridization
FTpA	FLAG-TEV-prot A tag
IF	Immunofluorescence
IP6	inositol hexaphophate
kda	kilodalton
KH domain	K-homology domain
mNET-seq	mammalian native elongating transcript sequencing
mRNA	messenger ribonucleic acid
mRNP	messenger ribonucleoprotein particle
Msl5	Mud2 synthetic lethal 5
NPC	nuclear pore complex
NTR	nuclear transport factors
Nup	nucleoporin
OD	optical density
ORF	open reading frame
PAP	Peroxidase-anti-peroxidase
PAR-CLIP	photoactivatable ribonucleoside-enhanced crosslinking and immunoprecipitation
PCR	Polymerase chain reaction
PIC	preinitiation complex
poly(A)	Poly-adenaylation
Prp19C	Prp19 complex
py	polypyrimidine
RBP	RNA binding protein
RES complex	Retention and Splicing complex
RNAPII	RNA polymerase II
RRM	RNA recognition motif
RT	room temperature
S. cerevisiae	*Saccharomyces cerevisiae*
SC	synthetic complete
SDS-PAGE	Sodium dodecyl sulfate polyacrylamide gel electrophoresis

SF1	splicing factor 1
snRNA	small nuclear RNA
TAP	Tandem Affinity Purification
TBP	TATA-box binding protein
TEV	Tobacco etch virus
THSC	Thp1-Sac3-Sus1-Cdc31 complex
TREX	Transcription export
TSS	transcription start site
UTR	untranslated region
wt	wild-type
YPD	Yeast extract, peptone, dextrose

13 Publication

The Prp19C subunits Cwc15 and Syf2 function in TREX occupancy and transcription elongation.

Laura Henke-Schulz, Rashmi Minocha and Katja Sträßer1

2023 (manuscript in progress)

14 Danksagung

Zu allererst möchte ich meinen Dank an Katja Sträßer aussprechen, die mir die Gelegenheit gegeben hat, in ihrem Labor zu arbeiten. Ich bin dankbar für die Freiheiten und Möglichkeiten, die ich erhalten habe, sowie für deine kontinuierliche Unterstützung und die produktiven Diskussionen, die wir geführt haben.

Selbstverständlich möchte ich auch meiner Zweitgutachterin Prof. Dr. Elena Evguenieva-Hackenberg und den anderen Mitgliedern meiner Prüfungskommission, Prof. Dr. John Ziebuhr und Prof. Dr. Kai Thormann, meinen Dank aussprechen. Ich schätze es sehr, dass Sie sich die Zeit genommen haben, Teil meiner Prüfungskommission zu sein.

Des Weiteren möchte ich auch dem gesamten Labor meinen Dank aussprechen! Ich hatte stets Freude ins Labor zu gehen und Ihr wart ein Grund hierfür! Danke! Bei Wolle möchte ich mich bedanken, der mir stets technischen Support geboten hat. Egal, ob ein Gerät im Labor streikte oder Probleme auftraten, er hatte immer eine offene Tür und war zur Stelle, um zu helfen. Bei Cornelia möchte ich mich bedanken sowohl für das Korrigieren meiner Promotionsarbeit als auch für die fachlichen Diskussionen. Bei Kristin möchte ich mich bedanken, da sie mir den Einstieg ins Labor erleichtert hat und auch die wichtigsten Versuche beigebracht hat. Bei Johanna und Kristin möchte ich mich für die vielen Stunden bedanken, in denen wir sowohl über persönliche als auch wissenschaftliche Themen geplaudert haben, und auch für die gelegentlichen Denkanstöße. Ich freue mich darauf, viele weitere gute Gespräche mit euch zu führen!

Außerdem möchte ich mich noch bei meinen Studenten Laura, Carla, Sophie und Nils bedanken. Es hat mir großen Spaß bereitet euch neue Dinge beizubringen und ihr habt mir auch die ein oder andere Aufgabe abgenommen. Besonders möchte ich hier Nils hervorheben - vielen Dank für deine Unterstützung, nicht nur bei den Aufgaben im Zusammenhang mit dem Projekt, sondern auch darüber hinaus!

Ein ganz besonderer Dank gebührt meinen Eltern, die mich immer ermutigt haben, meinen eigenen Weg zu gehen. Ich danke euch dafür, dass ihr über die Jahre hinweg stets an mich geglaubt habt und mich unterstützt habt, auch wenn ihr selbst mit eigenen Herausforderungen konfrontiert wart. Ihr wart immer für mich da, und dafür bin ich euch zutiefst dankbar.

Zum Schluss möchte ich mich noch bei meinem Ehemann Nils bedanken. Danke, dass du immer für mich da bist. Danke, dass du nach so manch einer verkorksten Woche die Probleme relativiert hast und mich stets hast positiv in die nächste sehen lassen. Gerade das vergangen Jahr war nicht einfach für uns. Im vergangenen Jahr musste ich physisch sowie psychisch an meine Grenzen gehen, du warst stets an meiner Seite und hast dein Bestes gegeben mir jede Träne zu trocken. Ich könnte nicht aufgeregter, zuversichtlicher und freudiger in die Zukunft schauen mit der Gewissheit, dass du da bist!

15 Eidesstattliche Erklärung

Ich, Laura Henke-Schulz erkläre: Ich habe die vorgelegte Dissertation selbstständig und ohne unerlaubte fremde Hilfe und nur mit den Hilfen angefertigt, die ich in der Dissertation angegeben habe. Alle Textstellen, die wörtlich oder sinngemäß aus veröffentlichten Schriften entnommen sind, und alle Angaben, die auf mündlichen Auskünften beruhen, sind als solche kenntlich gemacht. Ich stimme einer evtl. Überprüfung meiner Dissertation durch eine Antiplagiat-Software zu. Bei den von mir durchgeführten und in der Dissertation erwähnten Untersuchungen habe ich die Grundsätze guter wissenschaftlicher Praxis, wie sie in der „Satzung der Justus-Liebig-Universität Gießen zur Sicherung guter wissenschaftlicher Praxis“ niedergelegt sind, eingehalten.

Gießen, den: .....

Unterschrift: .....

(Vorname, Nachname)

16 Appendix

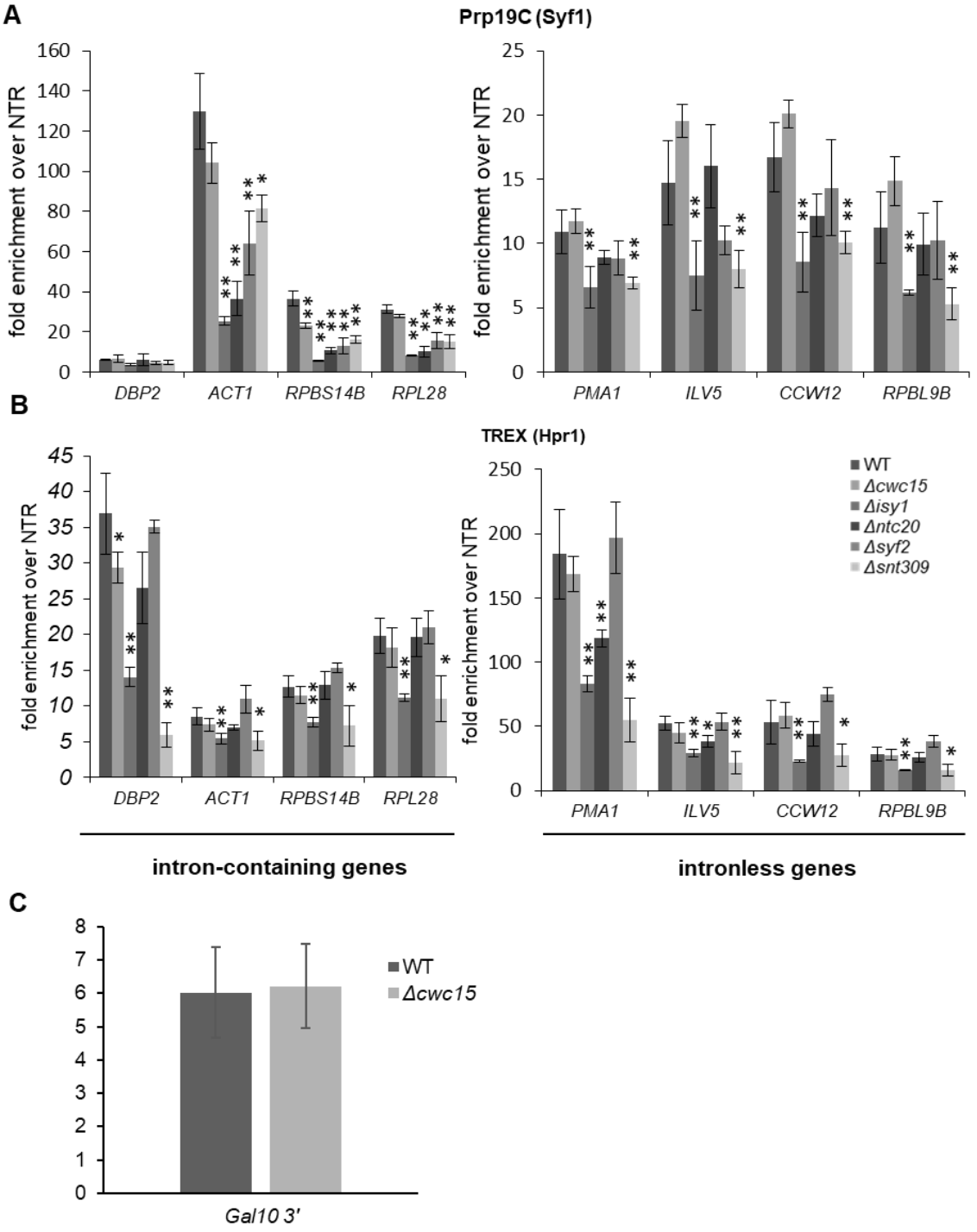

Appendix Figure 1: Prp19C occupancy is reduced in *Δsyf2* cells and TREX occupancy is reduced in *Δcwc15* cells. The occupancy of Syf1 (**A**) and Hpr1 (**B**) was assessed in wild-type cells (WT) and *Δcwc15*, *Δisy1*, *Δntc20 Δsyf2* and *Δsnt309* deletion mutants using chromatin immunoprecipitation (ChIP) at both intron-containing (left panel) and intronless genes (right panel). ChIPs were quantified by Real Time PCR using primer pairs that anneal to the 3' end of each gene. (**C**) Prior to crosslinking the cells were *CWC15* is deleted are induced with galactose

followed by a ChIP experiment. The ChIP was quantified by Real Time PCR using primer pair that anneal to the 3' end of *GAL10*.

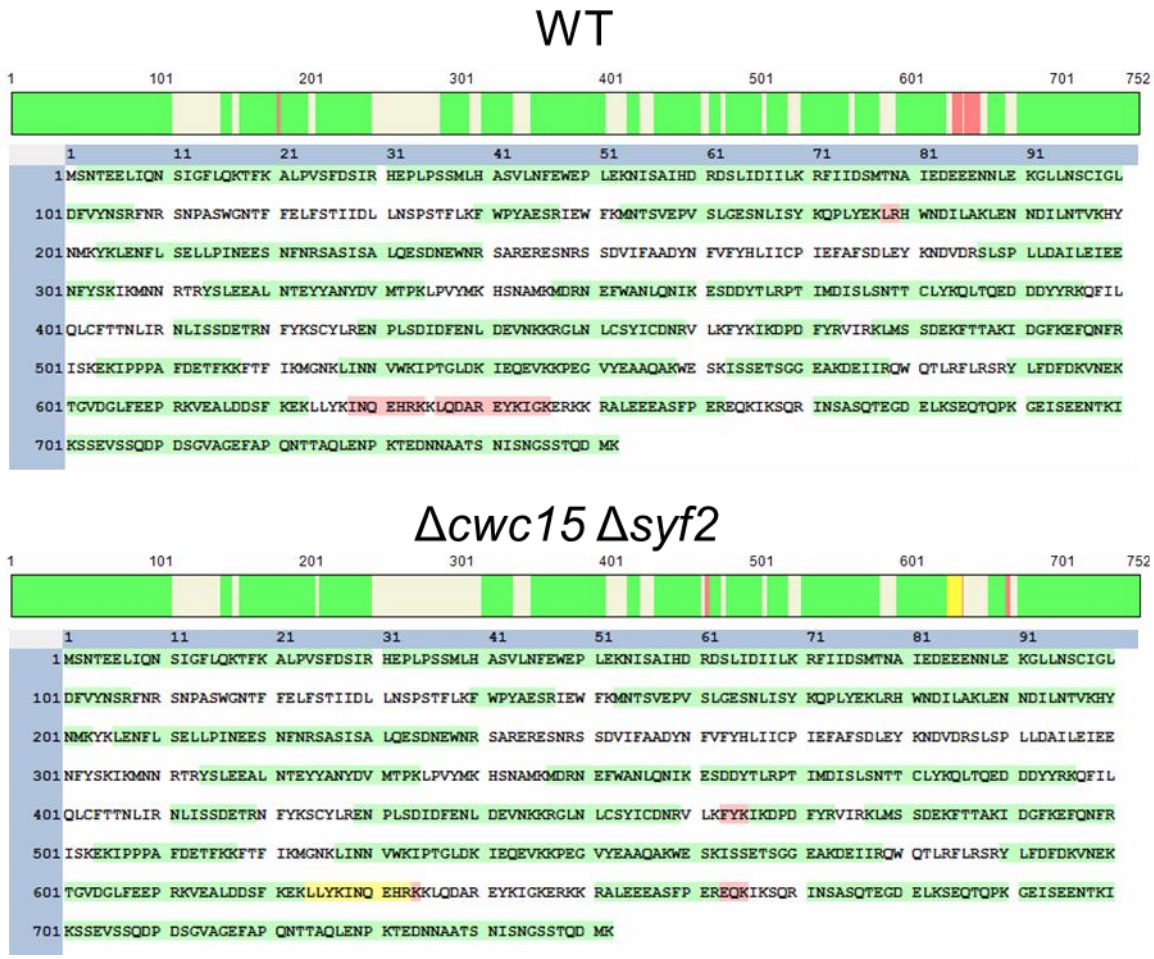

Appendix Figure 2: Mass spectrometry sequence analyses of wild-type and *Δcwc15 Δsyf2*. After Tap purification, the proteins were separated *via* SDS-PAGE. The presumed Hpr1-CBP band were cut out and analyzed by mass spectrometry. green: peptide with high confidence identified (FDR <1 %), yellow: with middle confidence identified (FDR 1-5 %), red: with low confidence identified (FDR >5 %). Mass spectrometry and analyses was performed by Günter Lochnit.

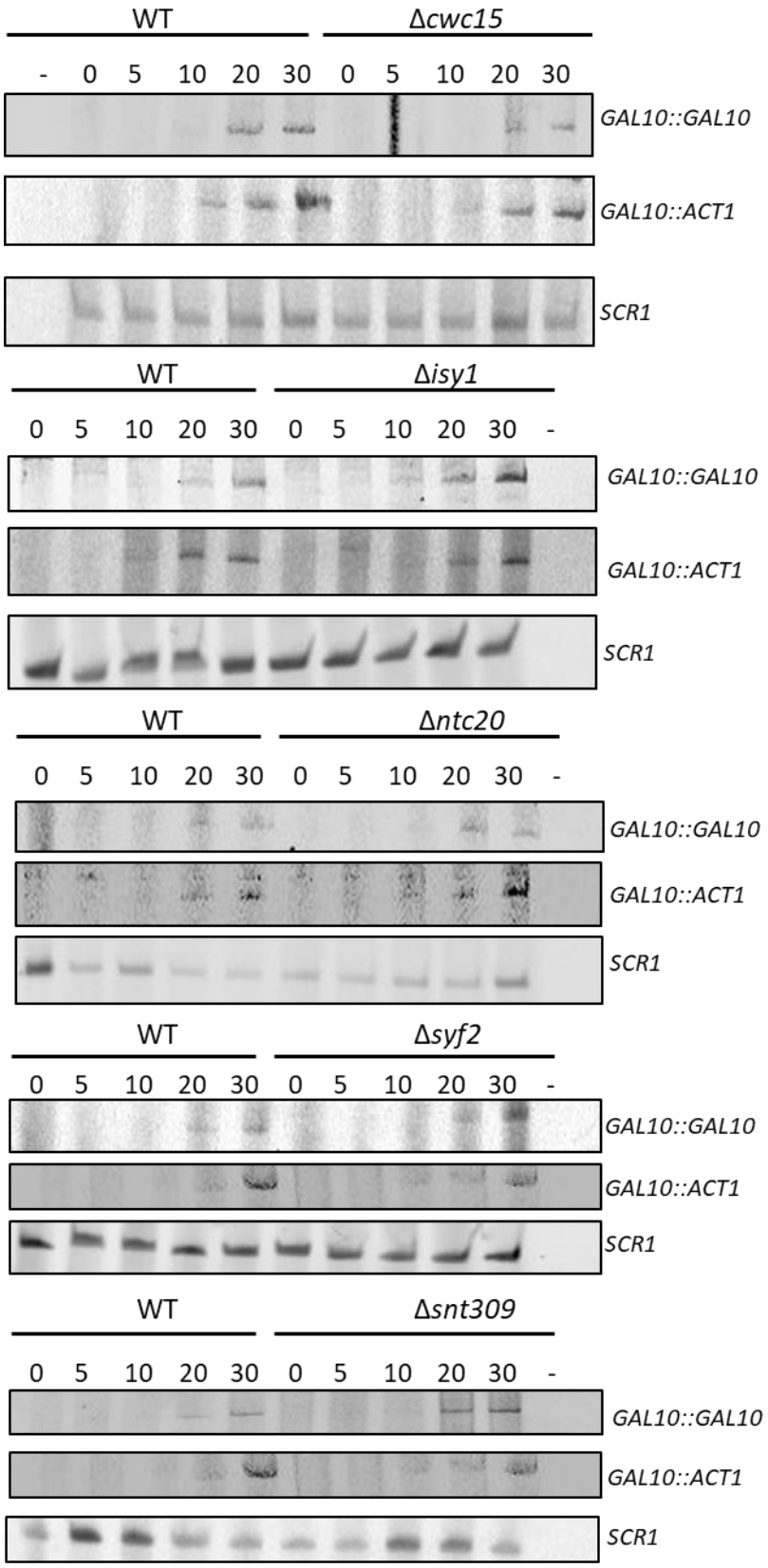

Appendix Figure 3: Exemplary urea-SDS-PAGE corresponding to the *in vivo* assay of Figure 17. The intronless, endogenous *GAL10* gene and plasmid-driven *ACT1* gene under both under the control of *GAL* promoter. Cells were grown in medium using raffinose as carbon source. Cells were grown to an OD_{600} of 0,8 and induced with galactose and total RNA was extracted from collected 0, 5, 10, 20 and 30 min. The

amount of synthesized *GAL10* and *ACT1* mRNA was analyzed by primer extension assay using 5' Cy5 labelled primers specific to *GAL10* and *ACT1* mRNA. The amount of *SCR1* RNA (-), an RNAPIII transcript, served as a loading control for the experiment.

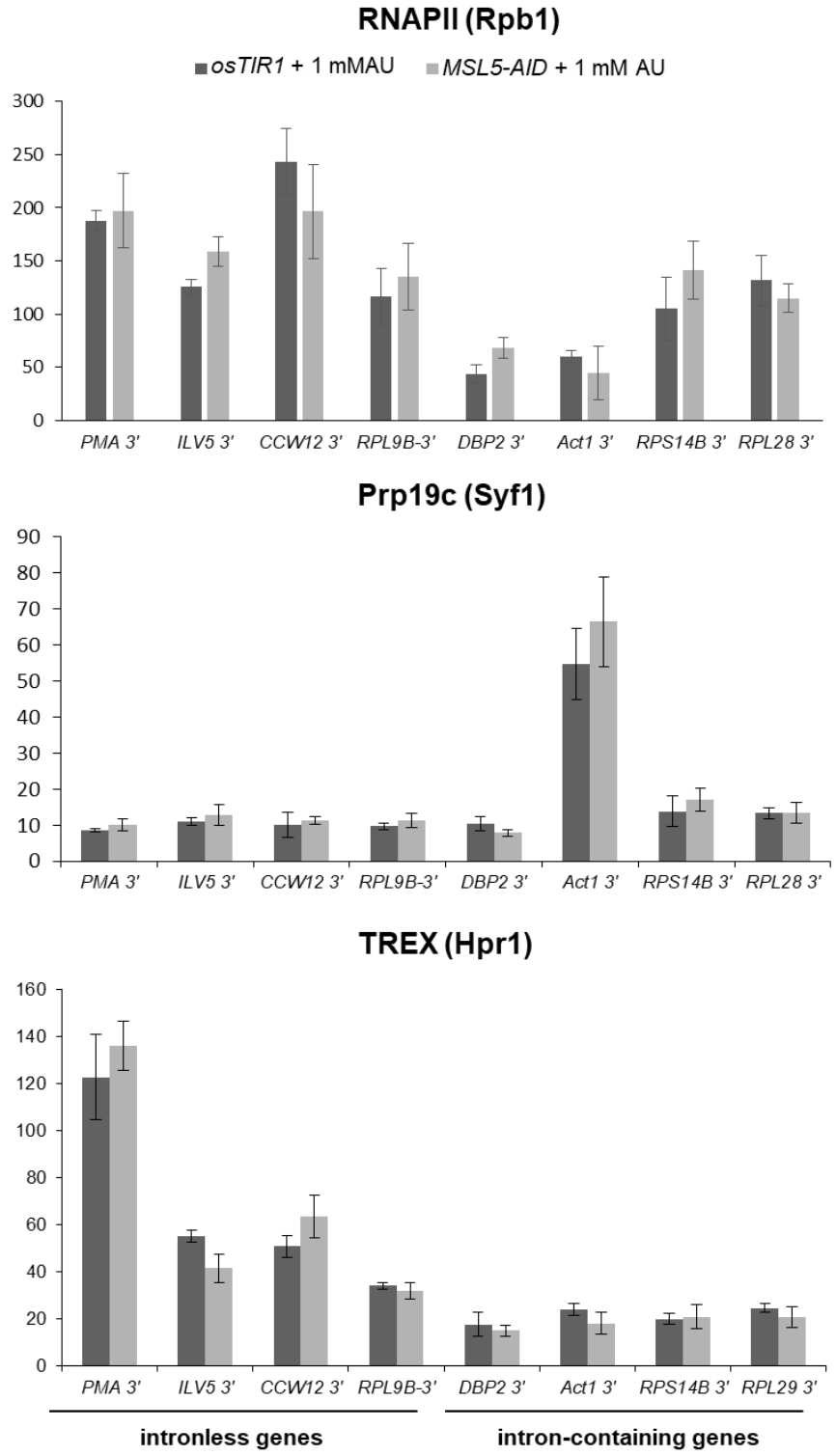

Appendix Figure 4: Control experiments for auxin addition for Figure 21A, 29A and B. RNAPII, Syf1 and Hpr1 occupancy in Tir1 cells under the addition of 1 mM of AU and Msl5-AID cell under the addition of 0 mM of AU. The occupancy was assessed using chromatin

immunoprecipitation (ChIP) at exemplary intron-containing (*DBP2, ACT1, RSP14B and RPL28*) and intronless genes (*PMA1, ILV5, CCW12 and RPL9B*). ChIPs were quantified by Real Time PCR using the primer pairs which bind at the 3' end of the gene.

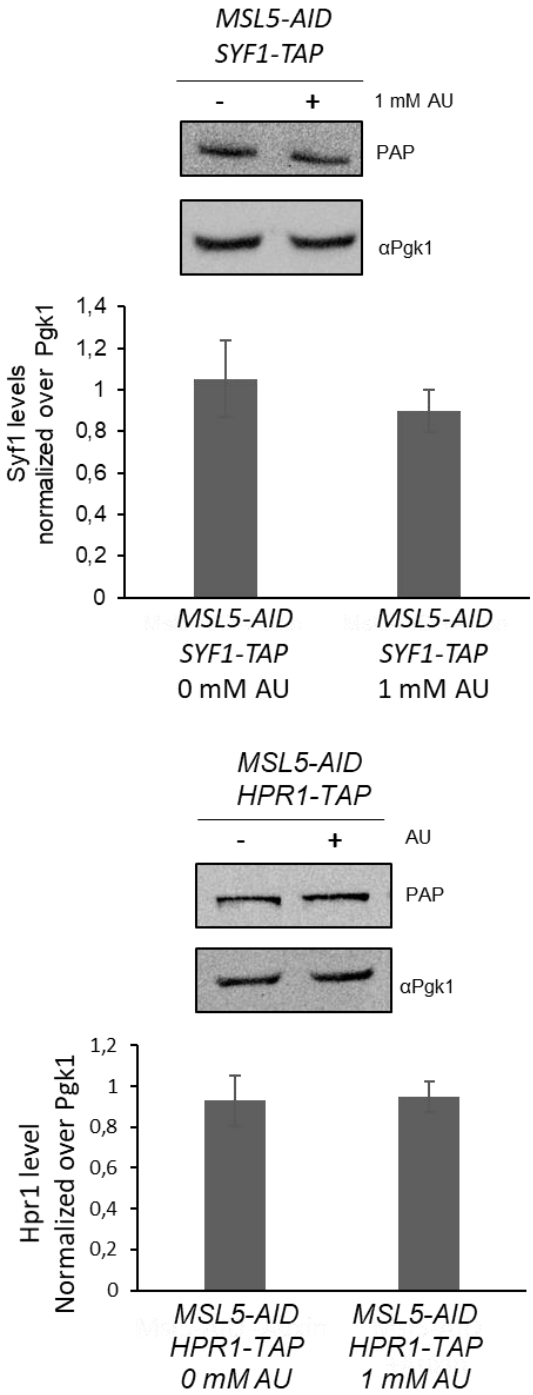

Appendix Figure 5: Depletion of Msl5 do not influence Syf1 and Hpr1 protein levels. Western blots and quantification of three independent experiments of total Syf1 and Hpr1 levels in whole cell lysates in *MSL5-AID* cells treated with 0 mM and 1 mM AU. The amount of *SYF1-TAP* and *HPR1-TAP* was quantified with an antibody directed against protein A (PAP) and normalized to the amount of Pgk1. Values for undepleted cells were set to 1.